GEOLOGICA ULTRAIECTINA

Mededelingen van de
Faculteit Geowetenschappen
Universiteit Utrecht

No. 250

Coupled transport in clayey materials with emphasis on induced electrokinetic phenomena

Katja Heister

GEOLOGICA ULTRAIECTINA

Mededelingen van de
Faculteit Geowetenschappen
Universiteit Utrecht

No. 250

Coupled transport in clayey materials with emphasis on induced electrokinetic phenomena

Katja Heister

Coupled transport in clayey materials with emphasis on induced electrokinetic phenomena

Gekoppeld transport in kleihoudende materialen met nadruk op geïnduceerde elektrokinetische verschijnselen

(met een samenvatting in het Nederlands)

Gekoppelter Transport in tonigen Materialien unter besonderer Berücksichtigung induzierter elektrokinetischer Phänomene

(mit einer Zusammenfassung in deutscher Sprache)

PROEFSCHRIFT

ter verkrijging van de graad van doctor aan de Universiteit Utrecht

op gezag van de Rector Magnificus, Prof. Dr. W.H. Gispen,

ingevolge het besluit van het College voor Promoties

in het openbaar te verdedigen op maandag 30 mei 2005 des ochtends te 10:30 uur

door

Katja Heister

geboren op 21 maart 1973 te Koblenz, Duitsland

Promotor: Prof. Dr. P.S.J. Van Cappellen

Department of Earth Sciences - Geochemistry

Faculty of Geosciences

Universiteit Utrecht

Co-promotor: Dr. Ir. J.P.G. Loch

Department of Earth Sciences - Geochemistry

Faculty of Geosciences

Universiteit Utrecht

The research described in this thesis was carried out at the Department of Earth Sciences – Geochemistry, Faculty of Geosciences, Universiteit Utrecht, The Netherlands.

The work was funded by TRIAS (project number 835.80.003 'Chemically and Electrically Coupled Transport in Clayey Soils and Sediments').

ISBN 90-5744-108-X

"The answer is ***everyday***."

From the motion picture 'The Sixth Sense', written and directed by M. Night Shyamalan, 1999.

Für meinen Vater.

Table of contents

Summary

Transport of water and solutes in clayey soils and sediments plays an important role in groundwater and waste management. In clay layers, water transport can be induced not only by gradients in hydraulic potential and solution density but also by gradients in salt concentration and electrical potential. Chemically and electrically driven water transport, chemical osmosis and electroosmosis, respectively, are significant in porous materials with hydraulic conductivity less than $1{\cdot}10^{-9}$ m/s, like e.g. clays.

Although the importance of these flows in clayey soils and sediments was recognized since the middle of the 20th century, chemical osmosis and electroosmosis are still absent in groundwater models. In these decades, much fundamental research on hydraulically, chemically and thermally driven flows was done by soil chemists and soil physicists and application of electroosmosis for dewatering of soil and slope stabilization and the use of electromigration as an in-situ remediation technique for contaminated soils were attempted. Neglecting chemically and electrically induced processes is not justified in e.g. salt-water intrusions in low coastal areas, depositories of polluted harbour sludge and long-term storage of radioactive waste or other toxic waste in clay formations. In these cases, groundwater and waste management relies on the low permeability and the high adsorptive capacity of the clay for limiting transfer of contaminant solutes through aquitards or from a waste disposal site. In coastal areas, seawater intrusion into aquifers is supposed to be restricted by Holocene clay layers. Contaminated clay or clayey sludge or sediment is subject to emission requirements for contaminants to the surrounding. In case of long-term storage of radioactive waste in clay formations, even small fluxes are of significance because processes can take place over a long period of time and human and environmental toxicity are large.

Chemical osmosis and electroosmosis are coupled flow phenomena that can be described within the framework of irreversible thermodynamics. In general, clay layers are subject to flows of fluid, electrical charge, solutes and heat. These flows can be induced by their conjugated driving forces, like e.g. fluid flow by a hydraulic potential gradient, and are called direct flows. Moreover, flows can be induced by non-conjugated driving forces, like e.g. fluid flow by a salt concentration gradient, which is termed chemical osmosis. These are called coupled flows.

Clay layers act as semipermeable membranes. Thus, they are able to permit the transport of some components of a solution while others are excluded from transport. Accordingly, a semipermeable membrane prevents the passage of a solute without affecting the passage of the solvent. This is caused by overlapping diffuse double layers of the clay particles inside the pores of the clay layer. Anions that attempt to migrate through the pores are repelled by the negative charge of the clay platelets; subsequently, to maintain electrical neutrality in the external solution, also the movement of cations through the clay is restricted. If a clay is able to restrict the transport of a solute completely, the membrane is ideal. However, in nature, a membrane is seldom ideal, and some of the salt ions will pass the membrane by diffusion. Accordingly, such non-ideal membranes do not restrict the passage of solutes completely. The degree of ideality is expressed by the reflection coefficient, which can be calculated together with a number of other transport parameters for the transport of ions and water through semipermeable membranes using the coupled flow equations.

The aim of this thesis is to quantify the effect of induced electrical potential gradients on the transport of water and ions in clay layers by means of laboratory experiments. Electrical potential gradients can be induced by a hydraulic pressure gradient (streaming potential) or a salt concentration gradient (membrane potential).

For this purpose, permeameter set-ups were realized to perform bench-scale experiments on different clay materials. The materials studied were a commercially available bentonite as a reference material and two field clays. With coupled flow equations, transport parameters were calculated and the effect of the induced electrical potential gradients on the flow of water and ions was demonstrated. It was observed that the induced electrical potential gradients counteracted the flow of fluid in case of the streaming potential and the flows of fluid and solutes in the case of membrane potential. Subsequently, taking these effects not into account influenced the calculated transport parameters.

The results of this laboratory study will be used to validate a model, developed by the Environmental Hydrogeology Group of the Department of Earth Sciences, Utrecht University, which includes chemical osmosis and electroosmosis in groundwater transport.

Chapter 1

General introduction

Transport of water and solutes in clayey soils and sediment layers is of great importance in groundwater management. Groundwater aquifers in sedimentary regions usually are confined by aquitards consisting of clayey layers. Waste disposal sites are often constructed with clay liners. In both cases, groundwater and waste management relies on the low permeability and the high adsorptive capacity of the clay for limiting distribution of contaminant solutes to or from an aquifer or from a waste disposal site. In coastal regions, seawater intrusion into aquifers is supposed to be restricted by Holocene clay layers. Contaminated clay or clayey sludge or sediment is subject to emission requirements for contaminants to the surroundings. Water balances for polder areas or other diked regions are dependent on flow of water through clay layers.

In addition to gradients in hydraulic potential and solution density, water transport in clay layers can also be driven by salt concentration gradients resulting in chemical osmosis and electrical potential gradients resulting in electroosmosis. Chemically and electrically driven water transport is significant in porous materials with a low hydraulic conductivity. However, at present, these driving forces and fluxes are virtually neglected in groundwater models. The aim of this thesis is to demonstrate and quantify the effects of induced electrical potential gradients on water and solute flow in clay layers. Use will be made of the theory of irreversible thermodynamics. With the obtained transport parameters, a new model, which does include these coupled transport phenomena, will be developed and validated by the Environmental Hydrogeology Group of the Department of Earth Sciences, Utrecht University.

Clay minerals and diffuse double layers

Clayey materials consist for the most part of clay size particles. One should distinguish between particles of 'clay size', which are particles $\leq$ 2µm (Mitchell, 1993), and clay minerals, which are secondary aluminium silicates belonging to the family of phyllosilicates. Clay as a size fraction also includes other minerals like sesquioxides and fine primary silicate minerals. Although clay minerals are commonly of the size of clay fraction, size is not the significant parameter. From here on, we mean clay minerals, when clay is discussed.

Clay minerals exhibit properties crucial for coupled flow phenomena, which are in general caused by their crystallographic structure. There is a huge variation in chemical and physical structure of clay minerals, but basically, all are characterized by a platy morphology and a perfect basal cleavage (Deer et al., 1985). Clay minerals consist of combinations of sheets of silica tetrahedrons and sheets of aluminium or magnesium octahedrons. The different clay mineral groups are characterized by the stacking arrangements of these sheets and the manner in which two successive two- (tetrahedron-octahedron[1]) or three-sheet (tetrahedron-octahedron-tetrahedron[2]) layers are held together (Mitchell, 1993). Accordingly, the clay minerals can be classified in groups like e.g. kaolinite (1:1), smectite, illite

[1] t-o stacks Ξ 1:1 clay minerals

[2] t-o-t stacks Ξ 2:1 clay minerals

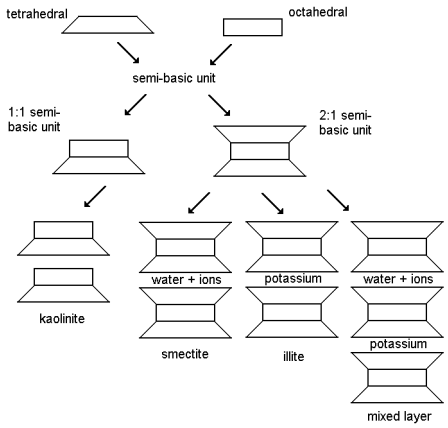

Figure 1.1: Structural classification of the clay minerals.

and mixed layer (2:1) (Fig. 1.1). Differences among minerals within the groups result primarily from differences in the type and amount of isomorphous substitution within the crystal structure. Isomorphous substitution means that a cation of suitable size, other than normally found, is present in the crystal lattice without a substantial change in the crystal structure. Due to isomorphous substitution, clay minerals are negatively charged. Thus, in an aqueous medium, a diffuse double layer develops. Different theories about the structure of diffuse double layers like the Gouy type and the Stern type models were developed (cf. van Olphen, 1977; Bolt, 1979), and even the applicability of the diffuse double-layer theory is called into question (cf. McBride, 1997; Grasso et al., 2002; McBride and Baveye, 2002). However, we will follow the approach of Gouy-Chapman (cf. Bolt, 1976; Bolt, 1979), and we will see later on that the phenomena observed in this study can satisfactorily be described with this theory.

Accordingly, to obtain electrical neutrality, the negative charge of the clay particle is balanced by the attraction of cations close to the surface of the particle. Negatively charged anions are repelled from the clay. The charged clay surface together with the water layer with excess charge of cations, the so-called counter-ions, forms the diffuse double layer. Far away from the clay particle surface in the bulk solution, cation and anion concentrations equal the equilibrium concentration (Fig. 1.2). The thickness of the diffuse double layer decreases with increasing electrolyte concentration and with increasing valence of the cation, and further depends on the dielectric constant of the medium and the temperature (Mitchell, 1993).

Due to their electrical charge, in free solution, the clay particles repel each other. But under an overburden load, if the clay particles are forced more closely together, diffuse double layers will overlap. In this case, like in a dehydrated clay, the double layers are truncated (Fig. 1.3). The water film within the truncated double layers is completely dominated by the electrical restrictions imposed

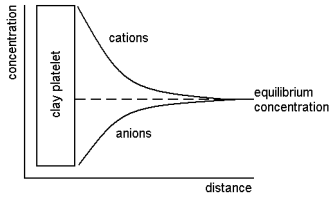

Figure 1.2: Distribution of cations and anions in the close vicinity of a clay platelet according to the diffuse double-layer theory.

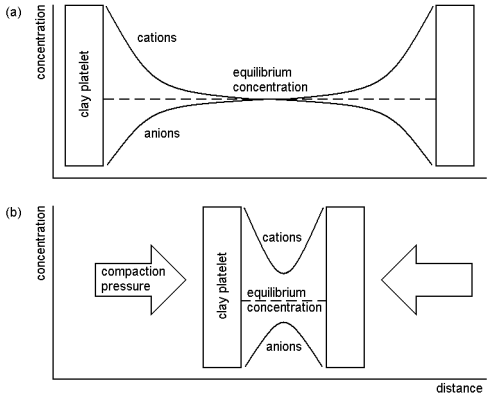

Figure 1.3: Distribution of cations and anions in the vicinity of clay platelets. The dispersed situation is shown in (a) where the diffuse double layers of the clay particles do not overlap. Under an overburden pressure, as shown in (b), the clay platelets are forced more closely together which results in an overlap of their diffuse double layers.

on ion transfer. The cation concentration is higher and the anion concentration is lower than in the equilibrium solution. This latter effect is known as 'negative adsorption', 'anion exclusion' or 'Donnan exclusion' (Mitchell, 1993; Horseman et al., 1996).

Clay layers as semipermeable membranes

In transport processes, compacted clay layers act as semipermeable membranes. Generally, a membrane is 'a selective barrier between two phases, the term 'selective' being inherent to a membrane or a membrane process' (Mulder, 1991). Semipermeability is defined as the ability to permit the transport of some components of a solution while others are excluded from transport (Tuwiner, 1962). Accordingly, a semipermeable clay membrane prevents the passage of a solute without affecting the passage of the solvent (Mitchell, 1993). Due to overlapping diffuse double layers in the pores, anions that attempt to migrate through the water film are repelled by the negative charge of the clay platelets. In order to maintain electrical neutrality in the external solution, cations will tend to remain with their co-ions. So, their movement through the clay will also be restricted (Fritz, 1986).

If a clay membrane is subject to a concentration gradient of a certain solute, the solvent will flow through the membrane until the imposed concentration gradient is levelled out. This phenomenon is called osmosis and best known from biology, where cell walls of plants and animals are capable of restricting the passage of salts and sugars but allow water to pass in or out of the cell. However, earth science showed that clays or materials with a high clay content are also capable to act as semipermeable membranes (Kharaka and Berry, 1973; Hanshaw and Coplen, 1973; Fritz and Marine, 1983; Keijzer et al., 1999). Furthermore, other comparable phenomena are imaginable as well. They are termed coupled flow phenomena and will be described later.

First, let us have a closer look at the semipermeable membrane. According to the definition of semipermeability, the passage of a solute through a semipermeable membrane is totally restricted. This implies that the membrane is ideal. In nature, however, a membrane is seldom ideal. In case of osmosis, water will pass the membrane while salt ions are rejected, but some of the salt ions will pass the membrane by diffusion, thereby lowering the induced osmotic pressure. Accordingly, such non-ideal or 'leaky' membranes do not restrict the passage of solutes completely. The degree of ideality is expressed by the reflection coefficient, σ (Katchalsky and Curran, 1967). The reflection coefficient

Table 1.1: Direct and coupled flow phenomena (Mitchell, 1993;Yeung, 1994; Horseman et al., 1996).

Flow J	Gradient X			
	Hydraulic	Electrical	Chemical	Thermal
Fluid	Hydraulic conduction *Darcy s law*	Electroosmosis	Chemical osmosis	Thermoosmosis
Current	Streaming potential	Electrical conduction *Ohm s law*	Diffusion and membrane potentials	Thermoelectricity Seebeck effect
Ion	Streaming current	Electrophoresis	Diffusion *Fick s law*	Thermal diffusion of electrolyte Soret effect
Heat	Isothermal heat transfer	Peltier effect	Dufour effect	Thermal conduction *Fourier s law*

varies between zero and one. If the membrane is ideal, the reflection coefficient equals one. In porous media without semipermeability, the reflection coefficient is zero. Consequently, clay membranes, which exhibit semipermeable behaviour but are not ideal semipermeable, have a reflection coefficient between zero and one.

The reflection coefficient can be calculated together with a number of other transport parameters for the transport of ions and solution through semipermeable membranes. A feasible framework to describe these transport processes is the set of coupled flow equations used in irreversible thermodynamics.

Coupled flow phenomena and equations of irreversible thermodynamics

Although some processes like diffusion and osmosis in porous media have been known for a couple of centuries, their role in geotechnical problems was given attention since the middle of the 20th century (Mitchell, 1991). Russell (1933) was the first who suggested that reverse osmosis could explain the formation of subsurface brines, which often have a higher chloride concentration than seawater, and encouraged further research in this field. Thereafter, Casagrande (1949) suggested application of electroosmosis for dewatering of soil and slope stabilization, and Winterkorn (1947, 1955) noted similarities between chemical osmosis, electroosmosis and thermoosmosis and suggested a generalization of Darcy's law to include contributions from electrical and thermal gradients. Subsequently, Olsen (1969, 1972) studied flows of various types in geological processes, and much more fundamental research on chemically, hydraulically and thermally driven flows was done by

researchers in soil chemistry and soil physics (e.g. Kemper and Quirk, 1972; Hanshaw and Coplen, 1973; Kharaka and Berry, 1973; Fritz and Marine, 1983; Keijzer et al., 1999).

But even though the appearance of coupled flow phenomena seems to be widespread, they are only significant relative to direct hydraulic flows in porous media if the hydraulic conductivity is less than $1 \cdot 10^{-9}$ m/s (Mitchell, 1991). Therefore, we study compacted clay layers, as they are known for their low hydraulic conductivity.

Accordingly, flows in porous media, e.g. in clay layers, are flows of fluids, electrical charge, solutes and heat and can be described with the coupled flow equations of irreversible thermodynamics (cf. Katchalsky and Curran, 1967). In this regard, it has been well established that each flux J_i relates linearly to its conjugated driving force X_i:

$$J_i = L_{ii} X_i \tag{1.1}$$

where L_{ii} is the conductivity coefficient of this flow.

For each of the four fluxes, we can write an analogous equation. One example is the flux of water that is directly related to the hydraulic gradient by the hydraulic conductivity coefficient. This is widely known as Darcy's law. For the fluxes of electrical charge, solutes and heat, similar equations are established known as Ohm's law, Fick's law and Fourier's law, respectively.

In all these cases, the flux is induced by its conjugated driving force. They are called direct flow phenomena. In most cases, however, there are simultaneous flows of different types, even when only one driving force is acting. Strictly speaking, a gradient of one type can cause a flux of another type according to

$$J_i = L_{ij} X_j \tag{1.2}$$

in which L_{ij} is the coupling coefficient (Katchalsky and Curran, 1967; Yeung and Mitchell, 1993; Yeung, 1994).

These are coupled flow phenomena. One example, as mentioned, is osmosis. Here, a concentration gradient induces a flow of water. As there are four types of fluxes and gradients, twelve coupled flow phenomena are possible. The matrix of all flow phenomena is shown in Table 1.1. The direct flow phenomena are on-diagonal, whereas the coupled flow phenomena are off-diagonal (Mitchell, 1993; Yeung, 1994; Horseman et al., 1996).

The matrix can be translated into coupled flow equations. In this study, we neglect heat flow and temperature gradients because temperature is easily kept constant under laboratory conditions. So, we obtain:

$$\begin{aligned} J_v &= L_{11}\nabla(-P) + L_{12}\nabla(-E) + L_{13}\nabla(-\mu) \\ I &= L_{21}\nabla(-P) + L_{22}\nabla(-E) + L_{23}\nabla(-\mu) \\ J_s &= L_{31}\nabla(-P) + L_{32}\nabla(-E) + L_{33}\nabla(-\mu) \end{aligned} \tag{1.3}$$

in which J_v is the water flux density in m/s, I is the electrical current density in A/m^2, J_s is the solute

flux density in mol/m²·s, P is the hydraulic pressure in N/m², E is the electrical potential in V, μ is the chemical potential in J/mol and L_{11} to L_{33} are the phenomenological coefficients in their corresponding units (Katchalsky and Curran, 1967; Yeung, 1990; Yeung and Mitchell, 1993).

Furthermore, the cross-coupled coefficients are related to each other according to

$$L_{ij} = L_{ji} \quad (i, j = 1,2,3,...) \tag{1.4}$$

This reciprocal relation was demonstrated by Onsager (1931a, b).

So, for Eq. 1.3, we end up with three direct and three independent coupled coefficients. With this set of equations, it is possible to describe direct and coupled flows of water, electrical charge and solutes due to hydraulic, electrical and chemical potential gradients.

Electrokinetic phenomena

Coupling between electrical, hydraulic and chemical flows and gradients in mixtures of charged solids and water can be responsible for a couple of electrokinetic phenomena. Figure 1.4 gives a schematic overview of those that are of importance in the author's opinion.

The most widely known is probably electrophoresis. In this case, a DC field is placed across a colloidal suspension of charged particles, which are attracted electrostatically to one of the electrodes and repelled from the other. On the other hand, the movement of charged particles in a suspension during gravitational settling generates an electrical potential gradient, defined as migration or sedimentation potential. It is caused by viscous drag of the water that retards the movement of the diffuse double-layer cations relative to the particles. While these two phenomena involve discrete particle transport in an aqueous suspension, the following phenomena involve water transport through a continuous fixed particle network.

In case of electroosmosis, an electrical potential gradient is applied across a porous solid medium. The ions are attracted to the cathode and anode, respectively. Thereby, they exert a viscous drag on the water around them. In a medium composed of negatively charged particles, like clay minerals, there is a net water flow towards the cathode, which is termed electroosmosis. Otherwise, when water is caused to flow through a clay under a hydraulic pressure gradient, the diffuse double-layer charges are displaced in the direction of flow, which results in an electrical potential difference between the two opposite ends of the soil mass called streaming potential (Mitchell, 1993; Yeung, 1994).

Electroosmosis has been given the most attention in geotechnical engineering because of its practical value for transporting water in fine-grained soils. Applications are dewatering, soft ground consolidation, injection, containment and extraction of chemicals in the ground (Mitchell, 1993). Since the 1980s, the application of DC is also used for soil remediation (e.g. Renaud and Probstein, 1987; Acar et al., 1993; Probstein and Hicks, 1993; Chung and Kang, 1999). Charged species of contaminants in soil solution are attracted to the respective electrode where they can be removed from the soil. Uncharged species can be dragged along with the water transported by electroosmosis.

Since we will study transport in compacted clay membranes, electrophoresis and migration or sedimentation potential are ignored in this investigation. Moreover, we will confine our interest to induced electrical potential gradients. By applying Onsager's reciprocal relations, the magnitude of

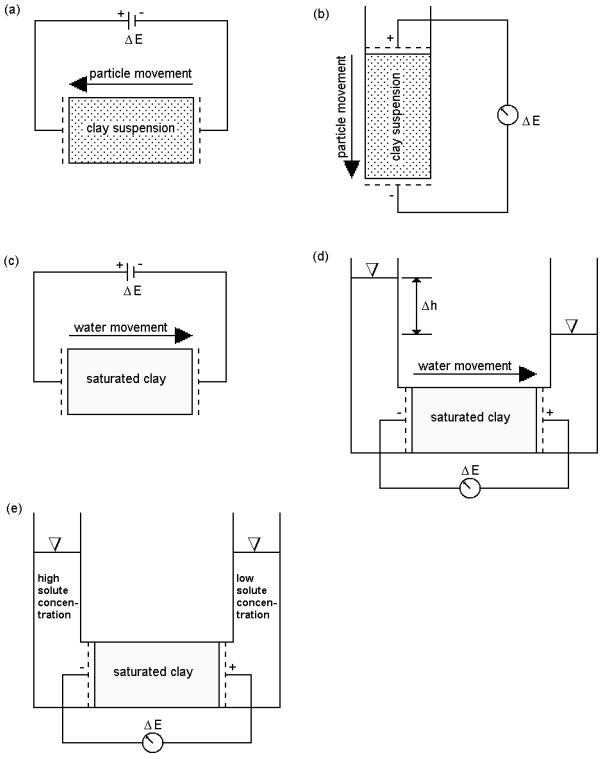

Figure 1.4: Schematic overview of the electrokinetic phenomena described in the text. (a) Electrophoresis. (b) Migration or sedimentation potential. (c) Electroosmosis. (d) Streaming potential. (e) Membrane potential.

electroosmosis can be predicted from the streaming potential. Since streaming potentials do not involve the transport of solutes or gradients of chemical potential, we, furthermore, will study electrical potential gradients induced by gradients of chemical potential. These are called membrane potentials and have first been considered by Henderson (1907). The membrane potential is defined as an electrical potential gradient induced by a concentration gradient across a membrane under isothermal conditions and constant pressure (Kobatake et al., 1965).

Although in literature, authors use various terms to describe the same phenomena, we will stick to the nomenclature listed in Table 1.1 throughout the whole thesis.

Social relevance and framework of this research

Transport of water and solutes in clayey soils and sediments plays a crucial role in groundwater management. But in nearly all existing water transport models, water movement is only driven by differences in hydraulic potential and solution density. Chemical osmosis and electroosmosis, the movement of water driven by a concentration gradient or an electrical potential gradient, respectively, are absent in groundwater models. In recent years, the importance of coupled flows in clayey soils and sediments was noticed and first experimental studies underlining this were published (e.g. Keijzer, 2000). Moreover, the incorporation of osmotic transport in existing models is on its way (Bader and Kooi, 2005).

There are various scenarios imaginable where neglecting coupled transport processes may not be

justified. One example is the regional hydrology in low coastal areas with large salinity gradients as in The Netherlands, where spatial variations in water level are very small. Here, even a small osmotic flux could have a strong effect. This was emphasized by De Haven (1982), who computed as an example the effect of osmotic fluxes on groundwater movement in the Haarlemmermeer polder, The Netherlands.

Another example are depositories of polluted harbour sludge, which is a clayey sediment, and therefore commonly deposited without sealing clay layers. According to calculations of De Haven (1982), a concentration difference of 4800 ppm Cl^- can cause an osmotic pressure of approximately 7 bar. Comparing the resulting chemical osmosis with the small fluxes allowed by Dutch legislation for emission of water from harbour sludge deposits, osmotic fluxes are expected to have a strong effect and should therefore be definitely taken into account in modelling calculations for the design of such deposits.

A third example, receiving much attention in the last decades, is the long-term storage of radioactive waste in clay formations. To investigate the fate of radioactive waste deposited in the clay, in-situ laboratories were set up in potential host rocks, like the Hades Underground Research Laboratory in the Boom Clay formation in Mol, Belgium and the Mont Terri Laboratory in the Opalinus Clay formation in Canton Jura, Switzerland. In these cases, small fluxes are of significance because processes can take place over a long period of time and human and environmental toxicity are high.

All examples highlight the social relevance of this research topic.

The present thesis is part of a cooperative project funded by TRIAS (Tripartite Approach to Soil System Processes), which is entitled 'Chemically and Electrically Coupled Transport in Clayey Soils and Sediments'. TRIAS consists of three funding partners, NWO (Netherlands' Organisation of Scientific Research), Delft Cluster and SKB (Foundation for the Development and Transfer of Knowledge of Soils). The objective of this project is to model water and solute transport in clayey soils and sediments, where chemical or electrical gradients are present. The project is divided into three different approaches, each of them resulting in a Ph.D. thesis, i.e. laboratory studies of coupled transport phenomena on different sample materials, field studies of osmotic transport at different field sites and model development and validation to incorporate chemical osmosis and electroosmosis in an existing transport model.

The participants in the cooperative project are Utrecht University, Department of Earth Sciences – Geochemistry (laboratory studies), Vrije Universiteit Amsterdam, Department of Hydrology and Geo-environmental Sciences (field studies) and Utrecht University, Department of Earth Sciences – Environmental Hydrogeology, formerly Technical University of Delft, Faculty of Civil Engineering and Geosciences (model development and validation).

This thesis is presented by the Geochemistry group and deals with the laboratory investigation of chemically and electrically coupled transport in clayey materials.

Outline of the thesis

After a description of the clay materials used in the experiments (**Chapter 2**), the stability of clay membranes is investigated in **Chapter 3**. This is of importance for all following experiments with clay membranes that get in contact with solutions of ionic strength above their flocculation value. If structural changes of the clay occur due to rearrangement of the clay particles by flocculation, this

will have a significant impact on the semipermeability of the membrane. Thereafter, in bentonite membranes, streaming potentials, i.e. electrical potential gradients induced by hydraulic flow, are studied in a flexible-wall permeameter and their effect on water transport is quantified (**Chapter 4**). In this laboratory set-up, gold electrodes are employed to measure the electrical potential gradient. The performance of gold electrodes may be questioned due to possible polarization of the electrodes. Therefore, the various types of reversible electrodes are reviewed and the feasibility of gold electrodes is compared with Ag/AgCl gel electrodes in streaming potential and electroosmosis experiments in bentonite membranes (**Chapter 5**). As it is concluded that both types of electrodes are unsuitable for our purpose, a rigid-wall permeameter with double-junction Ag/AgCl reference electrodes is developed (**Chapter 6**). With this set-up, membrane potentials, i.e. electrical potential gradients induced by a concentration gradient, are measured in bentonite membranes and their effect on water and solute transport is quantified. The same experiments on samples of two field clays are reported in **Chapter 7**, which, compared to the bentonite, show different semipermeable behaviour. Finally, **Chapter 8** critically summarizes the results obtained, underlines the conclusions that can be drawn from this study and gives an outlook to possible further investigation of this complex subject.

References

Acar, Y.B., Alshawabkeh, A.N. and Gale, R.J., 1993. *Fundamentals of extracting species from soils by electrokinetics.* Waste Management, 13: 141 - 151.

Bader, S. and Kooi, H., 2005. *Modelling of solute and water transport in semi-permeable clay membranes: Comparison with experiments.* Advances in Water Resources, 28: 203 - 214.

Bolt, G.H., 1976. *Surface interaction between the soil solid phase and the soil solution.* In: G.H. Bolt and M.G.M. Bruggenwert (Editors), Soil Chemistry. A. Basic Elements. Developments in Soil Science. Elsevier, Amsterdam, pp. 43 - 53.

Bolt, G.H., 1979. *The ionic distribution in the diffuse double layer.* In: G.H. Bolt (Editor), Soil Chemistry. B. Physico-chemical Models. Developments in Soil Science. Elsevier, Amsterdam, pp. 1 - 25.

Casagrande, L., 1949. *Electro-osmosis in soils.* Geotechnique, 1(3): 159 - 177.

Chung, H.I. and Kang, B.H., 1999. *Lead removal from contaminated marine clay by electrokinetic soil decontamination.* Engineering Geology, 53: 139 - 150.

De Haven, J.C., 1982. *Lowlands underground water as a physicochemical system, Appendix C,* Tweede Nota Waterhuishouding. SDU, Den Haag, The Netherlands, pp. 300 - 315.

Deer, W.A., Howie, R.A. and Zussman, J., 1985. *An Introduction to the Rock-Forming Minerals.* Longman, Harlow, Essex, UK, 528 pp.

Fritz, S.J. and Marine, I.W., 1983. *Experimental support for a predictive osmotic model of clay membranes.* Geochimica et Cosmochimica Acta, 47: 1515 - 1522.

Fritz, S.J., 1986. *Ideality of clay membranes in osmotic processes: A review.* Clays and Clay Minerals, 34(2): 214 - 223.

Grasso, D., Subramaniam, K., Butkus, M., Strevett, K. and Bergendahl, J., 2002. *A review of non-DLVO interactions in environmental colloidal systems.* Reviews in Environmental Science and Bio/Technology, 1: 17 - 38.

Hanshaw, B.B. and Coplen, T.B., 1973. *Ultrafiltration by a compacted clay membrane - II. Sodium ion exclusion at various ionic strengths.* Geochimica et Cosmochimica Acta, 37: 2311 - 2327.

Henderson, P., 1907. *Zur Thermodynamik der Flüssigkeitsketten.* Zeitschrift für physikalische Chemie, Stöchiometrie und Verwandtschaftslehre, 59: 118 - 127.

Horseman, S.T., Higgo, J.J.W., Alexander, J. and Harrington, F.J., 1996. *Water, Gas and Solute Movement Through Argillaceous Media.* CC-96/1, Nuclear Energy Agency, Organisation for Economic Co-Operation and Development, Paris, France.

Katchalsky, A. and Curran, P.F., 1967. *Non-Equilibrium Thermodynamics in Biophysics.* Harvard University Press, Cambridge, MA, USA, 248 pp.

Keijzer, T.J.S., Kleingeld, P.J. and Loch, J.P.G., 1999. *Chemical osmosis in compacted clayey material and the prediction of water transport.* Engineering Geology, 53: 151 - 159.

Keijzer, T.J.S., 2000. *Chemical Osmosis in Natural Clayey Materials.* Ph.D. Thesis, Universiteit Utrecht, Utrecht, The Netherlands, 166 pp.

Kemper, W.D. and Quirk, J.P., 1972. *Ion mobilities and electric charge of external clay surfaces inferred from potential differences and osmotic flow.* Proceedings of the Soil Science Society of America, 36: 426 - 433.

Kharaka, Y.K. and Berry, F.A.F., 1973. *Simultaneous flow of water and solutes through geological*

membranes. I. Experimental investigation. Geochimica et Cosmochimica Acta, 37: 2577 - 2603.

Kobatake, Y., Takeguchi, N., Toyoshima, Y. and Fujita, H., 1965. *Studies of membrane phenomena. I. Membrane potential.* Journal of Physical Chemistry, 69(11): 3981 - 3988.

McBride, M.B., 1997. *A critique of diffuse double layer models applied to colloid and surface chemistry.* Clays and Clay Minerals, 45(4): 598 - 608.

McBride, M.B. and Baveye, P., 2002. *Diffuse double-layer models, long-range forces, and ordering in clay colloids.* Soil Science Society of America Journal, 66: 1207 - 1217.

Mitchell, J.K., 1991. *Conduction phenomena: From theory to geotechnical practice.* Geotechnique, 41(3): 229 - 340.

Mitchell, J.K., 1993. *Fundamentals of Soil Behavior.* John Wiley and Sons, New York, 437 pp.

Mulder, M., 1991. *Basic Principles of Membrane Technology.* Kluwer Academic Publishers, Dordrecht, The Netherlands, 363 pp.

Olsen, H.W., 1969. *Simultaneous fluxes of liquid and charge in saturated kaolinite.* Proceedings of the Soil Science Society of America, 33: 338 - 344.

Olsen, H.W., 1972. *Liquid movement through kaolinite under hydraulic, electric, and osmotic gradients.* The American Association of Petroleum Geologist Bulletin, 56(10): 2022 - 2028.

Onsager, L., 1931a. *Reciprocal relations in irreversible processes I.* Physical Review, 37: 405 - 426.

Onsager, L., 1931b. *Reciprocal relations in irreversible processes II.* Physical Review, 38: 2265 - 2279.

Probstein, R.F. and Hicks, R.E., 1993. *Removal of contaminants from soils by electric fields.* Science, 260: 498 - 503.

Renaud, P.C. and Probstein, R.F., 1987. *Electroosmotic control of hazardous wastes.* Physicochemical Hydrodynamics, 9(1/ 2): 345 - 360.

Russell, W.L., 1933. *Subsurface concentration of chloride brines.* Bulletin of the American Association of Petroleum Geologists, 17(10): 1213 - 1228.

Tuwiner, S.B., 1962. *Diffusion and Membrane Technology.* Reinhold Publishing Corporation, New York, 421 pp.

van Olphen, H., 1977. *An Introduction to Clay Colloid Chemistry.* John Wiley, New York, 318 pp.

Winterkorn, H.F., 1947. *Fundamental similarities between electro-osmotic and thermo-osmotic phenomena.* Proceedings Highway Research Board, 27: 443 - 445.

Winterkorn, H.F., 1955. *Water movement through porous hydrophilic systems under capilary, electrical, and thermal potentials.* American Society for Testing Materials Special Technical Publication, 163: 27 - 35.

Yeung, A.T., 1990. *Coupled flow equations for water, electricity and ionic contaminants through clayey soils under hydraulic, electrical and chemical gradients.* Journal of Non-Equilibrium Thermodynamics, 15(3): 247 - 267.

Yeung, A.T. and Mitchell, J.K., 1993. *Coupled fluid, electrical and chemical flows in soil.* Geotechnique, 43(1): 121 - 134.

Yeung, A.T., 1994. *Effects of electro-kinetic coupling on the measurement of hydraulic conductivity.* In: D.E. Daniel and S.J. Trautwein (Editors), Hydraulic Conductivity and Waste Contaminant Transport in Soils. American Society for Testing and Materials, Philadelphia, pp. 569 - 585.

Chapter 2

Characterization of the sample materials

Abstract

The properties of three different clays, relevant for their semipermeability in the flow of fluids, electrical charge and solutes, were determined in the laboratory. Properties measured are e.g. mineralogical composition, specific surface area and cation exchange capacity. The three sample materials are a commercially available bentonite and two field clays. One, the Tertiary Boom Clay, originates from the Hades Underground Research Laboratory of SCK·CEN in Mol, Belgium; the other, the Holocene Calais Clay, is retained from the shallow subsurface of the polder Groot Mijdrecht, southeast of Amsterdam, The Netherlands. All clays investigated are found to have properties indicative for semipermeable behaviour.

2.1 Introduction

Water, electrical charge, solutes and heat flow through porous materials like e.g. soils and sediments. The laws of Darcy, Ohm, Fick and Fourier relate fluxes and conjugated gradients. Moreover, flows can also occur due to non-conjugated gradients. These coupled flows are significant in porous materials with a hydraulic conductivity of less than $1 \cdot 10^{-9}$ m/s (Mitchell, 1991). Commonly, compacted clays or clayey soils and sediments have such a low hydraulic conductivity. So, coupled flow phenomena may occur in these media.

One example of such coupled flows is chemical osmosis, a water flow induced by a concentration gradient. The occurrence of chemical osmosis in clayey materials was demonstrated many times in laboratory experiments (Letey and Kemper, 1969; Fritz and Marine, 1983; Malusis et al., 2001; Keijzer and Loch, 2001) and in the field (Neuzil, 2000). In this case, the clay acts as a semipermeable membrane by restricting the passage of solutes during the passage of water through the clay. The capability of a clay layer to act as a semipermeable membrane depends on several properties of the clay, e.g. the cation exchange capacity (CEC) and the cation occupation of the exchange complex.

To study coupled transport phenomena in clays, three different clayey materials were chosen, one commercially available bentonite and two field clays. First of all, it will be determined whether the clays are suitable for these experiments, i.e. whether or not they have semipermeable properties. Therefore, several standard laboratory analyses were performed to characterize these clays.

2.2 Description of the sample materials

2.2.1 Bentonite

The term bentonite was first employed by Knight (1898) describing a particular plastic and highly swelling clay, who named this clay after Fort Benton, Montana, which is close to the place of first retrieval. Bentonite is formed by the alteration of eruptive igneous rocks, usually tuffs and volcanic ash. The principal constituents are montmorillonite and beidellite; however, bentonite can also contain small amounts of cristobalite, zeolites, biotite, quartz, feldspar and zircon (Deer et al., 1985).

Two major varieties can be distinguished based on the major cation on the exchange complex. In Wyoming bentonite, Na^+ is the predominant exchangeable cation. This is a highly swelling type and traditionally used in drilling fluids and more recently for low permeable barriers for waste disposal sites. Ca^{2+} is the predominant exchange cation in the low- or non-swelling type, which is often used as filling agent or cleaning agent (Hosterman and Patterson, 1992).

Due to its expected semipermeable properties, a natural sodium bentonite was used in this project as a reference material. The bentonite is commercially available and sold as Portaclay A90 (Ankerpoort, Maastricht, The Netherlands). It was supplied as an air-dry powder and used without any pretreatment.

2.2.2 Boom Clay

The Boom Clay is a Tertiary (Oligocene) formation extending in northeastern Belgium. It crops out along a west-east line from the Scheldt estuary area in the west along the Rupel river and the Demer river to the Meuse river in the east and is slightly dipping to the northeast with a slope of 1 – 2%. Its thickness is increasing towards the northeast reaching about 102 m in the Mol area, northern Belgium.

The Boom Clay separates the overlying Neogene sandy sediments from the deeper sandy and clayey layers forming several aquifers and aquitards (Aertsens et al., 2004). The Boom Clay was deposited by the sea, which occupied a large part of northern Europe 30 – 36 Ma ago (Beaucaire et al., 2000). It is characterized by its banded structure essentially found in the alternation of siltier and more clayey beds of several decimeters thickness. The contrast between these beds is enhanced by the presence of bituminous organic matter accentuating the dark clay beds. Whereas organic matter is present essentially in the upper part of the formation, calcareous horizons, often with calcareous concretions called septaria, are distributed through the whole formation (Aertsens et al., 2004).

The Boom Formation can be divided into three stratigraphic units. They are, from the basis to the top, the Belsele-Waas Member, which is the siltiest part of the Boom Clay, the Terhage Member, which is characterized by pale grey clay and comprised the lowest proportion of coarser particles, and finally, the Putte Member, which is characterized by dark clay and the systematic presence of organic matter. On top of the Putte Member, the upper part of the Boom Formation, which is siltier, is deposited. It is called the 'Transition Zone' (Vanderberghe et al., 2001; Aertsens et al., 2004).

In the stratigraphic sequence of the Boom Clay Formation, climatically driven sea-level fluctuations at different scales ranging from Milankovitch orbital cycles to third-order eustacy cycles can be recognized. The sharp boundary between the grey Terhagen Member and the overlying black Putte Member indicates the initiation of suboxic conditions at the sea bottom (Laenen, 1998) and

must represent a widespread sudden paleogeographic event (Vanderberghe et al., 2001).

The Boom Clay sample investigated in this project originates from the Rupelian Putte Member from the upper part of the Boom Clay profile. The sample is taken during excavation works of the connexion gallery between the second shaft and the Test drift of the Hades Underground Research Laboratory from SCK·CEN in Mol, Belgium, in February 2002. The depth of the connexion gallery is 223 m below the ground level at Mol. After excavation, the clay was immediately packed in an aluminium-coated polyethylene foil under vacuum to avoid pyrite oxidation and desiccation. The clay was kept at 4°C to minimize microbial growth before it was transported to our laboratory. Here, the Boom Clay was air-dried and grounded in an agate mortar before analysis. Although in-situ conditions were anaerobic, no pyrite oxidation or acidification was observed.

2.2.3 Calais Clay

The Calais Clay, here sampled from the polder Groot Mijdrecht southeast of Amsterdam, The Netherlands, is a Holocene sediment. It is deposited on top of a Pleistocene coversand, an aeolian sediment from the Würm- or Weichsel-iceage and a following peat layer which was formed during the first stage of transgression.

During the rise of the sea level that continued during Atlanticum and early Subboreal, salt tidal sediments consisting of clay layers and more silty parts, the so-called deposits of Calais (de Jong, 1960), were deposited. In regression periods, peat layers were formed, which are intercalated in the marine sediments. In the polder Groot Mijdrecht, two phases of sedimentation of Calais Clay can be distinguished. The first deposits belong to the Watergraafsmeer deposits consisting of black clay sediments of brackish conditions with some sandy parts intercalated. Thereafter, the Wieringermeer deposits with a higher content of clay and less carbonate were deposited in a mudflat environment (Pons and Wiggers, 1959).

After 2200 BC, no further transgression took place. The environment changed to a more fresh-water environment due to riverine water flowing into the area. Subsequently, a significant peat layer formed on top of the Calais Clay (Bennema, 1949). In the 19th and 20th century, the peat layer was dug off, so that from then on, the clay occurred in a quite shallow position. Moreover, man lowered the groundwater level by pumping to reclaim land (Stichting voor Bodemkartering, 1970). At positions where subsequently oxidation is taking place, the Calais Clay can form 'acid sulphate soils'. Due to the large amount of organic matter and the salty or brackish condition, pyrite accumulated in the sediment. Under anaerobic conditions, soil bacteria reduce sulphate to sulphide-compounds. But if the soil is drained, sulphide is oxidized to sulphate and acid reacting sulphate precipitates like jarosite form. The degree in which this acidification takes place is dependent on the amount of alkaline cations at the exchange complex and carbonate in the soil, which will buffer the reaction until they are consumed (Poelman, 1966). A Calais Clay under anaerobic conditions with only a small amount of alkaline cations is called 'potential acid sulphate soil'.

The Calais Clay sample employed in this study originates from the northwestern part of the polder Groot Mijdrecht near Nessersluis from a depth of 1.6 – 1.8 m. In the grassland, the groundwater table is so high that the clay is fully water-saturated and in anaerobic conditions. Consequently, the clay is a potential acid sulphate soil because many yellow spots of acid reacting sulphate precipitates were formed during air-drying in the laboratory. Thereafter, the sample was grounded in an agate mortar and large pieces of organic material were removed in doing so before analysis.

2.3 Analytical methods

2.3.1 Mineralogy

The mineralogical composition of the three clays was determined with XRD analysis. X-ray diffractograms (XRD – Philips PW1710, CuKα radiation and Ni filter) were made of untreated powder samples without texture and of oriented samples after the removal of carbonates and organic matter.

2.3.2 Particle size distribution

The particle size distribution was determined with a Malvern Particle Sizer 2600 after removal of carbonates and organic matter and without any pretreatment with respect to the dispersion of the clay.

2.3.3 Specific surface area

The specific surface area was determined by sorption of ethylene glycol monoethyl ether (EGME). This method is favoured over the BET-N_2 method because it is more appropriate for clay-rich materials as EGME also adsorbs at the interparticle surfaces and therefore yields the total specific surface area. It is conceivable that already a small percentage of clay particles in the sample can contribute significantly to the specific surface area, which is accessible to solutes in aqueous phase (Ball et al., 1990).

After drying of the samples above P_2O_5, EGME was added and the samples were placed under vacuum above anhydrous $CaCl_2$ for 18 days and weighed to determine the retention of EGME on the surface area (van Reeuwijk, 1995).

2.3.4 Cation exchange capacity and cation occupation of the exchange complex

The cation exchange capacity (CEC) and the cation occupation of the exchange complex are strongly influencing the swelling and semipermeable behaviour of the clay. The cation occupation was determined by extraction with 0.01 M $BaCl_2$. The CEC was identified after a following extraction with 0.02 M $MgSO_4 \cdot 7H_2O$ according to Houba et al. (1995). After extraction, the cation concentrations in the supernatant solutions were measured using Inductively Coupled Plasma Optical Emission Spectrometry (ICP-OES, Spectro Ciros^{CCD}).

2.3.5 Carbonate content

The carbonate content was determined with the Scheibler method (Williams, 1948). Thereby, the samples were mixed with 1 M HCl and the release of CO_2 was measured volumetrically.

2.3.6 Organic carbon content

The organic carbon content was determined as loss of ignition by combustion in a sulphur/carbon analyzer (SC-144DR, Leco Corporation).

2.3.7 pH

Especially for the natural field samples, the pH is of interest because it indicates the degree of decomposition of the clay. pH values were measured after shaking the untreated samples in demineralized water for 24 hours with a Sentron Argus pH meter.

2.3.8 Flocculation value

The flocculation value is of particular importance with respect to the structure of clay. It was determined in a flocculation series test as described by van Olphen (1977). In a series of tubes, different NaCl concentrations were added to clay suspensions. The suspensions were mixed by shaking overnight, after which the tubes were allowed to stand. Settling rates, as determined by visual inspection of the position of the interface between sediment and clear supernatant water, were monitored up to 15 weeks. The flocculation value is the salt concentration marked by a sharp increase in settling volume. Accordingly, a flocculation value range is identified.

2.4 Results and discussion

All physical and chemical properties determined of the three clay samples, except the mineralogical composition, are listed in Table 2.1.

2.4.1 Mineralogy

The X-ray diffractograms show that the bentonite mainly consists of montmorillonite and some traces of illite and quartz (Fig. 2.1). Other mineral phases that might be expected like e.g. feldspar were not detected (Deer et al., 1985). In the Boom Clay, illite, smectite, kaolinite and some quartz were found (Fig. 2.2). This is in good agreement with quantitative analysis reported in literature where 60% clay minerals and 20% quartz were detected in Boom Clay. However, feldspar, pyrite or siderite, which might be expected, were not found (Bernier et al., 1997; Aertsens et al., 2004). For the Calais Clay, no literature data on the mineralogical composition were available. The main phases detected in the X-ray diffractograms are also illite, smectite, kaolinite and quartz (Fig. 2.3). If we compare the mineralogical composition of the three sample materials, we see that the main constituents are identical, but the proportions are varying.

2.4.2 Particle size distribution

The particle size distributions of the three sample materials are fairly similar. The main fraction of all samples is in the range of 2 – 60 μm. The percentage of particles < 2 μm decreases from the bentonite (14.96%) and the Boom Clay (12.56%) to the Calais Clay (9.15%). It is assumed that the reason for the dominance of the silt fraction is due to tactoid formation and clustering of the clay particles. Apparently, the clay is not well dispersed, since measurements were performed in aqueous solution without addition of dispersing agents.

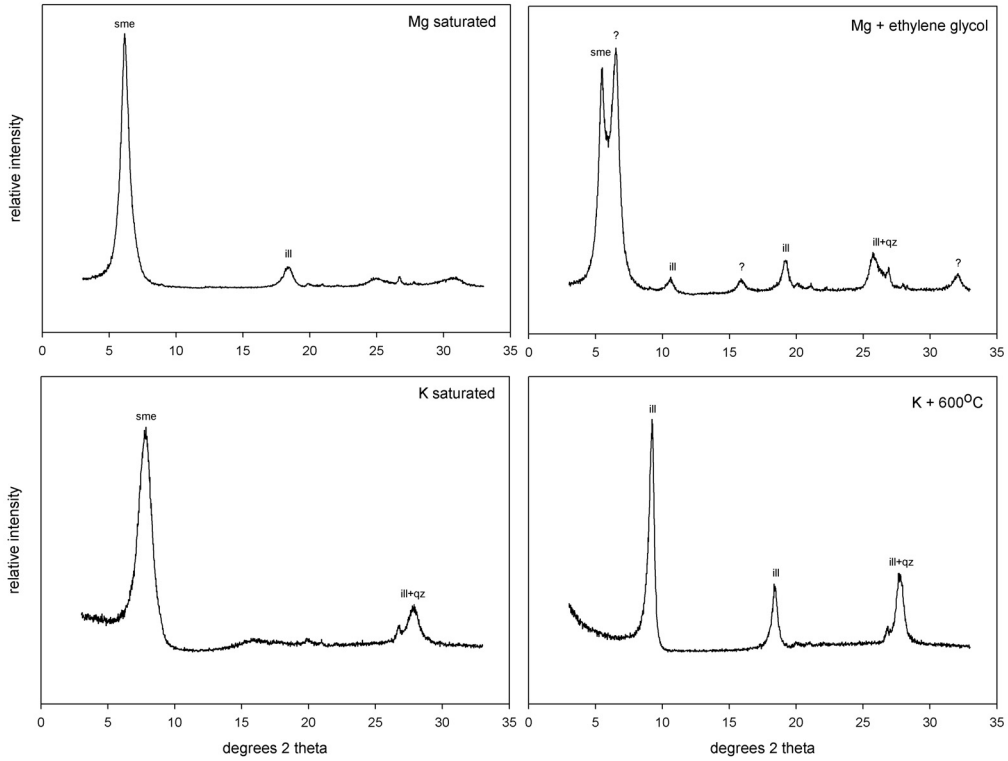

Figure 2.1: X-ray diffractograms of the pretreated oriented bentonite with designation of the different peaks to the minerals (ill = illite, kao = kaolinite, sme = smectite, qz = quartz).

2.4.3 Specific surface area

Values for the specific surface area reported in literature range from 10 – 20 m^2/g for kaolinite to up to 840 m^2/g for montmorillonite (Mitchell, 1993). The specific surface areas measured with the ethylene glycol monoethyl ether (EGME) method, which also includes the interlayer surfaces, are 611 m^2/g for the bentonite, 129 m^2/g for the Boom Clay and 88 m^2/g for the Calais Clay. This gradation is in good agreement with mineralogical composition. However, the measured values are at the lower end of the reported literature values (Mitchell, 1993; Petersen et al., 1996).

2.4.4 Cation exchange capacity and cation occupation of the exchange complex

The CEC of the bentonite was determined around 76 $cmol_c/kg$. The CECs of the two other clays are lower, respectively 23 $cmol_c/kg$ for the Boom Clay and 14 $cmol_c/kg$ for the Calais Clay. This is low compared to literature values for bentonite, 80 – 150 $cmol_c/kg$, and illite, 10 – 40 $cmol_c/kg$ (Mitchell, 1993). However, these low CEC-values correspond well with the small specific surface areas. Churchman and Burke (1991) established a clear correlation between the CEC and the specific surface area.

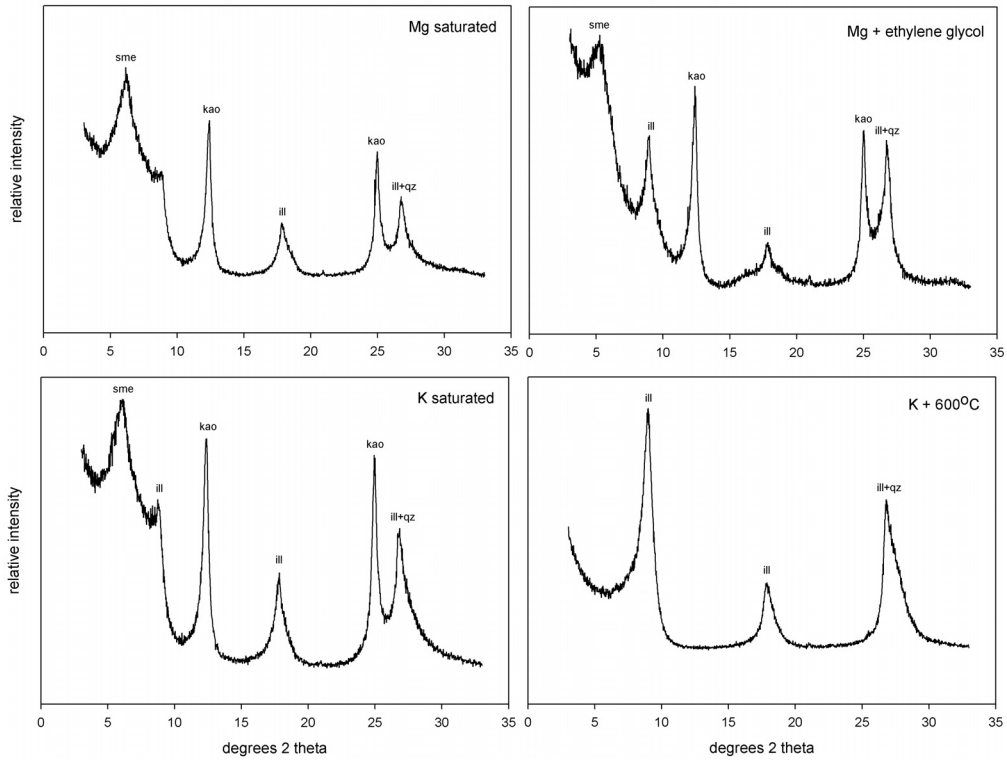

Figure 2.2: X-ray diffractograms of the pretreated oriented Boom Clay with designation of the different peaks to the minerals (ill = illite, kao = kaolinite, sme = smectite, qz = quartz).

For the bentonite, the dominant cation on the exchange complex was identified as Na^+ (53 $cmol_c/kg$) followed by Ca^{2+} (27 $cmol_c/kg$) and only small amounts of Mg^{2+} and K^+ (8 and 2 cmolc/kg, respectively). For the Boom Clay, also Na^+ was identified as main cation on the exchange complex (11 $cmol_c/kg$), but almost as much Ca^{2+} (11 $cmol_c/kg$) was found. Also here, only small amounts of Mg^{2+} (7 $cmol_c/kg$) and K^+ (4 $cmol_c/kg$) were detected. The main cation in the Calais Clay is Ca^{2+} with 12 $cmol_c/kg$, followed by Mg^{2+} (9 $cmol_c/kg$) and Na^+ (4 $cmol_c/kg$) and only a small amount of K^+ (1 $cmol_c/kg$). Ideally, the sum of the cations for each sample should add up to the value of the CEC. But in all samples, the sum of the cations is higher than the CEC. It is assumed that this is a result of the method used. Determinations were carried out in the presence of carbonate in the clays. Part of the measured cations might therefore originate from the carbonates and not from the exchange complex of the clay particles.

2.4.5 Carbonate content

The carbonate content is highest in the Boom Clay and the lowest in the Calais Clay. The very low carbonate content in the oxidized Calais Clay, compared to non-oxidized field material, is a result of acidification during oxidation. Most of the carbonate was already consumed by reaction with acid sulphate precipitates.

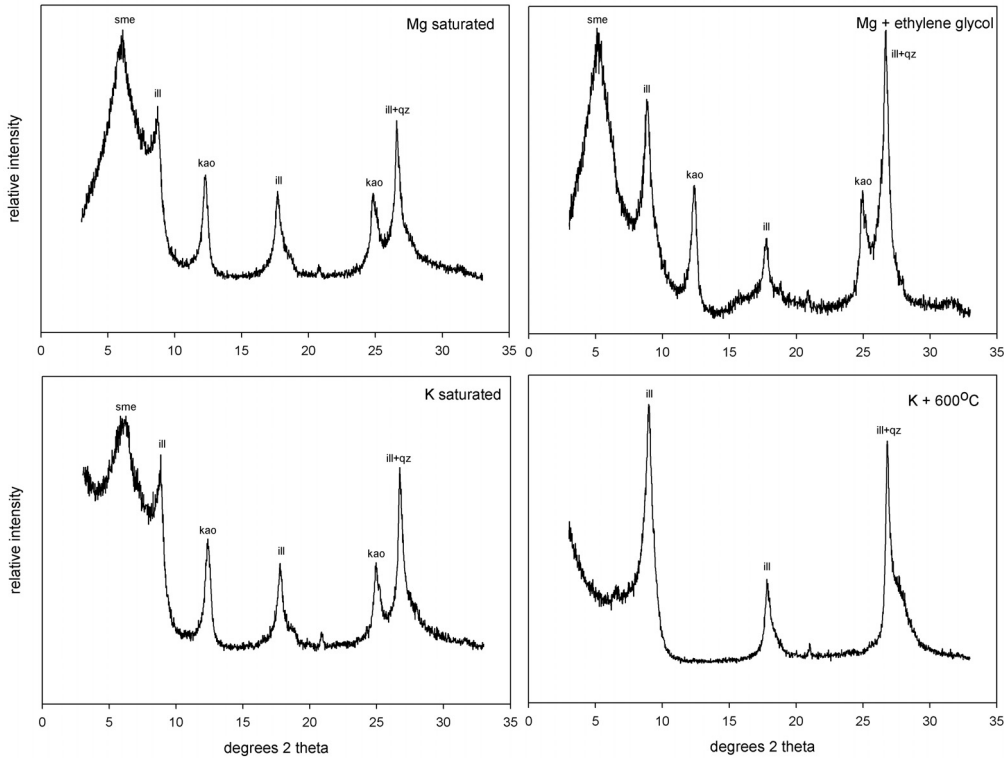

Figure 2.3: X-ray diffractograms of the pretreated oriented Calais Clay with designation of the different peaks to the minerals (ill = illite, kao = kaolinite, sme = smectite, qz = quartz).

2.4.6 Organic carbon content

The measured organic carbon content is an indication for the amount of organic matter present in the samples. It is highest in the Calais Clay and lowest in the bentonite. This is expected as organic matter usually is not present in bentonite, and the Calais Clay is assumed to be rich in organic matter due to intercalated peat layers and vegetation incorporated into the upper part of the soil column.

2.4.7 pH

The pH values measured correspond with the carbonate contents. Extremely high pH values were observed for the bentonite and the Boom Clay (10 and 9, respectively), whereas an acid pH of 3 was measured in the Calais Clay. This acid pH of the Calais Clay clearly demonstrates the acidification taken place during oxidation by drying and is visual by the yellow acid reacting sulphate precipitates that formed. Although the Boom Clay was exposed to oxygen in the same time as well, acidification was not measurable. No acid reacting sulphate precipitates were observed. The measured pH is close to values reported in literature of 8.5 (Maes et al., 1998, 1999). The bentonite is alkaline and not expected to acidify under aerobic conditions at all.

Table 2.1: Sample properties of the three clays, except the mineralogical composition.

			bentonite	Boom Clay	Calais Clay
particle size fraction	> 60 µm	%	3.14	0.87	0.86
	2 — 60 µm	%	81.9	86.55	89.99
	< 2 µm	%	14.96	12.58	9.15
specific surface area	EGME[1]	m^2/g	611 ± 9	129 ± 9	88 ± 8
cation exchange capacity		$cmol_c/kg$	75.7 ± 2.8	22.9 ± 3.0	14.0 ± 0.4
cation occupation by	Na^+	$cmol_c/kg$	53.0 ± 1.9	11.2 ± 0.2	3.5 ± 0.2
	K^+	$cmol_c/kg$	1.5 ± 0.1	3.6 ± 0.1	1.0 ± 0.0
	Ca^{2+}	$cmol_c/kg$	26.6 ± 0.6	10.7 ± 0.2	11.6 ± 0.4
	Mg^{2+}	$cmol_c/kg$	7.8 ± 0.0	7.2 ± 0.2	9.0 ± 0.2
carbonate content		wt%	0.63	2.76	0.29
C_{org} content		wt%	0.13	1.26	3.69
pH			10	9	3
flocculation value range		M NaCl	0.00 — 0.02	0.00 — 0.02	0.02 — 0.04

[1] ethylene glycol monoethyl ether

2.4.8 Flocculation value

The flocculation value determined with a flocculation series test yields a concentration range in which the actual flocculation value is located (van Olphen, 1977). The flocculation value range for the bentonite and the Boom Clay is between 0.00 – 0.02 M NaCl and for the Calais Clay between 0.02 – 0.04 M NaCl. The flocculation value is predominantly dependent of the valence of the cation. In literature, flocculation values for monovalent cations are reported to be 0.025 – 0.15 M (van Olphen, 1977).

The importance of the flocculation value for the structure of the clay is discussed in detail by Heister et al. (2004).

2.5 Conclusions

The bentonite has the highest amount of swelling clay minerals, the highest specific surface area and the highest CEC with Na^+ as the dominant cation on the exchange complex. The Boom Clay has less clay minerals and also a smaller specific surface area and CEC with Na^+ as the dominant cation. The Calais Clay has the lowest content of clay minerals, the lowest specific surface area and CEC. Moreover, the Calais Clay is acidified and acid reacting sulphate precipitates were formed.

Together with the highest content of organic carbon of the three clays, this leads to the conclusion that the Calais Clay has the highest impureness. Other analyses like carbonate content underline this.

From the analysis it is assumed that all three clay samples could show semipermeable behaviour regarding the flows of fluids, electrical charge and solutes. All clays investigated are found suitable for experiments on coupled flow phenomena. It is presumed that the bentonite will exhibit the most semipermeable behaviour, whereas the Calais Clay will show least semipermeable behaviour.

Acknowledgements

We thank Dr. Pierre De Cannière and his colleagues from SCK·CEN in Mol, Belgium for collaboration and providing us with Boom Clay material.

We also like to thank Ana Maria Garavito and her colleagues at the Vrije Universiteit of Amsterdam, The Netherlands, who provided us with Calais Clay material.

References

Aertsens, M., Wemaere, I. and Wouters, L., 2004. *Spatial variability of transport parameters in the Boom Clay.* Applied Clay Science, 26: 37 - 45.

Ball, W.P., Buehler, C., Harmon, T.C., Mackay, D.M. and Roberts, P.V., 1990. *Characterization of a sandy aquifer material at the grain scale.* Journal of Contaminant Hydrology, 5: 253 - 295.

Beaucaire, C., Pitsch, H., Toulhoat, P., Motellier, S. and Louvat, D., 2000. *Regional fluid characterisation and modelling of water-rock equilibria in the Boom clay Formation and in the Rupelian aquifer at Mol, Belgium.* Applied Geochemistry, 15: 667 - 686.

Bennema, J., 1949. *Het oppervlakteveen in West-Nederland.* Boor en Spade, 3: 139 - 149.

Bernier, F., Volckaert, G., Alonso, E. and Villar, M., 1997. *Suction-controlled experiments on Boom clay.* Engineering Geology, 47: 325 - 338.

Churchman, G.J. and Burke, C.M., 1991. *Properties of subsoils in relation to various measures of surface area and water content.* Journal of Soil Science, 42: 463 - 478.

de Jong, J.D., Hageman, B.P. and van Rummelen, F.F.F.E., 1960. *De holocene afzettingen in het deltagebied.* Geologie en Mijnbouw, 39: 654 - 660.

Deer, W.A., Howie, R.A. and Zussman, J., 1985. *An Introduction to the Rock-Forming Minerals.* Longman, Harlow, Essex, UK, 528 pp.

Fritz, S.J. and Marine, I.W., 1983. *Experimental support for a predictive osmotic model of clay membranes.* Geochimica et Cosmochimica Acta, 47: 1515 - 1522.

Heister, K., Keijzer, T.J.S. and Loch, J.P.G., 2004. *Stability of clay membranes in chemical osmosis.* Soil Science, 169(9): 632 - 639.

Hosterman, J.W. and Patterson, S.H., 1992. *Bentonite and Fuller's Earth Resources of the United States.* U.S. Geological Survey Professional Paper, 1522, Washington, 45 pp.

Houba, V.J.G., van der Lee, J.J. and Novozamsky, I. (Editors), 1995. *Soil Analysis Procedures. Other Procedures. Soil and Plant Analysis. A Series of Syllabi, 5B.* Department of Soil Science and Plant Nutrition, Wageningen Agricultural University, Wageningen, The Netherlands.

Keijzer, T.J.S. and Loch, J.P.G., 2001. *Chemical osmosis in compacted dredging sludge.* Soil Science Society of America Journal, 65: 1045 - 1055.

Knight, W.C., 1898. *Bentonite.* Engineering and Mining Journal, 66(17): 491.

Laenen, B., 1998. *The geochemical signature of relative sea-level cycles recognised in the Boom Clay.* Aardkundige Mededelingen, 9: 61 - 82.

Letey, J. and Kemper, W.D., 1969. *Movement of water and salt through a clay-water system: Experimental verification of Onsager reciprocal relation.* Proceedings of the Soil Science Society of America,

33: 25 - 29.

Maes, N., Moors, H., De Cannière, P., Aertsens, M. and Put, M., 1998. *Determination of the diffusion coefficient of ionic species in Boom Clay by electromigration: Feasibility study.* Radiochimica Acta, 82: 183 - 189.

Maes, N., Moors, H., Dierckx, A., De Cannière, P. and Put, M., 1999. *The assessment of electromigration as a new technique to study diffusion of radionuclides in clayey soils.* Journal of Contaminant Hydrology, 36: 231 - 247.

Malusis, M.A., Shackelford, C.D. and Olsen, H.W., 2001. *A laboratory apparatus to measure chemico-osmotic efficiency coefficients for clay soils.* Geotechnical Testing Journal, 24(3): 229 - 242.

Mitchell, J.K., 1991. *Conduction phenomena: From theory to geotechnical practice.* Geotechnique, 41(3): 229 - 340.

Mitchell, J.K., 1993. *Fundamentals of Soil Behavior.* John Wiley & Sons, New York, 437 pp.

Neuzil, C.E., 2000. *Osmotic generation of 'anomalous' fluid pressures in geological environments.* Nature, 403: 182 - 184.

Petersen, L.W., Moldrup, P., Jacobsen, O.H. and Rolston, D.E., 1996. *Relations between specific surface area and soil physical and chemical properties.* Soil Science, 161(1): 9 - 21.

Poelman, J.N.B., 1966. *De Bodem van Utrecht, Toelichting bij Blad 6 van de Bodemkaart van Nederland, Schaal 1:200.000.* Stichting voor Bodemkartering, Wageningen, The Netherlands, 107 pp.

Pons, L.J. and Wiggers, A.J., 1959. *De holocene wordingsgeschiedenis van Noordholland en het Zuiderzeegebied.* Tijdschrift van het Koninklijk Nederlandsch Aardrijkskundig Genootschap, 76: 104 - 152.

Stichting voor Bodemkartering, 1970. *Toelichting bij Kaartblad 31 Oost Utrecht.* Bodemkaart van Nederland, Schaal 1:50.000, Wageningen, The Netherlands, 153 pp.

van Olphen, H., 1977. *An Introduction to Clay Colloid Chemistry.* John Wiley, New York, 318 pp.

van Reeuwijk, L.P. (Editor), 1995. *Procedures for Soil Analysis.* Technical Paper, 9. International Soil Reference and Information Centre, Wageningen, The Netherlands.

Vandenberghe, N. et al., 2001. *Stratigraphical correlation by calibrated well logs in the Rupel Group between North Belgium, the Lower-Rhine area in Germany and Southern Limburg and the Achterhoek in The Netherlands.* Aardkundige Mededelingen, 11: 69 - 84.

Williams, D.E., 1948. *A rapid manometric method for the determination of carbonate in soils.* Proceedings of the Soil Science Society of America, 13: 127 - 129.

Chapter 3

Stability of clay membranes in chemical osmosis*

Katja Heister, Thomas J.S. Keijzer and J.P. Gustav Loch

Abstract

In an earlier study on chemical osmosis in clay membranes, a slow dissipation of the osmotically induced hydraulic pressure difference was observed. This non-ideal behaviour of the clay as a semipermeable membrane was explained by diffusion of salt through the clay as a result of the imposed salt concentration gradient. In addition, it was postulated that diffusion of salt causes shrinkage of the electrical double layers of the clay platelets, enhancing flocculation and making the clay more permeable.

In the present study, experiments were performed to investigate the flocculation and hydraulic permeability behaviour of a bentonite when permeated by gradually increasing salt solutions. The flocculation value was determined by flocculation series tests with NaCl solutions at different clay suspension densities. The tests show that the Na-montmorillonite used has a flocculation value below 0.02 M NaCl.

Hydraulic conductivity experiments were conducted using a flexible-wall permeameter with NaCl solutions of different ionic strengths on a clay sample with a thickness of approximately 2 mm. During the experiments, an overburden pressure of 4 bar was applied to prevent swelling. For all NaCl solutions used, both above and below the flocculation value, the hydraulic conductivity stayed constant with values of approximately $2.3 \cdot 10^{-12}$ m/s. This implies that flocculation does not take place in osmosis experiments, and shrinkage of the diffuse part of the electrical double layers of the clay platelets seems to be compensated for by the overburden pressure. Therefore, the dissipation of an osmotically induced hydraulic pressure difference is more likely to be explained by diffusion of salt through the clay.

Keywords
bentonite, clay membrane, diffuse double layer, flexible-wall permeameter, flocculation, salt

3.1 Introduction

Flocculation behaviour is of importance in several applications of clay. Clay suspensions are known to flocculate when salt is added beyond a definite amount. However, it is not clear how a consolidated clay layer reacts when in contact with fluids of ionic strength above the flocculation value of the clay.

* Heister, K., Keijzer, T.J.S. and Loch, J.P.G. 2004. Stability of clay membranes in chemical osmosis. Soil Science 169 (9): 632 – 639.

Quirk and Schofield (1955) determined electrolyte concentration threshold values below which the permeability of the tested soils decreased. They explained the decrease in permeability by swelling of the clay, resulting in the blocking of larger conducting pores. Mesri and Olson (1971) concluded that the most important variable determining the permeability of clays is the degree of flocculation of the clay particles, which influences the distribution of void sizes and shapes. At low electrolyte concentrations, the clay platelets have a tendency to disperse uniformly through the available space, leading to channels that are almost all the same size.

In recent years, much attention has been paid to the hydraulic conductivity of geosynthetic clay liners (GCL), the main component of which is bentonite. Geosynthetic clay liners are used in sealing applications like landfill systems where they can make contact with waste leachates of high ionic strength. In the laboratory, Petrov et al. (1997) noticed increasing hydraulic conductivity, caused by a more flocculated clay fabric, which resulted in an increase in 'effective' pore space. Petrov and Rowe (1997) observed that this hydraulic conductivity is dependent on three main factors: the void ratio, the concentration of the permeant salt solution and the initial clay fabric. Concentrated salt solutions have the potential to promote face-to-face flocculation and domain formation of the clay platelets. Egloffstein (2001) reported increasing hydraulic conductivities of GCLs in landfill capping systems, which he attributed to the ion concentration of the leachates that cause e.g. ion exchange reactions. During a laboratory experiment on chemical osmosis in clays, Keijzer and Loch (2001) observed a slow dissipation of the osmotically induced pressure difference. They attributed this non-ideal behaviour of the clay membranes to diffusion of salt, decreasing the osmotic gradient and reducing the osmotic water flux. In addition, it was postulated that increasing salt concentration by diffusion enhances flocculation and makes the clay membrane more permeable.

The minimum salt concentration that causes flocculation or coagulation of a suspension is called the flocculation value. It can be measured in a simple flocculation series test (van Olphen, 1991), and is dependent on the type of the clay and the valence of the cations of the salt. In this study, the flocculation and hydraulic conductivity behaviours of a compacted bentonite layer, when permeated by gradually increasing salt solutions, were investigated. Both types of tests were performed on commercially available Na-montmorillonite and NaCl solutions in order to avoid the influence of the valence of the cation. The flocculation series test was repeated with different clay concentrations ranging from 0.06 wt% to 2 wt% inasmuch as the solid concentration is expected to affect the behaviour of the suspension (Kotlyar et al., 1996). The hydraulic conductivity tests were performed under overburden pressure on compacted clay samples using NaCl solutions of increasing ionic strength. The hydraulic conductivity is regarded as a measure of the state of the clay structure. For the discussion, it is assumed that the clay is homogeneously dispersed. However, in reality, a consolidated clay like this will not be homogeneously dispersed but will have a microstructure with packets of clay particles and wider pores filled with a clay gel (Pusch and Weston, 2003; Yong, 2003). Therefore, what is discussed here as processes in a homogeneous gel may actually apply to a network of clay gel.

3.2 Theoretical background

The negative surface charge of smectite-type particles is balanced by an accumulation of counter-ions at the surface. The charged surface and the distributed charge in the adjacent water film are

together termed the diffuse double layer. The classical Gouy-Chapman theory provides a model for ion distributions and double layer thickness.

In suspensions, the clay platelets surrounded by the diffuse layers of counter-ions are repelled from each other by electrostatic forces. In a compacted clay, however, the double layers of adjacent clay platelets may overlap. Because of the small pore sizes and the electrical fields within them, the passage of ions and molecules through a compacted clay layer is restricted. Thus, the clay exhibits membrane properties, giving rise e.g. to chemical osmosis (Fritz and Marine, 1983; Fritz, 1986; Mitchell, 1993).

The thickness of the double layer according to the Gouy-Chapman theory is sensitive to variations in electrolyte concentration, cation valence, the dielectric constant of the solution and temperature (Mitchell, 1993). At constant surface charge, increasing the concentration in the equilibrium solution or increasing the valence of the counter-ions results in compression of the double layer.

Although compacted clay layers act as semipermeable membranes, in natural systems, this semipermeability is seldom ideal. The non-ideality of a membrane is expressed by the reflection coefficient, σ, which is defined as the ratio of the developed hydraulic pressure over the applied osmotic pressure at equilibrium, i.e. at zero solution flux (Katchalsky and Curran, 1967). An ideal membrane has a reflection coefficient of 1; no solutes can pass the membrane. In non-ideal membranes such as clay layers, the reflection coefficient varies between 0 and 1, depending on the type of clay, cation exchange capacity and exchangeable cations, compaction and salt concentration in the equilibrium solution. In non-ideal membranes, diffusion of solutes occurs in response to a chemical gradient. The resulting salt concentration increase will cause shrinkage of the double layers, further reducing the semipermeability of the clay membrane.

Below its flocculation value, sodium montmorillonite in dilute suspensions exists as particles typically containing two to three lamellae (van Olphen, 1991), whereas calcium montmorillonite exists in so-called tactoids or quasicrystals, each consisting of up to 10 clay platelets (Blackmore and Miller, 1961; Norrish and Quirk, 1954). In mixed Na-Ca montmorillonite systems, Ca^{2+} is on the interlayer surfaces between individual clay platelets and does not form a diffuse layer. Na^{+} is on the external surface (Shainberg and Otoh, 1968). In this case, the clay behaves like a system with a much lower particle surface area (Shainberg et al., 1971). Because of its location, exchangeable Na^{+} should have a large effect on flocculation of Na-Ca mixed systems because in these systems, flocculation depends on interactions between clay tactoids (Oster et al., 1980). At low solute concentration, the tactoids are repelled from each other by electrostatic forces (Abend and Lagaly, 2000).

At low clay concentrations, the clay particles can move freely through the suspension. When they encounter each other in a suspending medium at ionic strength above the flocculation value, they collide to form flocs. These flocs are large particles that are the result of the aggregation of smaller particles and have random structures (Logan and Wilkinson, 1990). With increasing salt concentration, the collision efficiency increases.

At high clay concentrations and in a suspending medium at an ionic strength greater than the flocculation value of the clay, the particles stick together immediately and form a voluminous gel. Within the gel, the particles are agglomerated by edge-to-face contact (cardhouse structure) in one single floc (van Olphen, 1991). Large amounts of the dispersing medium are enclosed in the network of the particles. A schematic summary of the various forms of clay agglomeration is given in Table 3.1.

At low salt concentrations, any interaction involves attraction between the edges and the faces of the clay platelets, whereas at higher salt concentrations, there is also attraction between the faces.

There is likely a continuous transition from edge-to-face structure, cardhouse structure, to face-to-face structure, so-called band-type structure (Abend and Lagaly, 2000). At high salt concentrations, the forces between the faces become strongly attractive and the particle network of the gel is contracted and disrupted. Consequently, distinct particles form that settle to a dense sediment.

3.3 Material and methods

A commercially available Wyoming bentonite, Ankerpoort Colclay A90™ batch 61203, was used in all experiments. This bentonite consists primarily of montmorillonite with only traces of quartz.

Table 3.1: The behaviour of clay suspensions.

	low clay concentration	high clay concentration
salt concentration below flocculation value	dispersed low settling rate *dense sediment*	dispersed low settling rate *dense sediment*
salt concentration above flocculation value	flocculated high settling rate *flocs*	flocculated very high settling rate *gel*

Table 3.2: Sample properties of the bentonite clay. Adapted from Keijzer (2000).

cation exchange capacity		$cmol_c/kg$	68.3 ± 1.3
cation occupation[1] by	Na^+	$cmol_c/kg$	48.4 ± 0.3
	K^+	$cmol_c/kg$	1.4 ± 0.1
	Ca^{2+}	$cmol_c/kg$	23.5 ± 0.9
	Mg^{2+}	$cmol_c/kg$	4.2 ± 0.2
organic matter content		wt%	0.20
carbonate content		wt%	0.79
particle density		g/cm^3	2.64
specific surface area	N_2-BET	m^2/g	47 ± 4
	EGME[2]	m^2/g	556 ± 13

[1] Cation exchange capacity and cation occupation are determined by two different methods. Therefore it is possible that sum of the base cation occupation is larger than the CEC as it is expected that some of the Ca^{2+} is due to the carbonate content of the bentonite.

[2] ethylene glycol monoethyl ether

Properties of the bentonite are given in Table 3.2.

The flocculation value was determined by a flocculation series test using visual inspection of the settling volumes (van Olphen, 1991). In a series of tubes, NaCl-concentrations of 0.00 M, 0.02 M, 0.04 M, 0.06 M, 0.08 M, 0.10 M, 0.12 M, 0.20 M, 0.40 M and 0.60 M were added to clay suspensions. The suspensions were mixed by shaking overnight, after which the tubes were allowed to stand. Settling rates, as determined by the position of the interface between sediment and clear supernatant water, were monitored for up to 15 weeks. The flocculation value is marked by a sharp increase in settling volume. The test was repeated with clay suspension densities of 0.06, 0.08, 0.1, 0.15, 0.2, 0.25, 0.5, 1 and 2 wt%.

To derive information about the degree of flocculation or dispersion in a compacted clay layer when in contact with fluids of different ionic strength, i.e. in an osmosis experiment, a clay sample (thickness approx. 2 mm, diameter 50 mm) was prepared and transferred into a flexible-wall permeameter for hydraulic conductivity measurements (Fig. 3.1). The flexible-wall permeameter was located in a cylindrical pressure cell (141 mm outer diameter, and 115 mm internal diameter) filled with de-aired water. An overpressure of approx. 4 bar was applied on the permeameter to prevent the clay from swelling. Falling head tests were conducted, whereby the water flow was measured gravimetrically at regular time intervals at a drainage port in the outflow reservoir. The first hydraulic conductivity experiment was performed on a clay sample prepared and flushed with tap water, subsequently flushed with a NaCl solution with the same ionic strength, and flushed thereafter with more concentrated NaCl solutions of 0.6 M and 1 M. Because of the low hydraulic conductivity and the duration of the experiments, a large hydraulic head gradient (between 327 and 149) was applied. A second experiment was performed on a clay prepared and flushed with deionized water and subsequently flushed with a 1 M NaCl solution. The gradient in this experiment varied from 132 for deionized water to 126 for the NaCl solution.

The hydraulic conductivity, k_h in m/s, was determined using Darcy's law:

$$J_w = k_h A \frac{\Delta p}{x} \qquad (3.1)$$

in which J_w is the measured water flux in m^3/s, A is the cross section of the sample in m^2, Δp is the applied hydraulic pressure difference in m solution across the sample, and x the thickness of the sample in m.

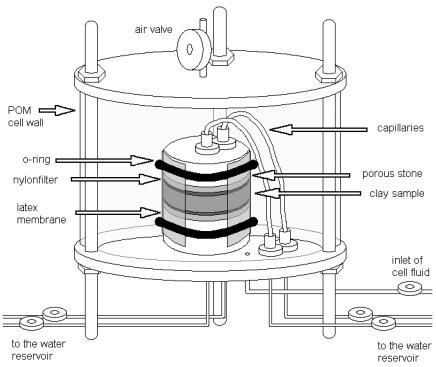

Figure 3.1: Schematic drawing of the flexible-wall permeameter within the pressure cell showing the position of the sample between the porous stones and the filters. Drawing not to scale.

3.4 Results and discussion

3.4.1 Flocculation tests

The suspension tubes were monitored at regular time intervals over a period of up to 15 weeks. After several weeks of standing, depending on the concentration of the solids, no further consolidation was observed. The derived flocculation value was between 0.02 M NaCl and 0.00 M NaCl for all clay concentrations. Figure 3.2 shows a typical example of a flocculation series test, where the flocculation value is marked by the sharp increase in settling volume at 0.02 M NaCl. Generally, flocculation values of clay in solutions of monovalent ions range between 25 and 150 mmol/l, and, in solutions of divalent ions, between 0.5 and 2.0 mmol/l (van Olphen, 1991). Because the bentonite is not sodium saturated and because it also contains calcium on the exchange complex, the flocculation value is somewhat lower than that for solutions with monovalent ions. Cation exchange will take place at the interlayer positions, freeing the Ca^{2+} to enter into the solution (Frenkel et al., 1978).

Depending on the clay and salt concentrations in the tubes, the suspensions showed different behaviours. In dilute suspensions and salt concentrations above or equal to 0.02 M NaCl, the clay

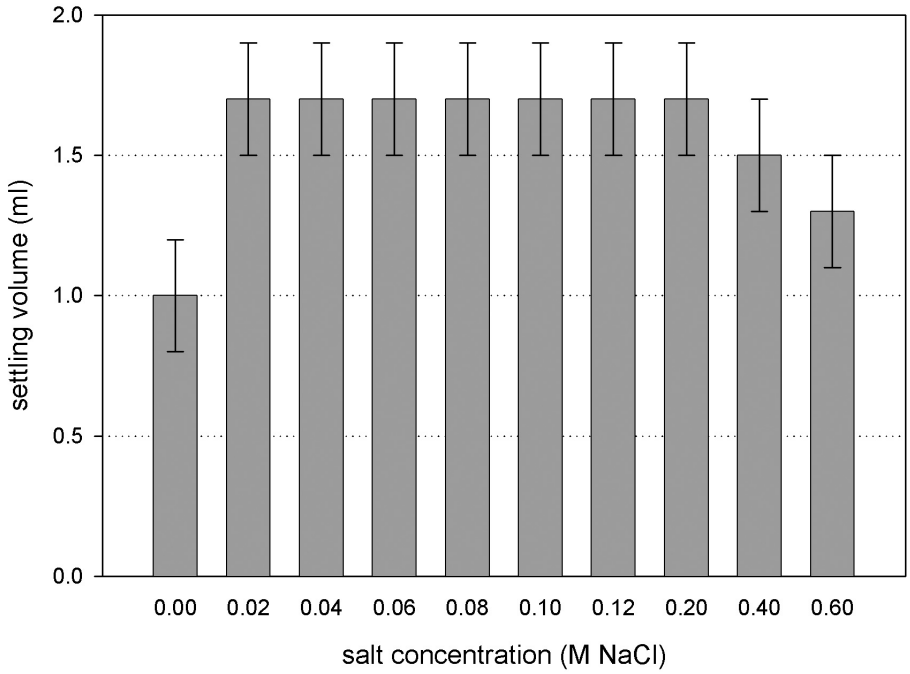

Figure 3.2: Result of a flocculation series test for a clay concentration of 0.08 wt%. The bars show the final settling volume in the tubes at the end of the experiment and the experimental error. There is a sharp increase in settling volume between 0.00 M and 0.02 M NaCl that marks the flocculation value. The volume of the sediment at 0.40 M and 0.60 M NaCl is obviously shrunken due to strongly attractive face-to-face structures at high salt concentrations.

platelets flocculated and settled slowly. In dense suspensions of a clay concentration ≥ 0.5 wt% and the same range of salt concentrations, the reaction time was very short, and a voluminous gel was formed that occupied almost the entire available volume of the suspension (Figs. 3.3 and 3.4). Settling of flocs or gelation was followed by slow consolidation.

There was a smooth transition between flocculation and gelation between 0.15 wt% and 0.5 wt%, where both flocculation and gelation occurred depending on the amount of electrolyte. In this transition zone, high electrolyte concentrations cause flocculation, whereas in low concentrated electrolytes, gelation occurs. Gelation was observed at clay concentrations above 0.5 wt%. The division in a flocculation phase at low concentrations and a gel phase at high clay concentrations is

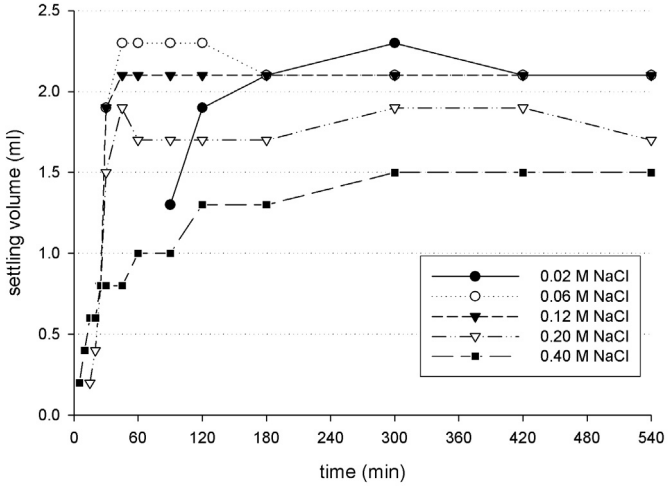

Figure 3.3: Settling velocity of a dilute clay suspension, 0.08 wt% clay concentration, showing typical curves for flocculation. The measurements started when a sharp sediment – water interface was observed.

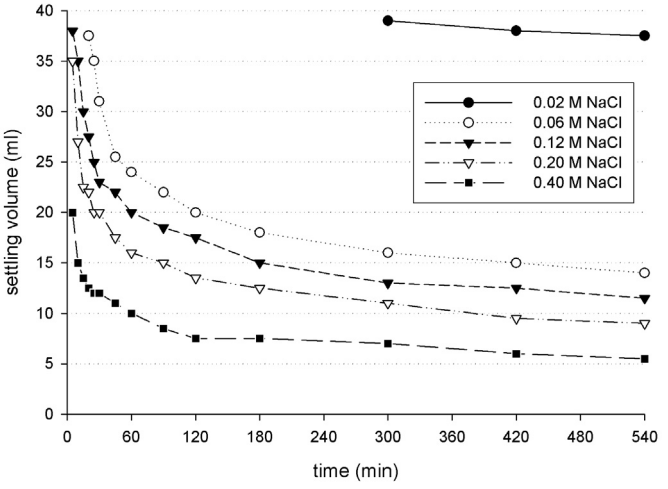

Figure 3.4: Settling velocity of a dense clay suspension, 1 wt% clay concentration, showing typical curves for gelation.

also proven by Monte Carlo model calculations. At a transitional stage, the flocs form a gel, which exhibits a nearly incompressible cardhouse network structure (Dijkstra et al., 1995).

The volume of the gel is sensitive to the salt concentration of the dispersing medium. With increasing amounts of salt, typically above 0.20 M NaCl, the volume of the gel decreased due to the strongly attractive forces that contract and disrupt the network of the clay particles (Fig. 3.2).

3.4.2 Hydraulic conductivity tests

The first hydraulic conductivity test was performed initially with tap water, then with increasing salt concentrations up to 1 M NaCl. After a start-up period with fluctuating hydraulic permeabilities and clay consolidation by the overburden load, the hydraulic conductivity reached a constant value, which did not change even if the solutions in the reservoirs were changed. Steady water flow was obtained after about 0.5 displaced pore volumes of the sample. The solutions were changed after two, three and four cumulative displaced pore volumes. The measured steady-state hydraulic conductivity for the clay had an average value of $2.3 \pm 0.9 \cdot 10^{-12}$ m/s. The data of this experiment are summarized in Table 3.3.

Table 3.3: Hydraulic conductivity of the clay sample during the first run.

used solution	hydraulic conductivity k_h (m/s)	cumulative displaced pore volumes	average gradient
tap water	$2.4 \pm 0.7 \cdot 10^{-12}$	2	327
0.357 M NaCl	$1.7 \pm 0.4 \cdot 10^{-12}$	3	162
0.6 M NaCl	$1.6 \pm 0.0 \cdot 10^{-12}$	4	175
1 M NaCl	$3.5 \pm 0.4 \cdot 10^{-12}$	6	149

Before installing the second sample – now with deionized water – into the permeameter, the clay was allowed to absorb much more water until saturation was reached. Applying the overburden pressure in the cell resulted in stronger consolidation of the sample compared with the first experiment. After reaching equilibrium, the hydraulic conductivity was in the same order of magnitude, $2.4 \pm 0.2 \cdot 10^{-12}$ m/s. After about six pore volumes were displaced by the permeate, the deionized water was replaced by 1 M NaCl. Subsequently, additional 12 pore volumes were displaced, but the hydraulic conductivity of the clay remained constant ($2.3 \pm 0.2 \cdot 10^{-12}$ m/s). This indicates clearly that the ionic strength of the solution does not influence the hydraulic conductivity of the clay under the applied overburden pressure (Fig. 3.5).

The unchanged hydraulic conductivity of clay samples below and above the flocculation value shows that the ionic strength of the solutions had no influence on the pore structure of the clay under the chosen experimental conditions. The effective pore size distribution – the effective pore size is defined as the size of the fraction of the pores that participates in water flow (Bear, 1979) – remained unchanged. This implies that flocculation or gelation, which would cause an increase in the hydraulic permeability, does not take place. The overburden pressure apparently dominates the structure and

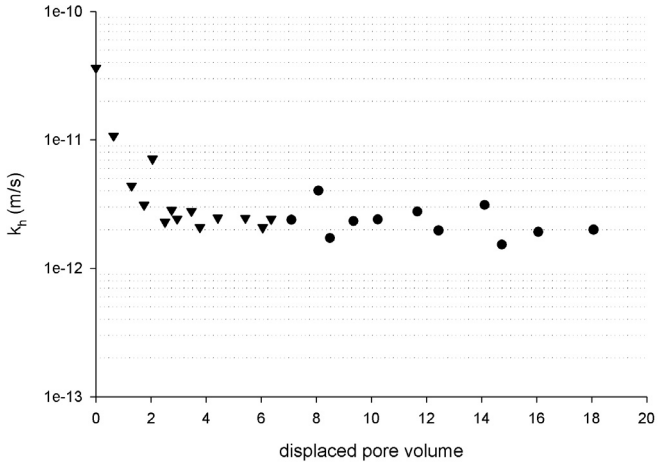

Figure 3.5: Hydraulic conductivity of the clay sample in the second experiment. The triangles show the development of the hydraulic conductivity with deionized water in the reservoirs. The bullets indicate the hydraulic conductivity with 1 M NaCl solution. After a start-up period, distinguishable by a decrease in hydraulic conductivity, a steady state was achieved. The hydraulic conductivity did not continue to change during the experiment although the solutions were changed.

behaviour of the clay. When a solution of sufficiently high electrolyte concentration enters the clay membrane, the extent of the double layers of the clay platelets decreases. When the double layers shrink in the presence of overburden pressure, further consolidation is encouraged. The samples were compacted immediately after the pressure was applied in the cell, resulting in a decrease in porosity. Measurements of the samples before and after the experiments show that the porosity had decreased, e.g. in the first experiment from 0.56 to 0.39.

The thickness of the double layer of a clay platelet can be calculated according to Mitchell (1993):

$$\frac{1}{\kappa} = \left(\frac{\varepsilon_0 \varepsilon k T}{2 n_0 e^2 v^2} \right)^{0.5} \qquad (3.2)$$

where $1/\kappa$ is the thickness of the double layer in m, ε_0 is the permittivity of vacuum, ε the dielectric constant of water, k the Boltzmann's constant, T the temperature, n_0 the electrolyte concentration in ions/m^3, and v the valence of the cation.

It is clear from this equation that the thickness of the double layer is dependent on the electrolyte concentration. In contact with deionized water and in the absence of overburden pressure, the double layers will swell to infinity. With increasing electrolyte concentration, the thickness of the double layer reduces from 5.1 Å at 0.357 M NaCl to 3.0 Å at 1 M NaCl. In the presence of overburden pressure, overlap will cause double layers to become truncated.

To verify that the double layers in the clay sample overlapped, the average pore size had to be calculated. For that purpose, it was assumed that the thickness of a clay platelet is 10 Å (Mitchell, 1993). Measurements show that only about half of the volume of a specimen is occupied by clay platelets. Assuming that all clay platelets are arranged parallel and are distributed uniformly throughout the specimen, an average pore size similar to the particle size, i.e. 10 Å, can be assumed (Yong, 2003). This is of the same order of magnitude as twice the calculated double layer thickness in the applied electrolyte concentration range. Thus, we infer that throughout the experiment the

pore space within the specimen is of the same magnitude as the double layer space and, therefore, overlapping of the double layers is possible.

This study indicates that as long as there is an overburden load on the clay, the clay platelets will approach each other to the same degree that their double layers shrink. This can be explained by means of the midpoint potential between the two truncated double layers of adjacent clay platelets. If the overburden pressure equals the swelling pressure of the clay at equilibrium, the swelling pressure will not change during the experiment because the overburden pressure is constant. According to Adamson (1990), the swelling pressure is directly related to the midpoint potential. Therefore, the midpoint potential also remains unchanged, which implies that the adjacent double layers approach each other to the same degree as they decrease in thickness. Apparently, the effective pore size distribution remains unchanged. At a given void ratio and low overburden load, Studds et al. (1998) observed an increase in effective porosity as a result of increasing solution strength. Dixon et al. (1985) suggested that the effective porosity of a clay is less than the total pore space because some of the pore space is occupied by surface or bound water, which has greater viscosity than free water. Double layer thickness decreases with increasing solution concentration. Consequently, at a given void ratio, the effective porosity of a clay will increase as the solution concentration increases. However, because the overburden load in this study was sufficient to compact the clay and reduce its void ratio upon increasing the salt concentration, the effective pore space may remain unchanged. The influence of flocculation or gelation on the distribution of pore sizes and shapes, as postulated by Mesri and Olson (1971), is apparently inhibited by the applied overburden pressure inasmuch as it does not influence the effective pore size distribution.

A very slight form of flocculation or tactoid formation cannot be excluded, however, but it will be too small to change hydraulic conductivity and effective pore size distribution. Locally reduced water flow caused by aggregation of some clay platelets will be compensated by pore widening elsewhere.

Accordingly, the dissipation of an osmotically induced pressure difference in the chemical osmosis experiments reported by Keijzer and Loch (2001) is more likely to be explained by diffusion, with the effect of reducing the salt concentration difference across the membrane (Fritz, 1986; Whitworth and Fritz, 1994). This could be proven by laboratory measurements of chemical osmosis in geosynthetic clay liners (Malusis et al., 2001). The overall effect is a net decrease in the chemico-osmotic pressure difference across the clay membrane, resulting in a decrease in the induced hydraulic pressure difference across the specimen. A rapid increase in osmotically induced hydraulic pressure difference, followed by a slight decrease, was also observed in a laboratory experiment by Elrick et al. (1976). The time required for the dissipation of the observed induced hydraulic pressure difference correlates well with the time required to achieve steady-state diffusion (Shackelford and Lee, 2003).

3.5 Conclusions

The flocculation value of bentonite clay can be determined by a flocculation series test. Depending on the clay concentration of the suspension, flocculation in dilute suspensions or gelation in dense suspensions occurs at the ionic strength of the solution above the flocculation value.

During hydraulic conductivity tests on clay membranes in a flexible-wall permeameter under a constant overburden load of about 4 bar, the ionic strength of the permeate had no influence on

hydraulic conductivity. Effective pore size distribution apparently remained unchanged. It is concluded, therefore, that flocculation or gelation of the clay membrane, resulting in a rearrangement of the clay platelets, does not take place at the applied overburden pressure. The clay platelets approach each other in the same degree that their double layers shrink.

Dissipation of osmotically induced hydraulic pressure differences in chemical osmosis experiments under sufficiently high overburden pressure cannot be explained by flocculation. The non-ideality of the membrane behaviour can more likely be accounted for by the diffusion of salt through the clay.

References

Abend, S. and Lagaly, G., 2000. *Sol-gel transitions of sodium montmorillonite dispersions.* Applied Clay Science, 16: 201 - 227.

Adamson, A.W., 1990. *Physical Chemistry of Surfaces.* John Wiley & Sons, Inc., New York, 777 pp.

Bear, J., 1979. *Hydraulics of Groundwater.* McGraw-Hill, New York, 569 pp.

Blackmore, A.U. and Miller, R.D., 1961. *Tactoid and osmotic swelling in calcium montmorillonite.* Proceedings America Soil Science Society, 25: 169 - 173.

Dijkstra, M., Hansen, J.P. and Madden, P.A., 1995. *Gelation of a clay colloid suspension.* Physical Review Letters, 75(11): 2236 - 2239.

Dixon, D.A., Gray, M.N. and Thomas, A.W., 1985. *A study of the compaction properties of potential clay-sand buffer mixtures for use in nuclear fuel waste disposal.* Engineering Geology, 21: 247 - 255.

Egloffstein, T.A., 2001. *Natural bentonites - influence of the ion exchange and partial desiccation on permeability and self-healing capacity of bentonites used in GCLs.* Geotextiles and Geomembranes, 19: 427 - 444.

Elrick, D.E., Smiles, D.E., Baumgartner, N. and Groenevelt, P.H., 1976. *Coupling phenomena in saturated homo-ionic montmorillonite: I. Experimental.* Soil Science Society of America Journal, 40: 490 - 491.

Frenkel, H., Goertzen, J.O. and Rhoades, J.D., 1978. *Effects of clay type and content, exchangeable sodium percentage, and electrolyte concentration on clay dispersion and soil hydraulic conductivity.* Soil Science Society of America Journal, 42: 32 - 39.

Fritz, S.J. and Marine, I.W., 1983. *Experimental support for a predictive osmotic model of clay membranes.* Geochimica et Cosmochimica Acta, 47: 1515 - 1522.

Fritz, S.J., 1986. *Ideality of clay membranes in osmotic processes: A review.* Clays and Clay Minerals, 34(2): 214 - 223.

Katchalsky, A. and Curran, P.F., 1967. *Non-equilibrium Thermodynamics in Biophysics.* Havard University Press, Cambridge, MA, 248 pp.

Keijzer, T.J.S., 2000. *Chemical Osmosis in Natural Clayey Materials.* Ph.D. thesis, Universiteit Utrecht, Utrecht, The Netherlands, 166 pp.

Keijzer, T.J.S. and Loch, J.P.G., 2001. *Chemical osmosis in compacted dredging sludge.* Soil Science Society of America Journal, 65: 1045 - 1055.

Kotlyar, L.S., Sparks, B.D. and Schutte, R., 1996. *Effect of salt on the flocculation behavior of nano particles in oil sands fine tailings.* Clays and Clay Minerals, 44(1): 121 - 131.

Logan, B.E. and Wilkinson, D.B., 1990. *Fractal geometry of marine snow and other biological aggregates.* Limnology and Oceanography, 35(1): 130 - 136.

Malusis, M.A., Shackelford, C.D. and Olsen, H.W., 2001. *A laboratory apparatus to measure chemico-osmotic efficiency coefficients for clay soils.* Geotechnical Testing Journal, 24(3): 229 - 242.

Mesri, G. and Olson, R.E., 1971. *Mechanisms controlling the permeability of clays.* Clays and Clay Minerals, 19: 151 - 158.

Mitchell, J.K., 1993. *Fundamentals of Soil Behavior.* John Wiley & Sons, Inc., New York, 437 pp.

Norrish, K. and Quirk, J.P., 1954. *Crystalline swelling of montmorillonite.* Nature, 173: 255 - 256.

Oster, J.D., Shainberg, I. and Wood, J.D., 1980. *Flocculation value and gel structure of sodium/calcium montmorillonite and illite suspensions.* Soil Science Society of America Journal, 44: 955 - 959.

Petrov, R.J. and Rowe, R.K., 1997. *Geosynthetic clay liner (GCL) - chemical compatibility by hydraulic conductivity testing and factors impacting its performance.* Canadian Geotechnical Journal, 34(6): 863 - 885.

Petrov, R.J., Rowe, R.K. and Quigley, R.M., 1997. *Comparison of laboratory-measured GCL hydraulic conductivity based on three parameter types.* Geotechnical Testing Journal, 20(1): 49 - 62.

Pusch, R. and Weston, R., 2003. *Microstructural stability controls the hydraulic conductivity of smectite buffer clay.* Applied Clay Science, 23: 35 - 41.

Quirk, J.P. and Schofield, R.K., 1955. *The effect of electrolyte concentration on soil permeability.* Journal of Soil Science, 6(2): 163 - 178.

Shackelford, C.D. and Lee, J.-M., 2003. *The destructive role of diffusion on clay membrane behavior.* Clays and Clay Minerals, 51(2): 186 - 196.

Shainberg, I. and Otoh, H., 1968. *Size and shape of montmorillonite particles saturated with Na/Ca ions.* Israel Journal of Chemistry, 6: 251 - 259.

Shainberg, I., Bresler, E. and Klausner, Y., 1971. *Studies on Na/Ca montmorillonite systems. 1. The swelling pressure.* Soil Science, 111(4): 214 - 219.

Studds, P.G., Stewart, D.I. and Cousens, T.W., 1998. *The effects of salt solutions on the properties of bentonite-sand mixtures.* Clay Minerals, 33: 651 - 660.

van Olphen, H., 1991. *An Introduction to Clay Colloid Chemistry.* Krieger Publishing Company, Malabar, Florida, 318 pp.

Whitworth, T.M. and Fritz, S.J., 1994. *Electrolyte-induced solute permeability effects in compacted* smectite membranes. Applied Geochemistry, 9: 533 - 546.

Yong, R.N., 2003. *Influence of microstructural features on water, ion diffusion and transport in clay soils.* Applied Clay Science, 23: 3 - 13.

Chapter 4

A new laboratory set-up for measurements of electrical, hydraulic and osmotic fluxes in clays*

Katja Heister, Pieter J. Kleingeld, Thomas J.S. Keijzer and J.P. Gustav Loch

Abstract

If clays are subject to flows of fluid, electrical charge, chemicals or heat, in most cases, flows of different types occur simultaneously, even if only one driving force is acting. These are so-called coupled flows. Examples of coupling phenomena are streaming potential and electroosmosis, induced by the flows of fluid and electrical charge, respectively.

Since the 1960s, laboratory devices have been constructed to measure streaming potentials and/or electroosmosis in clays or clayey soils. Due to their mechanical and hydraulic properties, clays are not easy to work with. Consequently, laboratory devices have to deal with various complications. A new design for an experimental set-up is proposed. Contrary to earlier devices, the clay sample is mounted in a flexible-wall permeameter, which avoids side-wall leakage caused by the possible swell or shrink of the clay. Gold-coated gauze electrodes completely cover the surfaces of the sample, which are in contact with the solution reservoirs that ensure one-dimensional flow. In addition, the thickness of the sample is monitored during the experiment. The chemical composition of the reservoir fluids is controlled during the experiment. The device is flexible with respect to changing the solutions of both reservoirs independently, applying different hydraulic gradients, and measuring or applying electrical potentials. Finally, it is possible to mount undisturbed clay samples in the set-up, keeping them as in-situ during the whole experiment.

With this set-up, an extensive program of measurements of coupling phenomena like streaming potentials, electroosmosis and membrane potentials in a sodium montmorillonite is started. Preliminary results of streaming potential measurements are presented and demonstrate that the build-up of a streaming potential due to a hydraulic gradient is a reproducible process that influences the water flow through the clay, and that the extent of the streaming potential depends on the salt concentration of the permeating solution.

Keywords
bentonite, coupled flow, electroosmosis, flexible-wall permeameter, irreversible thermodynamics, streaming potential

* Heister, K., Kleingeld, P.J., Keijzer, T.J.S. and Loch, J.P.G., 2005. A new laboratory set-up for measurements of electrical, hydraulic, and osmotic fluxes in clays. Engineering Geology, 77(3-4): 295 - 303.

4.1 Introduction

Membrane properties of clay are caused by the surface charge of the clay platelets and can be described by the double layer theory. Direct relations exist between flow of, respectively, fluids, electrical charge, dissolved chemicals and heat through clays and their corresponding driving force. In most cases, these flows are coupled, e.g., a streaming potential is induced during water flow under a hydraulic pressure gradient (Yeung and Mitchell, 1993; Yeung, 1994). Streaming potentials of several tens of millivolts have been measured in clays (Mitchell, 1993). In an externally applied electrical potential field, a fluid flow is created by the migrating ions exerting a viscous drag on the water around them. In a clay of negatively charged particles, a net water flow toward the cathode occurs known as electroosmosis (Mitchell, 1993). Due to the low permeability of clays, coupled flow is relatively more important than in soils of higher permeability.

From the end of the 1980s until now, much research was done on electroremediation of soils by application of a DC current. Since the effectiveness of remediation depends on several properties of the soil (e.g., porosity, degree of saturation, mineralogy and composition of the pore water), the geometry of the configuration of the electrodes and the current density, bench-scale experiments are necessary to determine the best arrangement of the equipment. For this purpose, different devices have been developed through the years.

In the past, fixed-wall permeameters have been developed, where the clay or soil sample is fitted into a cell between two filters. Both sides of the sample are connected to a solution reservoir. Inert electrodes like carbon or platinum or reversible electrodes like Ag/AgCl electrodes are placed at the interfaces of the sample (in large samples also within the sample) or in the solution reservoirs. If the

Table 4.1: Direct and coupled flow phenomena (Mitchell, 1993; Yeung, 1994; Horseman et al., 1996).

Flow J	Gradient X			
	Hydraulic	Electrical	Chemical	Thermal
Fluid	Hydraulic conduction *Darcy s law*	Electroosmosis	Chemical osmosis	Thermoosmosis
Current	Streaming potential	Electrical conduction *Ohm s law*	Diffusion and membrane potentials	Thermoelectricity Seebeck effect
Ion	Streaming current	Electrophoresis	Diffusion *Fick s law*	Thermal diffusion of electrolyte Soret effect
Heat	Isothermal heat transfer	Peltier effect	Dufour effect	Thermal conduction *Fourier s law*

system is insulated so that short-circuiting is avoided, streaming potentials are induced, which can be measured when a hydraulic gradient is applied (e.g., Olsen, 1962; Gairon and Swartzendruber, 1975; Kocherginsky and Stucki, 2001). Electroosmosis can be observed by applying an electrical potential gradient across the sample (e.g., Yeung et al., 1992; Acar et al., 1995; Grundl and Michalski, 1996; Kim et al., 2001). But especially for clays and clay-rich materials, the fixed-wall permeameters suffer from incomplete control over the stresses that act on the specimen and possible leakage along the interface between the sample and the wall of the permeameter (Daniel et al., 1984).

The aim of the present study was to develop a flexible-wall permeameter set-up that is capable of measuring streaming potentials and electroosmosis in clays and clay-rich materials.

4.2 Coupled phenomena

A mathematical description for coupled phenomena can be found in the literature of irreversible thermodynamics (Katchalsky and Curran, 1967; Yeung and Mitchell, 1993). Table 4.1 gives a summary of all coupled flow phenomena in porous media (Mitchell, 1993; Yeung, 1994; Horseman et al., 1996). The direct flow phenomena are on-diagonal, whereas the coupled flow phenomena are off-diagonal.

In theoretical analysis of coupled hydraulic and electrical flows in the absence of gradients of chemical potential and temperature, the fluxes are determined to be the fluid flux density and the electrical current density. The conjugated driving forces are the hydraulic pressure gradient and the electrical potential gradient. Thus the coupled flow equations are:

$$J_v = L_{11}\nabla(-P) + L_{12}\nabla(-E) \tag{4.1}$$

$$I = L_{21}\nabla(-P) + L_{22}\nabla(-E) \tag{4.2}$$

where J_v is the fluid flux density in m/s, I is the electrical current density in A/m², P is the hydraulic pressure in N/m², E is the electrical potential in V, and L_{11} to L_{22} are the phenomenological transport coefficients expressed in the corresponding units (Yeung, 1994). The negative signs in Eqs. 4.1 and 4.2 indicate that the flows of fluid and electrical charge are in the direction of decreasing hydraulic pressure and electrical potential.

When hydraulic conductivity is measured, the electrical current must vanish, as the electrical circuit is always open. If I=0, Eq. 4.2 reduces to:

$$\nabla(-E) = -\frac{L_{21}}{L_{22}}\nabla(-P) \tag{4.3}$$

thus giving the gradient of the streaming potential generated by the applied hydraulic pressure gradient. The phenomenological coefficients L_{12}, which, according to the reciprocal relations of Onsager (1931a, b) is equal to L_{21}, L_{22} can be determined from measurement of the coefficients of the electroosmotic conductivity and the electrical conductivity of the porous medium. As in electroosmosis usually $\nabla(-P) = 0$, Eqs. 4.1 and 4.2 reduce to:

$$J_v = L_{12}\nabla(-E) \tag{4.4}$$

$$I = L_{22}\nabla(-E) \tag{4.5}$$

Therefore, it follows that:

$$L_{12} = k_e \tag{4.6}$$

where k_e is the coefficient of electroosmotic conductivity in m^2/Vs and:

$$L_{22} = \kappa \tag{4.7}$$

with κ is the bulk electrical conductivity of the porous medium in S/m. Due to Onsager's reciprocity theorem, the equality of L_{12} and L_{21} causes the equivalence between streaming potential and electroosmosis:

$$\left(\frac{J_v}{I}\right)_{\Delta P=0} = -\left(\frac{\Delta E}{\Delta P}\right)_{I=0} \tag{4.8}$$

which is known as Saxén's law (Yeung, 1990, 1994; Yeung and Mitchell, 1993).

4.3 Design of the experimental set-up for measurement of streaming potentials and electroosmosis in clayey materials

Based on earlier studies described in literature and our own demands, the following requirements were established:

1. The device should not electrically short-circuit the sample.
2. Side-wall leakage caused by the possible swell or shrink of the sample should be avoided.
3. All parts in contact with the solutions should be corrosion- and chemical resistant and should not evoke additional potentials.
4. The solutions in the reservoirs should be independently replaceable and controllable.
5. Homogeneous flow through the sample should be obtained.
6. Hydraulic, electrical and chemical gradients should be applicable accurately across the sample.
7. The volume flow rates of solution, induced potentials and reservoir electrical conductivities should be measurable.
8. The electrodes should be placed at the interface of the sample to obtain a one-dimensional flow through the sample.
9. It should be possible to connect different controlling or measuring devices to the set-up without disturbing it.
10. The device should be flexible in exerting different accurately defined back-pressures on the sample.
11. The temperature during the experiment should be kept constant.
12. It should be possible to saturate the sample in-situ in the permeameter to keep it undisturbed

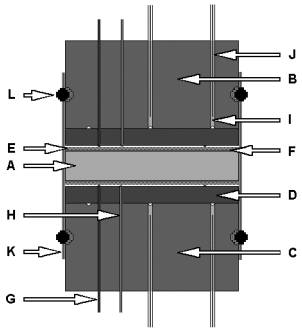

A: clay sample
B: hard rubber top cap
C: hard rubber pedestal
D: porous stone
E: goldplated nylon-filter
F: Millipore filter
G: gold-wire for potential measurement
H: pH electrode
I: flow-channel
J: gold-wire for electrical conductivity measurement
K: neoprene membrane
L: o-ring

Figure 4.1: Schematic drawing of the embedding of the sample. The drawing is not to scale.

during the whole experiment.

13. The geometry of the sample should be monitored during the experiment.
14. It should be possible to measure the pH of the solutions at the interface of the sample.

The set-up consists of a flexible-wall permeameter in which the clay sample is connected to two reservoirs. Within a Plexiglas cell (internal diameter 70 mm, external diameter 90 mm), the sample, which has a diameter of 50 mm and a variable thickness of several millimeters up to several centimeters, is mounted between two 0.45 μm Millipore filters and two porous stones (ELE Intertest, Etten-Leur, The Netherlands). The porous stones are pasted marginally on a pedestal on the bottom plate of the cell and on the top cap, respectively, both made of hard rubber. On the surface of each

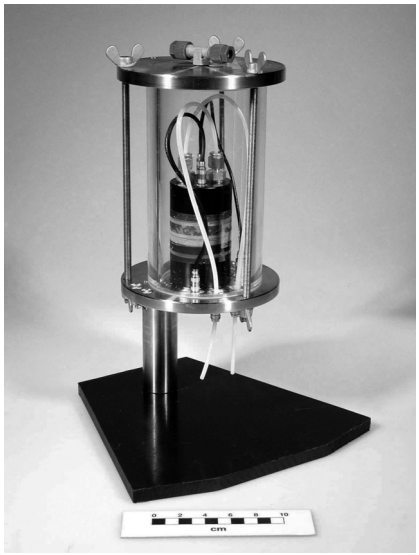

Figure 4.2: The photograph shows the permeameter cell without sample before it is connected to the reservoirs. The polyacetat top cap and base pedestal are clearly visible within the cell. For clearness, there is no neoprene membrane or cell filling shown.

porous stone, an annular gold wire is imprinted. In-between the Millipore filters and the porous stones, a goldplated nylon filter is situated. The nylon filter has a vapour-deposited gold grid that is in contact with the gold wire on the porous stone. Thus, the nylon filters act as electrodes that are situated very close to the interface of the sample. Between the two opposite goldplated filters, induced electrical potentials can be measured or electrical potentials can be applied. The porous stones are part of the fluid reservoirs in which it is possible to measure electrical conductivity of the solutions between two gold wires, which are led into the solution reservoirs close to the porous stones. Two flow channels on each side, electrical connections and the connection to the solid state pH ISFET electrode (Sentron, Roden, The Netherlands) are led through the pedestal and the top cap, respectively, and out of the cell in an insulated and pressure-tight way. A schematic overview of the embedding of the sample is given in Figure 4.1. From the pedestal to the top cap, the sample is wrapped in two neoprene membranes, each with a thickness of 0.2 mm (Piercan, Paris, France) and subsequently fitted with o-rings. The cell around the sample is filled with silicone oil, on which a pressure up to 5 bar can be applied by argon gas. For illustration, Figure 4.2 shows a photograph of the cell without sample and neoprene membranes.

To ensure electrical insulation, the reservoirs are made of plastics (PVDF/ PTFE/ POM/ PMMA). Each reservoir can be filled independently by use of peristaltic pumps (Ismatec Reglo-MS Analog) with PharMed tubings (Dépex, De Bilt, The Netherlands). The reservoirs can be variably equipped with devices to apply different hydraulic heads or collecting outflow solution.

Normally, the clay sample is saturated before the experiment outside the permeameter in a seawater resistant stainless steel mould with an internal diameter of 50 mm and then placed into the permeameter. During this procedure, there is a risk of disturbing the sample. To avoid disturbance, it is also possible to saturate a sample in-situ, thus within the permeameter with a low back-pressure in the cell. The thickness of the sample during the swelling period and the following experiment can be monitored by use of a digital slide gauge that is placed on the top cap and the bottom plate and is operative in silicone oil.

To minimize temperature effects, the whole set-up is situated in a temperature controlled room at 25°C ± 0.4°C.

4.4 Sample preparation

For a first experiment to measure streaming potentials in clays, a commercially available bentonite, marketed under the name Colclay A90™ (Geertruidenberg, The Netherlands), was used. It is a sodium montmorillonite with a third of the exchange complex occupied by calcium. An amount of 5.0 g of the air-dried powdered bentonite was weighed into a stainless steel mould with an internal diameter of 50 mm between two porous stones of the same diameter. Subsequently, the clay was subjected to a compaction pressure of 20.3 MPa for approximately 30 minutes. This compaction was done to obtain an easy-to-handle sample. After compaction, the mould was placed into a 0.01 M NaCl solution and the clay is allowed to swell in vertical direction. After 5 days, the clay was completely saturated. Consequently, a sample was obtained with a thickness of 3.8 mm and a diameter of 50 mm. The sample was then placed into the permeameter and the cell was filled with silicone oil until the top cap was completely submerged. Next, a pressure of 1 bar was applied to the cell by use of argon gas. The silicone oil prevents diffusion of gas through the membrane or along

Table 4.2: Measured sample properties.

			0.01 M NaCl	0.357 M NaCl
Before the experiment:				
	volume	cm^3	7.50	5.43
	surface of sample	cm^2	19.55	19.72
	thickness of sample	cm	0.383	0.275
After the experiment:				
	volume	cm^3	8.52	6.50
	surface of sample	cm^2	22.15	21.03
	thickness of sample	cm	0.384	0.309

the o-rings into the sample. Both reservoirs were filled by use of peristaltic pumps with the same solution used for saturating the clay, viz. 0.01 M NaCl, to eliminate chemical gradients at the start of the experiment. In the reservoir at the bottom-end of the sample, an inflow-device was installed consisting of a vessel filled with the solution, in which a constant hydraulic pressure of 0.5 bar is maintained by nitrogen gas. In the other reservoir, a tube for gravimetrical measurements of the outflow was installed. The tube has a water lock to prevent evaporation. The electrodes at the interfaces of the sample were connected to a high impedance multi-channel controller (R305 – Consort, Turnhout, Belgium) to read off the induced electrical potential across the sample in millivolts.

To study the influence of ionic strength, a similar experiment with the same bentonite using a 0.357 M NaCl solution was performed. The fabrication and mounting procedure remained the same and the same experimental procedure was followed. Sample properties of both experiments are summarized in Table 4.2.

4.5 Results

The potential difference across the clay is monitored from the moment the electrodes were connected to the controller. In both experiments, it is observed that, before starting the experiment, the clay has a potential difference of about -20 mV with the inflow side as the reference representing an electrical gradient of approximately -5 V/m. It is assumed that this potential has been built up during swelling when the solution can only flow unidirectionally into the clay. During the assembling of the cell, the potential can vary. These effects and the initial potential difference have to be eliminated at the start of the experiment by short-circuiting the goldplated filter-electrodes for approximately 10 minutes. Accordingly, the potential difference over the clay immediately vanishes. When the short-circuit is abrogated and hydraulic flow is initiated, an electrical potential development is observed. This is the point in time when the hydraulic conductivity measurement starts.

During the experiment, the hydraulic conductivity of the clay is determined by a constant head

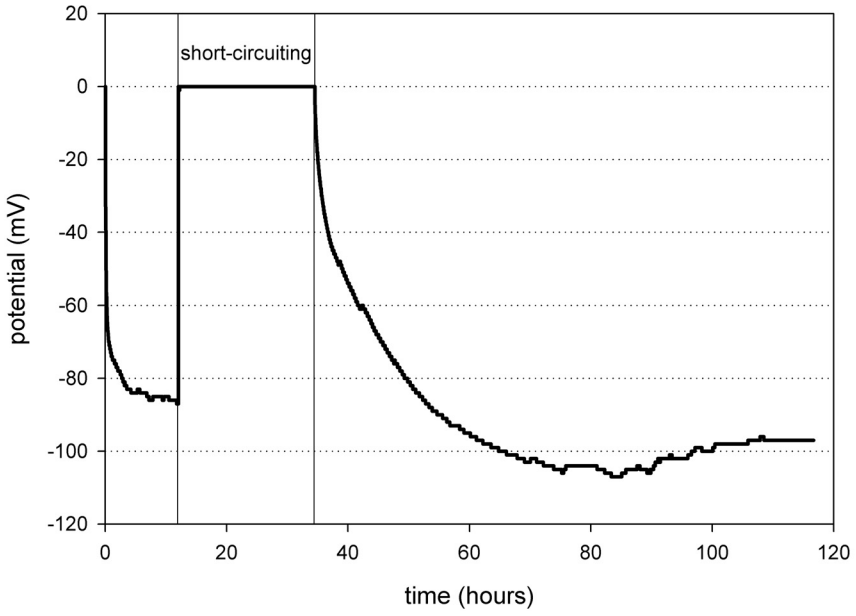

Figure 4.3: Electrical potential measurement of the sample with 0.01 M NaCl solution. The hydraulic pressure amounts 0.5 bar at a thickness of the bentonite sample of 0.384 cm. It is shown that after a period of short-circuiting the build-up of the potential is a repeatable process.

test. The NaCl solution is forced through the clay with a pressure of 0.5 bar and the flow rate is determined gravimetrically by weighing the outflow of the sample at regular time intervals. Measured and calculated fluxes and gradients are presented in Table 4.3. The build-up of electrical potential difference across the clay is exponential in time (Fig. 4.3). Within nearly 2 days, a stable potential of about -100 mV (again the inflow side is the reference) is achieved. The potential development is

Table 4.3: Water fluxes and driving forces measured in the experiments. J_v and J_h are measured gravimetrically, whereas J_e is calculated.

			0.01 M NaCl	0.357 M NaCl
total water flux density	J_v	m/s	$2.65 \cdot 10^{-8}$	$3.62 \cdot 10^{-8}$
under non-short-circuited conditions				
hydraulic induced water flux density	J_h	m/s	$3.05 \cdot 10^{-8}$	$6.05 \cdot 10^{-8}$
under short-circuited conditions				
electrical induced water flux density	J_e	m/s	$-3.91 \cdot 10^{-9}$	$-2.43 \cdot 10^{-8}$
hydraulic gradient	i_h	-	1304	1814
electrical gradient	i_e	V/m	-24	-19

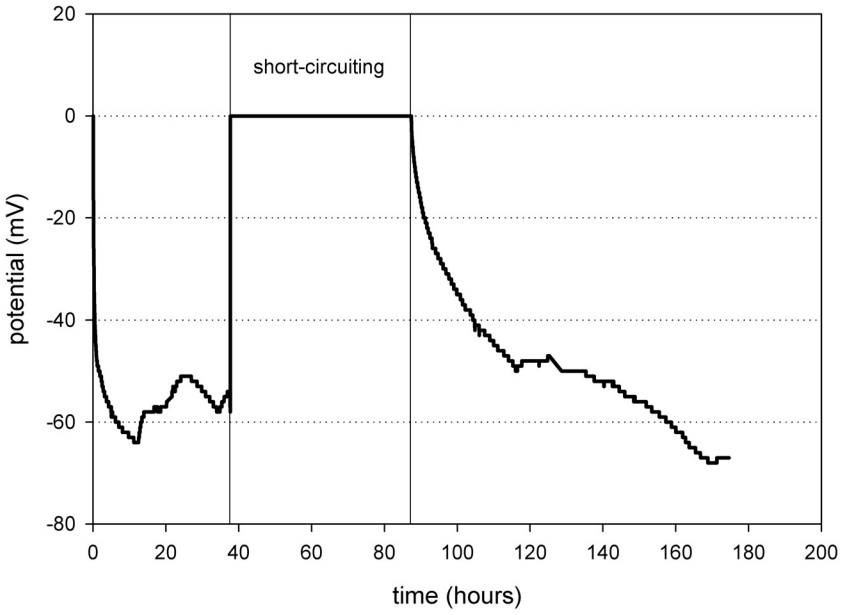

Figure 4.4: Electrical potential measurement of the sample with 0.357 M NaCl. Also in this experiment, the hydraulic pressure amounts 0.5 bar. The thickness of the bentonite sample is 0.309 cm. After a period of short-circuiting, a similar and repeatable build-up of the potential was observed. In comparison to the previous experiment, the potential difference is smaller.

reproducible because, after a period of short-circuiting the clay, a potential difference develops again exponentially in time with comparable values.

The potential development in the second experiment with 0.357 M NaCl solution is comparable to the previous experiment, which means that the build-up of potential difference is again exponential in time and reproducible after a period of short-circuiting (Fig. 4.4). There is a difference in the extent of the potential; in this case, a relatively stable potential is achieved at about -70 mV. Also in this experiment, the reference electrode is located in the inflow reservoir.

The two experiments show that the electrical potential difference, induced by the pressure difference across the clay, is dependent on the salt concentration. The higher the salt concentration in solution, the lower the induced electrical potential gradient. This is in accordance with earlier investigations in which was observed that the streaming potential decreases as the electrolyte concentration increases (Ahmad, 1963; Abaza and Clyde, 1969).

The hydraulic conductivity was determined both under short-circuited and non-short-circuited conditions. In both experiments, a water flow in the same order of magnitude was obtained. Moreover, it is clearly shown that the total water flow under non-shorted conditions is smaller than the hydraulic induced water flow under shorted conditions. Under non-short-circuited conditions, an electrically induced water flow is counteracting the hydraulic flow (Tab. 4.3).

4.6 Discussion

To facilitate analysis of the data measured with the set-up, Eqs. 4.1 and 4.2 can be rewritten as:

$$J_v = L_{11}\gamma_f i_h + L_{12} i_e \tag{4.9}$$

$$I = L_{21}\gamma_f i_h + L_{22} i_e \tag{4.10}$$

where J_v is the measured fluid flux density in m/s, γ_f is the unit weight of the fluid in N/m^3, i_h is the dimensionless hydraulic gradient, I is the electrical current density in A/m^2, i_e is the electrical potential gradient in V/m, and L_{11} to L_{22} are the phenomenological coefficients. Eq. 4.9 can be rewritten as:

$$J_v = J_h + J_e \tag{4.11}$$

with

$$J_h = L_{11}\gamma_f i_h \tag{4.12}$$

and

$$J_e = L_{12} i_e \tag{4.13}$$

When the clay is short-circuited, the water flow is solely driven by the hydraulic head. Therefore, for calculating the hydraulic conductivity, Darcy's law can be applied according to:

$$J_h = k_h^{\star} i_h \tag{4.14}$$

where $k_h^{\star}$ is the hydraulic conductivity at short-circuited condition, which is related to L_{11} according to Eq. 4.12:

$$k_h^{\star} = L_{11}\gamma_f \tag{4.15}$$

In the experiments, constant hydraulic conductivity coefficients, $k_h^{\star}$, of $2.34 \cdot 10^{-11}$ m/s at 0.01 M NaCl, and $3.33 \cdot 10^{-11}$ m/s at 0.357 M NaCl were measured (Tab. 4.4), which is close to the minimum of $1 \cdot 10^{-11}$ m/s reported for saturated fine-grained soils (Mitchell, 1993). For the calculations, the thickness and surface area of the samples at the end of the experiments were used. It is assumed that the change in thickness and surface area due to the overburden pressure occurs at the beginning of the experiment.

If the clay is not short-circuited, an electrically induced water flow counteracts the hydraulic induced water flow. Accordingly, $k_h^{\star}$ has to be supplemented by an electrically induced electroosmotic conductivity coefficient, k_e. Because J_v, J_h, and i_e were measured, $k_e = L_{12}$ (Eq. 4.6) can be calculated by substituting Eqs. 4.11 and 4.13. In these experiments, k_e values of $1.63 \cdot 10^{-10}$

Table 4.4: Calculated flow parameters derived from water fluxes and driving forces.

			0.01 M NaCl	0.357 M NaCl
hydraulic conductivity coefficient	k_h^*	m/s	$2.34 \cdot 10^{-11}$	$3.33 \cdot 10^{-11}$
electroosmotic conductivity coefficient	k_e	m^2/Vs	$1.63 \cdot 10^{-10}$	$1.28 \cdot 10^{-9}$
electrical conductivity coefficient	κ	S/m	$8.68 \cdot 10^{-5}$	$1.20 \cdot 10^{-3}$

m^2/Vs for 0.01 M NaCl, and $1.28 \cdot 10^{-9}$ m^2/Vs for 0.357 M NaCl were derived. In literature, reported values of k_e in fine-grained soils lie between $1 \cdot 10^{-8}$ and $1 \cdot 10^{-9}$ m^2/Vs (Mitchell, 1993). Accordingly, also in this case, there is a relatively good consistency of the measured values with literature data, although the k_e in the 0.01 M NaCl experiment is somewhat lower than the literature minimum.

Due to Onsager's reciprocal relations:

$$L_{12} = L_{21} = k_e \tag{4.16}$$

Eq. 4.3, applicable at non-short-circuited conditions, can be rewritten as:

$$i_e = -\frac{L_{21}\gamma_f}{L_{22}} i_h \tag{4.17}$$

Accordingly, $L_{22} = \kappa$ can be calculated. In these experiments κ was found to be $8.68 \cdot 10^{-5}$ S/m at 0.01 M NaCl and $1.20 \cdot 10^{-3}$ S/m at 0.357 M NaCl. All coefficients are summarized in Table 4.4.

In most soils, the electrical conductivity is in the range of 0.01 to 0.1 S/m (Yeung and Mitchell, 1993). The actual value depends on several properties of the soil such as porosity, degree of saturation, composition of the pore water, mineralogy, soil structure and temperature (Mitchell, 1993). Because the solid-phase composition of the porous medium is the same in both experiments, the shift in electrical conductivity is only caused by the composition of the fluid phase. Accordingly, the electrical conductivity of the 0.01 M NaCl experiment is significantly lower than in the experiment with higher ionic strength, indicating that electrical conduction is larger in solution of higher ionic strength. However, in both experiments, the electrical conductivity is lower than the range stated by Yeung and Mitchell (1993). It is assumed that the low values obtained in the experiments are due to the compact homogeneous fabric of the clay samples. Hence, the hydraulic conductivity is very low compared to average soils. Electrical conductance mainly takes place in the fluid phase, as the solid phase is only a poor conductor. In these experiments, the mobility of ions is hindered by the overlap of the diffuse double layers of the clay platelets.

The electroosmotic conductivity coefficient, k_e, is identical to both phenomenological coefficients L_{12} and L_{21}. Thus, this coupling coefficient can be used to predict the electroosmotic water transport when electrical gradients are applied across a sample. This is very useful information for the design of electroosmosis experiments.

4.7 Conclusions and outlook

A new laboratory set-up for measurements of electrical, hydraulic and osmotic fluxes in clays and

clay-rich materials is realized. Two experiments were performed on bentonite to study the dependency of the streaming potential on the ionic strength of solution.

It was shown that under non-short-circuited conditions, a streaming potential difference over the clay arose, the extent of which is dependent on the salt concentration of the solution: the higher the ionic strength, the lower the potential gradient.

The water flux under non-short-circuited conditions was in both experiments lower than under short-circuited conditions. This is due to the fact that under non-shorted conditions, an electrically induced water flow occurs, counteracting the hydraulic flow.

The hydraulic, electroosmotic and electrical conductivity coefficients were calculated. The hydraulic and electroosmotic conductivity coefficients are comparable with data in literature. The electrical conductivity coefficient is lower than the values reported for soils in literature. This is presumably due to the compact fabric of the clay with overlapping diffuse double layers of the clay platelets.

The results, obtained with this laboratory device, indicate that this set-up is utilizable for measuring electrokinetic phenomena in clays and clayey materials. The data obtained until now can be used for adjusting and supplementing the device for following experiments. In following steps, a fluid flow can be observed by applying an electrical potential gradient across the clay via the electrodes at the surfaces of the sample. Furthermore, chemical gradients will be created by changing the solution at one side of the clay, and the resultant hydraulic and electrical fluxes will be quantified. In a next step, the pH-electrodes need to be modified, as measuring the pH in the current set-up creates interferences with the electrical potential measurements. As a result, pH measurements were not yet performed during the described experiments.

References

Abaza, M.M.I. and Clyde, C.G., 1969. *Evaluation of the rate of flow through porous media using electrokinetic phenomena.* Water Resources Research, 5(2): 470 - 483.

Acar, Y.B. et al., 1995. *Electrokinetic remediation: Basics and technology status.* Journal of Hazardous Materials, 40: 117 - 137.

Ahmad, M.U., 1963. *A laboratory study of streaming potentials.* Geophysical Prospecting, 12: 49 - 64.

Daniel, D.E., Trautwein, S.J., Boynton, S.S. and Foreman, D.E., 1984. *Permeability testing with flexible-wall permeameters.* Geotechnical Journal, 7(3): 113 - 122.

Gairon, S. and Swartzendruber, D., 1975. *Water flux and electrical potentials in water-saturated bentonite.* Proceedings of the Soil Science Society of America, 39(5): 811 - 817.

Grundl, T. and Michalski, P., 1996. *Electroosmotically driven water flow in sediments.* Water Research, 30(4): 811 - 818.

Horseman, S.T., Higgo, J.J.W., Alexander, J. and Harrington, F.J., 1996. *Water, Gas and Solute Movement Through Argillaceous Media.* CC-96/1, Nuclear Energy Agency, Organisation for Economic Co-Operation and Development, Paris, France.

Katchalsky, A. and Curran, P.F., 1967. *Non-Equilibrium Thermodynamics in Biophysics.* Harvard University Press, Cambridge, MA, USA, 248 pp.

Kim, S.-O., Moon, S.-H. and Kim, K.-W., 2001. *Removal of heavy metals from soils using enhanced electrokinetic soil processing.* Water, Air, and Soil Pollution, 125: 259 - 272.

Kocherginsky, N.M. and Stucki, J. W., 2001. *Supported clay membrane: A new way to characterize water and ion transport in clays.* Advances in Environmental Research, 5: 197 - 201.

Mitchell, J.K., 1993. *Fundamentals of Soil Behavior.* John Wiley & Sons, Inc., New York, 437 pp.

Olsen, H.W., 1962. *Hydraulic flow through saturated clays.* Clays and Clay Minerals, 9: 131 - 161.

Onsager, L., 1931a. *Reciprocal relations in irreversible processes I.* Physical Review, 37: 405 - 426.

Onsager, L., 1931b. *Reciprocal relations in irreversible processes II.* Physical Review, 38: 2265 - 2279.

Yeung, A.T., 1990. *Coupled flow equations for water, electricity and ionic contaminants through clayey soils under hydraulic, electrical and chemical gradients.* Journal of Non-Equilibrium Thermodynamics, 15(3): 247 - 267.

Yeung, A.T., Sadek, S.M. and Mitchell, J.K., 1992. *A new apparatus for the evaluation of electro-kinetic processes in hazardous waste management.* Geotechnical Testing Journal, 15(3): 207 - 216.

Yeung, A.T. and Mitchell, J.K., 1993. *Coupled fluid, electrical and chemical flows in soil.* Geotechnique, 43(1): 121 - 134.

Yeung, A.T., 1994. *Effects of electro-kinetic coupling on the measurement of hydraulic conductivity.* In: D.E. Daniel and S.J. Trautwein (Editors), Hydraulic Conductivity and Waste Contaminant Transport in Soils. American Society for Testing and Materials, Philadelphia, pp. 569 - 585.

Chapter 5

Comparing the influence of electrode materials in electrokinetic experiments: Evidence from literature and laboratory measurements

Katja Heister, Pieter J. Kleingeld and J.P. Gustav Loch

Abstract

In the laboratory, commonly two types of electrodes are used to measure electrokinetic effects like streaming potentials in clays and other earth materials. On the one hand, reversible Ag/AgCl electrodes are used, whereas in other studies, noble metal oxidation-reduction electrodes like platinum or gold are employed. This paper shortly outlines the different types of electrodes and their application in earlier studies.

Thereafter, streaming potentials measured in a commercially available bentonite with de-aired NaCl solution inside a flexible-wall permeameter are reported. This flexible-wall permeameter is equipped with a pair of Ag/AgCl electrodes and a pair of gold electrodes to be able to compare directly the performance of those two types of electrodes. It turned out that the measurements of the Ag/AgCl electrodes were not stable in time due to the development of air bubbles in the outflow reservoir, which was caused by the pressure release after the solution had passed the clay membrane. On the other hand, it was shown that the measurements of the gold electrodes were influenced due to polarization of the electrodes and additional unknown effects. This could be shown in an electroosmosis experiment. Therefore, it was concluded that the Ag/AgCl electrodes, as long as they were in secure contact with the reservoir solution, measured the electrical potential more correctly.

With the coupled flow equations of irreversible thermodynamics, hydraulic, electroosmotic and electrical conductivity coefficients were calculated. Comparing these with literature data, it was shown that the values obtained with the Ag/AgCl electrodes were in good agreement with literature data and with results of a previous streaming potential experiment performed with this permeameter solely equipped with gold electrodes. Apparently, there are other factors influencing the performance of the electrodes, which have not been studied here, as they are not all known yet.

Keywords
coupled flow, electroosmosis, irreversible thermodynamics, oxidation-reduction electrodes, reversible electrodes, streaming potential

5.1 Introduction

The basic goal of this study is to measure and quantify electrokinetic effects in clays. Electrokinetic effects include streaming potentials and electroosmosis, which are coupled flow phenomena and can be defined by irreversible thermodynamics. Fluxes of fluid, electrical charge, solutes and heat can occur across a clay layer. Each of these fluxes can be driven by a conjugate gradient, i.e. a hydraulic, an electrical, a chemical and a thermal gradient, respectively. They are called direct flows. Contrary, coupled flows are driven by non-conjugate gradients (Katchalsky and Curran, 1967; Yeung and Mitchell, 1993). In the case of streaming potential, an electrical potential difference across the clay layer arises due to a hydraulic induced fluid flow through the clay, whereas in the case of electroosmosis, a fluid flow is caused by an applied electrical gradient across the clay (Yeung, 1994).

Because clays have a low hydraulic permeability, flow experiments take a long time. So a well-designed set-up is of great importance to study these phenomena in the laboratory. In this study, a flexible-wall permeameter connected to two solution reservoirs is used. A detailed description of this device will be given in a subsequent section.

Streaming potentials will be created by fluid flow through the clay and can be measured with electrodes on both sides of the sample. Like all parts of the set-up, the electrode material should be chosen carefully. From electrochemistry it is known that different electrode materials perform differently. Consequently, the choice of electrode will predominantly influence the measured potentials and the derived cross-coupling coefficients relating the coupled flow gradients.

In this study, two frequently used types of electrodes will be compared in experiments of streaming potential and electroosmosis in a bentonite clay. The electrode materials employed are gold as inert oxidation-reduction electrodes and Ag/AgCl electrodes with a single liquid junction.

Before discussing the experimental results, this paper will briefly outline the different types and modes of functioning of electrodes and review investigations of this topic elsewhere.

5.2 Electrodes

5.2.1 Classification of electrodes

In electrochemistry, the choice of electrode material is of particular importance because the properties of the material will directly influence the performance and thus the obtained results. For different applications, different requirements have to be fulfilled. Applying a current asks for different electrodes than measuring potentials. In practice, however, only few electrodes are commonly used. These are effectively standard, so-called 'reversible electrodes'.

In electrochemistry, 'reversible electrodes' are electrodes by which the equilibrium of a given reversible process is established at a rate satisfying the requirements of a given application. If equilibrium between the electrode and the solution is established slowly or not at all in the given time period, the electrode will in practice not attain a defined potential and cannot be used to measure individual thermodynamic quantities (Koryta et al., 1993).

Electrode equilibrium is a distribution equilibrium of charged species between the electrode material and the surrounding solution in a way that both phases must have at least one charged species in common. The magnitude of the potential difference between the phases is determined by the chemical potentials of this species in both phases.

Reversible electrodes may be divided into five groups (Yu and Ji, 1993):

- *Electrodes of the first kind:* These electrodes generally consist of a metal in equilibrium with a solution containing cations of that metal (cationic electrode – in the rare case of anionic electrodes, the equilibrium is established between the metal and the corresponding anions in solution). For this kind of electrode, only one interface is involved.
- *Electrodes of the second kind:* These electrodes consist of three phases: a metal, a low soluble salt containing that metal's cations, and a solution containing anions of that salt. Accordingly, two interface equilibria are involved, one between the metal and its salt, and the other between the salt and the solution. Examples are the calomel and the Ag/AgCl electrode.
- *Electrodes of the third kind:* These electrodes consist of four phases: a metal, a low soluble salt of that metal cation, another hardly soluble salt containing the same anions as the first salt, and a solution containing the cations of the second salt. Therefore, three interfaces are involved. This kind of electrode has only little practical utility due to the rather long time required to establish the three equilibria and has only been used in soil science. Double-junction electrodes belong to this group of electrodes.
- *Oxidation-reduction electrodes:* Contrary to the other types of electrodes, where the electrode potential originates from the transfer of ions between electrode and solution, with oxidation-reduction electrodes, the transfer of electrons induces the electrode potential. An inert metal electrode (usually platinum, gold or mercury) is dipped in a solution containing electrons. The electrode potential is determined by the electron activity of the solution, which in turn is determined by the relative activities of the reactants of the oxidation-reduction couple. Contrary to electrodes of the first kind, the reactants can be present in variable activities, while in the electrode of the first kind, one of the reactants, the electrode material, has a fixed activity.
- *Gas electrodes:* In principle, gas electrodes are electrodes of the first kind. The involved reaction is the equilibrium between a molecular gas and its ions. An inert metal is generally used as conductor. The most important electrode of this type is the standard hydrogen electrode at which equilibrium is established between hydrogen and H_3O^+ ions in solution through a platinum electrode.

Reversible electrodes are used in a broad range of applications. If we focus on the field of electrokinetic effects in soils, oxidation-reduction electrodes, e.g. platinum electrodes, and electrodes of the second kind, e.g. Ag/AgCl electrodes, are most commonly used. Therefore, we will give more attention to these two groups.

5.2.1.1 Oxidation-reduction electrodes

An oxidation-reduction electrode is also called an inert electrode because it can only transfer electrons but does not react with the solution chemically. In principle, its behaviour towards all oxidation-reduction systems is the same. Immersing such an electrode in a solution containing an oxidation-reduction system causes a potential difference at the interface electrode – solution owing to the transfer of electrons from the solution to the electrode or in a reversed direction (Yu and Ji, 1993).

In practice, however, there is no strictly inert electrode. Additionally to the transfer of electrons, other reactions like adsorption or deposition of components from the electrolyte and oxidation of the electrode material take place. These processes, termed 'poisoning of electrodes', can retard or

accelerate the electrode reaction or change its mechanisms (Koryta et al., 1993).

At present, the platinum electrode is still the most commonly used electrode for measurement of oxidation-reduction potentials of soils and water, although it can be oxidized by oxygen to form platinum oxides and can adsorb hydrogen and oxygen molecules as well as some organic and inorganic substances (Yu and Ji, 1993).

The second most widely used noble metal for this kind of electrodes is gold. Similar to platinum, the gold electrode in contact with an aqueous electrolyte can be covered by an oxide film. However, the electroanalytic activity for most charge transfer is considerably lower than for platinum.

5.2.1.2 Ag/AgCl electrodes as electrodes of the second kind

The Ag/AgCl electrode, which belongs to the electrodes of the second kind, is by far the most frequently employed because it is simple to prepare and gives very reproducible results. It is constructed by covering metallic silver by a layer of silver chloride and then immersing it in a solution containing chloride ions. The potential of the Ag/AgCl electrode is determined by the activity of Cl^- ions, so the electrode is reversible to Cl^- ions (Yu and Ji, 1993).

The Ag/AgCl electrode is normally used with a liquid junction of saturated or 3.5 M KCl solution. Potassium chloride is an obvious choice in most cases since the most important reference systems contain chloride. At the interface of the KCl solution and the solution of the system, ions will diffuse back and forth. If the mobilities of the two ion species comprising the electrolyte are different, a potential difference, the liquid junction potential, will be created between the two sides of the interface. Because K^+ and Cl^- have nearly the same ionic conductivity, liquid junction potentials are minimized (Galster, 1991; Rieger, 1994). The solubility of silver chloride in concentrated KCl solutions is very high (about $6 \cdot 10^{-3}$ M in saturated KCl solution at 25°C). Therefore, a small amount of AgCl should be added to the bridge solution to prevent dissolution of the AgCl during time (Yu and Ji, 1993).

If a too fast diffusion of potassium ions into the system solution should be inhibited, electrodes with thickened electrolytes can be used. The thickening agents form a relatively coarse network in the solution, so that ions can still retain their mobility within this network. This means that the electrical conductivity is not greatly affected, and additionally, it is not necessary to take effects of the medium into account. Although there is no outflow of electrolyte, diffusion still takes place in both directions. The thickening does not stop diffusion within the liquid junction, so that 'electrode poisons' can still gradually reach the electrode. Moreover, the electrolyte is slowly diluted by the sample solution, but this dilution is slowed down if the KCl solution is saturated and contains the solid salt (Galster, 1991).

5.2.2 Mode of functioning and the problem of polarization of electrodes

Metals are besides carbon the most important electrode materials. The charge transfer between the metal and the surrounding solution occurs by electrons. Within the metal, the electrons are loosely bound and form an 'electron gas' (Koryta et al., 1993). Under the influence of an external electric field, their originally random motion becomes oriented. Consequently, defects within the crystal lattice and in the surface structure (e.g. steps and kinks) will influence the charge transfer. Defects within the structure of the electrode can also be caused by unequal heating or mechanical stress, especially in the manufacturing process. It is beneficial to have a smooth and large surface of the

electrode in contact with the solution to enable a fast charge transfer to obtain reliable measurements.

If spurious potential drifts are measured, polarization of the electrode is accounted to be one of the main problems. In the case of an ideal polarized electrode, no movement of charge is allowed between the electrode itself and the solution phase. In contrast, an ideal non-polarized electrode allows free and unimpeded exchange of electrons across the interface. It should be mentioned here that although the existence of an electrical double layer around the electrode in solution is characteristic for polarized electrodes, it is also present at non-polarized electrodes even though the origin in the latter case is different and involves charge transfer across the interface (Crow, 1994).

Often, the problem of electrode polarization could be avoided by using Ag/AgCl electrodes instead of oxidation-reduction electrodes (Ahmad, 1964; Sprunt et al., 1994). But also the use of salt bridges or mathematical corrections can eliminate polarization (Korpi and de Bruyn, 1971).

However, the polarization problem was also observed by the use of Ag/AgCl electrodes (Morgan et al., 1989). In this case, amendment was achieved by the use of freshly made Ag/AgCl electrodes and placing the electrodes outside the fluid motion. Fluid motion causes the 'stirring effect', which under unfavourable conditions, amounts to as much as 40 mV (Galster, 1991). The stirring effect can be reduced by the employment of an additional salt bridge, by increasing the rate of electrolyte outflow out of the liquid junction, by reducing the liquid junction potential using another ion pair in the liquid junction solution, or – of course – by reducing the flow rate in the neighbourhood of the electrode (Yu and Ji, 1993; Galster, 1991).

From the aforementioned, the conclusion can be drawn that potential measurements are greatly affected by the type of electrode and electrode material. Obviously, there is no ideal electrode, and concessions have to be made for each experiment. So the type of ions, the running time of the experiment or the sources of spurious potentials, like e.g. polarization, liquid junction potentials or stirring effects, are among other things of importance for choosing the best kind of electrode.

5.3 Overview of former investigations

Laboratory devices for measuring streaming potentials and electroosmotic water transport in clays and soils have been developed since the 1960s. Although the objectives of these studies were different, there are only a few different electrode materials used, namely mostly Ag/AgCl electrodes as electrodes of the second kind and platinum and carbon electrodes as inert oxidation-reduction electrodes. In the 1960s and 1970s, the determination of streaming potential was the predominant goal, and so Ag/AgCl electrodes were most commonly used (e.g. Olsen, 1962; Jacazio et al., 1972; Elrick et al., 1976). Since the 1980s, with increasing significance of the application of electroosmosis, measuring electrical potentials differences takes a back seat and the use of inert electrodes to apply electrical potentials directly to the samples is on the rise. In the beginning, platinum was preferentially employed (e.g. Renaud and Probstein, 1987; Baraud et al., 1997), but in the meantime, carbon or rather graphite electrodes become more important (e.g. Hicks and Tondorf, 1994; Grundl and Michalski, 1996; Azzam and Oey, 2001; Suèr et al., 2003), since carbon electrodes prevent corrosion and introduction of secondary corrosion products (Hamed and Bhadra, 1997; Chung and Kang, 1999). It is obvious that the shift of main focus from detection to application of electrical potentials asks for different electrode materials. Consequently, recent studies to compare different electrode materials to detect electrical potentials are barely found in literature.

Most comparisons of the behaviour of different electrode materials for measuring streaming potentials are already published in the 1960s and 1970s. Ahmad (1964) could not obtain reliable potential readings with platinum electrodes when measuring the streaming potential of a silica sand column because the electrodes exhibited a so-called flow-potential, i.e. a potential difference that usually persists even when the liquid flow is stopped. According to Ahmad (1964), not all electrodes show this behaviour, so, thereupon, he used Ag/AgCl electrodes, which do not exhibit this flow-potential. Similarly, Abaza and Clyde (1969) detected flow-potentials with platinized platinum electrodes. However, they concluded that similar values for streaming potentials and streaming currents could be obtained for platinized platinum electrodes and Ag/AgCl electrodes by making a correction for the flow-potential. The flow-potential is the difference in potential after the flow has stopped and can therefore be directly measured. The subtraction of the flow-potential from the measured streaming potential is also recommended by Korpi and de Bruyn (1971) although this correction does not consider that the polarization potential changes with time and direction of flow. The reason for this change is the formation or dissolution of oxides films at unequal rates on the surface of each electrode. These errors can be avoided by the use of electrodes of the second kind. However, according to Korpi and de Bruyn (1971), at higher salt concentrations, it is possible to make reliable corrections for the polarization effects through the record of potentials during and after streaming.

Seemingly, most of the polarization problems of the electrodes can be solved by the use of electrodes of the second kind like Ag/AgCl electrodes. However, it should be mentioned that polarization problems of the electrodes were also encountered with Ag/AgCl electrodes by Sprunt et al. (1994), who compared the performance of gold and Ag/AgCl electrodes in streaming potential measurements. This problem could be minimized by monitoring the polarization and replacing the electrodes by fresh electrodes when needed (Morgan et al., 1989; Sprunt et al., 1994).

5.4 Experimental

5.4.1 The set-up

Experiments are carried out with a flexible-wall permeameter in which a clay sample with a diameter of 50 mm and a thickness of several millimeters is connected to two fluid reservoirs, which can be filled independently of each other. The clay sample is mounted on a pedestal within a Plexiglas cell between two 0.45 μm Millipore filters and two porous stones (ELE Intertest, Etten-Leur, The Netherlands) to enable a uniform fluid flow through the clay. The porous stones are pasted marginally on the pedestal of the bottom plate of the cell and on the top cap, respectively. Both are made of hard rubber. Also the fluid reservoirs consist of plastics for electrical insulation. From the pedestal to the top cap, the sample is wrapped in two neoprene membranes with a thickness of 0.2 mm (Piercan, Paris, France) and sealed with o-rings. The cell is then filled with silicone oil, and an overburden pressure of 1 bar is applied by argon gas. Subsequently, the reservoirs are filled independently by use of peristaltic pumps (Ismatec Reglo-MS Analog) with PharMed tubings (Dépex, Houten, The Netherlands). The bottom reservoir is connected to a solution reservoir where a constant hydraulic head is applied. The top reservoir is connected to a tube collecting the outflow solution. Thus, the hydraulic conductivity can be determined gravimetrically by weighing the outflow solution at regular time intervals and applying Darcy's law.

Both reservoirs are equipped with electrodes to measure the potential gradient across the clay

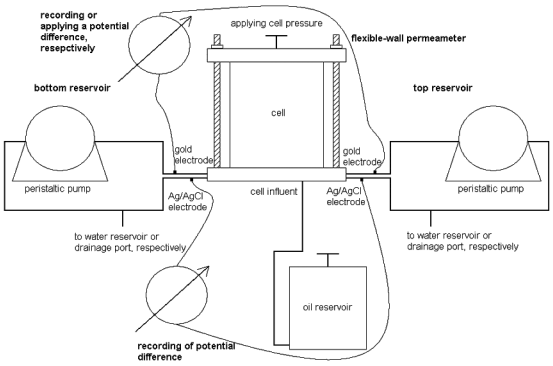

Figure 5.1: Schematic overview of the set-up. Drawing not to scale.

induced by hydraulic water flow, or to apply a potential gradient. A pair of reversible Ag/AgCl electrodes with a thickened KCl liquid junction (reference electrodes from Shindengen ISFET pH Meter KS501 – Wilten, Etten-Leur, The Netherlands) is installed to record induced potential differences. Common liquid junctions are not feasible due to the hydraulic pressure within the reservoirs that inhibits the required leakage of the liquid junction solution into the measuring solution. Ag/AgCl electrodes without liquid junction appeared to be too unstable in their measurements. To apply or to record a potential difference, respectively, depending on the type of experiment, electrodes consisting of gold wires with a diameter of 0.2 mm and a length of several centimeters are installed lengthwise in the reservoirs. Before installation, the gold wires consisting of 99.9% gold were first dawn-out and then annealed to eliminate stresses in the crystal lattice that can evoke notable potential differences.

All electrodes are connected to an electrometer multi-channel controller (R305 – Consort, Turnhout, Belgium) to read off the induced electrical potential across the sample in millivolts.

A schematic overview of the set-up is given in Figure 5.1.

5.4.2 Sample material

For sample material a commercially available bentonite is used. It consists mainly of montmorillonite with some traces of illite and quartz. Additional sample properties are given in Table 5.1. 5.0 g of air-dried powder was weighed into a stainless steel mould and compacted for 30 minutes at 20.3 MPa to obtain a disk with a diameter of 50 mm. Thereafter, the mould was placed in a bowl of 0.01 M NaCl solution in a way that the clay could take up the solution from the bottom up. In average, it takes two to three days to obtain a fully saturated clay sample, which now has a thickness of three to five millimeters. Now, the sample can be placed into the flexible-wall permeameter to perform the experiments.

5.5 Results

5.5.1 Streaming potential experiment

In the laboratory device described above, first a streaming potential experiment was performed with a bentonite saturated with 0.01 M NaCl. The solutions in the reservoirs were de-aired 0.01 M

Table 5.1: Sample properties of the bentonite.

cation exchange capacity		$cmol_c/kg$	75.7 ± 2.8
cation occupation by	Na^+	$cmol_c/kg$	53.0 ± 1.9
	K^+	$cmol_c/kg$	1.5 ± 0.1
	Ca^{2+}	$cmol_c/kg$	26.6 ± 0.6
	Mg^{2+}	$cmol_c/kg$	7.8 ± 0.0
C_{org}-content		wt%	0.13
carbonate content		wt%	0.63
specific surface area	EGME*	m^2/g	611 ± 9

* ethylene glycol monoethyl ether

NaCl solutions. A hydraulic head of 0.5 bar was applied to force the water through the clay membrane. To determine the hydraulic conductivity, the outflow solution was collected and weighed at regular time intervals. At the same time, the potential across the clay was measured with both Ag/AgCl and gold electrode pairs.

After a short time short-circuiting of both electrode pairs in order to eliminate potential effects, which could occur during mounting the sample in the set-up and to obtain a comparable initial situation, both electrode pairs showed a development of an electrical potential gradient that arose across the clay membrane. Surprisingly, the potentials developed were of opposite sign. With the gold electrode, a streaming potential of around 14.76 V/m was measured, whereas the Ag/AgCl electrodes

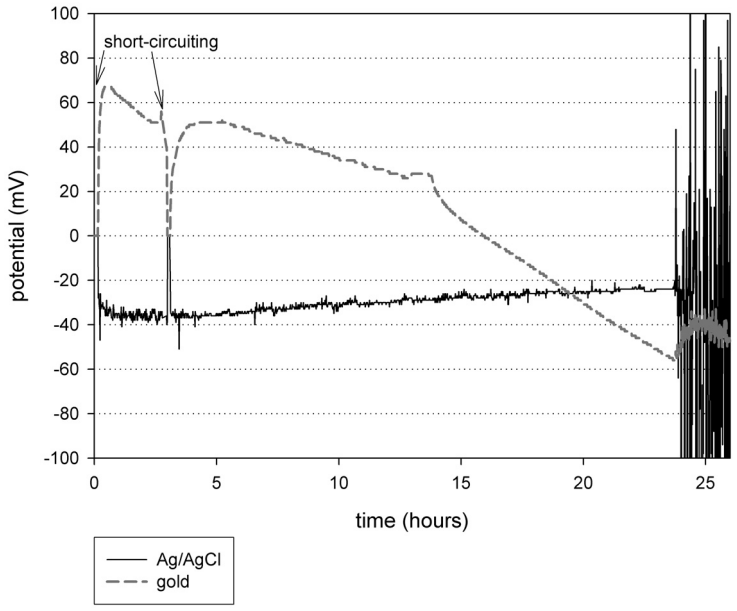

Figure 5.2: The potential development in the streaming potential experiment. Both pairs of electrodes are short-circuited at time zero and around three hours. After 24 hours the potential measurements of the Ag/AgCl electrodes start to fluctuate heavily due to air bubbles in the outflow reservoir.

denote a potential gradient of -10.63 V/m. These values were reproducible after short-circuiting the electrodes again. After nearly 11 hours, the potential gradient measured at the gold electrodes dropped dramatically to a minimum of -15.05 V/m. In the same time, the Ag/AgCl recordings kept quite constant. Only a small dissipation to -6.79 V/m was observed in a period of almost 21 hours. The development of the measured potentials is summarized in Figure 5.2.

In the experimental set-up described, the streaming potential is expected to be negative in the direction of the water flow. Due to this fact and the observation of instability of the readings of the gold electrodes, it is concluded that the Ag/AgCl electrodes measure the 'true' streaming potential. Unfortunately, the used Ag/AgCl electrodes also proved unsatisfactory. After a running time of the experiment of one day, the potential started to fluctuate heavily over a range of several hundreds of millivolts, which corresponds to a fluctuation of potential gradient of several tens of V/m. At the same time, small air bubbles were detected in the tubes of the outflow reservoir. Although de-aired solutions were used, the occurrence of air bubbles in the outflow reservoir could not be prevented. It is attributed to the fact that the solutions were never totally free of dissolved gases and that degassing occurs after the solution has passed the membrane. Obviously, the Ag/AgCl electrodes are very sensitive to those air bubbles, which hamper the contact between the electrodes and the solution. Even degassing valves in the close vicinity to the electrodes were no solution of this problem.

5.5.2 Electroosmosis experiment

Secondly, an electroosmosis experiment was performed, which, according to Onsager's reciprocal relations, is the contrary phenomenon to the streaming potential. From literature it is known that the unreliability of the gold electrodes is based on their mode of functioning and in particular on the problem of polarization. Like on all charged surfaces in solution, an electrical double layer develops around it, which hinders the exchange of electrons across the interface electrode – solution that is necessary for potential measurements. The build-up of an electrical double layer at the gold electrode can be visualized in an electroosmosis experiment.

The same bentonite material, NaCl solutions and experimental conditions like overburden load and hydraulic gradient were used in this experiment. Additional to the hydraulic gradient, an electrical potential difference was applied at the gold electrodes. Subsequently, the electrical potential difference was measured by the Ag/AgCl electrodes. It is known that the resistances of the interfaces electrode – solution influence the measured potential difference; however, this effect is not quantified in this study and thus not further taken into account.

Figure 5.3 shows a typical potential development. In this case, 300 mV were applied at the gold electrodes, resulting in an electrical potential gradient of 88.56 V/m. The Ag/AgCl electrodes measure the electrical potential of the solution in the reservoirs. It is clearly shown that the measured potential always differs significantly from the applied potential. This difference is attributed to the hydraulic induced electrical potential and can thus be defined as the streaming potential. Remarkable is a peak occurring immediately when the voltage is applied, which diminishes shortly after to a more or less stable electrical potential value. In this paper, the difference between the peak and subsequent stable measured potential value is referred as polarization potential. This polarization potential builds up in the first few hours after applying the potential at the gold electrodes and corresponds to the development of an electrical double layer at the gold electrodes, which hinders the charge transfer.

The same behaviour was observed by applying 150 mV (equivalent to 44.28 V/m) and similar

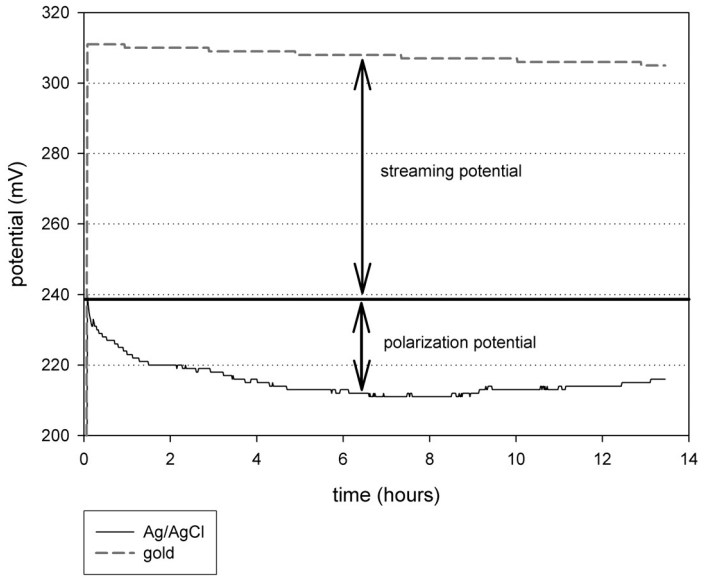

Figure 5.3: The potential development in the electroosmosis experiment. 300 mV are applied across the gold electrodes. Clearly visible is a peak close to time zero in the potential measurement of the Ag/AgCl electrodes that corresponds to the polarization potential.

observations were made by applying -300 mV and -150 mV, respectively. Particularly notable is the effect when the voltage gradient is reversed. The peak measured by the Ag/AgCl electrodes is analogous, but contrary to the observations before, no stable electrical potential value was achieved after more than 4.5 hours. One possible explanation for the development of the polarization potential could be that because the sign of the potential of the electrode has changed, also the sign of the electrical double layer in the solution has to change, which takes a remarkably longer time. Before the new double layer can be generated, first the ions of the previous double layer have to be repelled. On the other hand, the polarization potential could also be explained by adsorption of substances on the gold electrodes whose desorption will take longer time (Raistrick et al., 1987; Cao et al., 1994).

Unfortunately, however, it is not possible to calculate the charge accumulation in the electrical double layer at the electrode because the resistance of the solution phase was not measured in this experiment. An estimation with the supplementary determined electrical conductivity of the solution leads to unrealistic values of the charge accumulated at the electrode. It seems that the resistance of the clay membrane between the two reservoirs heavily influences the total resistance of the system, which is, consequently, not easy to determine. Several authors prefer AC methods to measure the resistance of porous media (Benaventea and Jonsson, 1998; Wong, 1999; Fievet et al., 2000; Ariza et al., 2001), but those methods lie beyond the scope of this paper.

The phenomenon of electroosmosis implies that a fluid flow is created by an applied electrical potential gradient (Mitchell, 1993; Yeung and Mitchell, 1993). This means that in case of the electroosmosis experiment described above, differences in fluid flow should be observed at different levels of electrical potential applied. Moreover, the fluid flow is also depending on the sign of the applied voltage.

In the experiment, NaCl solution was forced through the clay sample with a hydraulic head difference of 5 m, which resulted in a development of a streaming potential of around -11 V/m across the clay. Applying a voltage of the opposite sign should result in accelerating the fluid flow, whereas a voltage of the same sign should slow down the transport of water through the sample.

As already described, the water flux density was determined by gravimetrically weighing the outflow at regular time intervals. If a streaming potential is present, the total water flux density, which is composed of the hydraulic and the electrical induced water flux density, averages $2.81 \cdot 10^{-8}$ m/s. By short-circuiting the electrodes, the electrical potential gradient becomes zero, and thus, the electrical induced water flux density vanishes. The measured water flow, which is now equal to the hydraulic induced water flux density, is larger because there is no counteracting flow present. In this experiment, the hydraulic induced water flux density amounts to $3.21 \cdot 10^{-8}$ m/s. In case of applying a voltage of -300 mV across the sample, the water flow is even more hindered than by the streaming potential alone. Due to the larger counteracting electrical induced flux, the total water flux density is slightly less ($2.76 \cdot 10^{-8}$ m/s). However, the effect of the additional electrical induced water flux density is more pronounced in case of applying a voltage of +300 mV, which results in a co-acting electrical induced water flux density. The total water flux density then amounts to $6.05 \cdot 10^{-8}$ m/s. Unfortunately, it is not clear why applying +300 mV results in more deviation of the water flow than applying -300 mV. Maybe the order of applying the additional electrical potential gradients is of importance, which would imply that a steady water flow was probably not achieved yet within the time the hydraulic conductivity was measured.

5.6 Discussion

As already mentioned in the introduction, the flow of fluid and electrical charge across a semipermeable membrane can be expressed with the coupled flow equations of irreversible thermodynamics (Katchalsky and Curran, 1967). Streaming potential and electroosmosis are coupled flow phenomena by coupling fluid flow and electrical current. In the absence of a chemical potential and a temperature gradient, the fluxes are the volume flow rate of fluid per unit area and the electrical current density. Moreover, Onsager's reciprocal relations (Onsager, 1931a, b) are assumed to be valid. Consequently, the streaming current and electroosmosis are directly related to each other, which is known as Saxén's law (Yeung, 1990, 1994; Yeung and Mitchell, 1993).

To calculate the conductivity coefficients with the data measured, the equations are established as

$$J_v = k_h^{\star} i_h + k_e i_e \tag{5.1}$$

$$I = k_e \gamma_f i_h + \kappa i_e \tag{5.2}$$

where J_v is the fluid flux density in m/s, $k_h^{\star}$ is the hydraulic conductivity coefficient under short-circuited conditions in m/s, i_h is the hydraulic gradient, k_e is the electroosmotic conductivity coefficient in m^2/Vs, i_e is the electrical potential gradient in V/m, I is the electrical current density in A/m^2, γ_f is the unit weight of the fluid in N/m^3, and κ is the electrical conductivity coefficient in S/m.

In addition, the fluid flux described in Eq. 5.1 consists of a hydraulic and an electrical induced water flux:

$$J_v = J_h + J_e \tag{5.3}$$

where J_h and J_e are the hydraulic and electrical induced water flux densities in m/s, respectively.

For a detailed derivation, the reader is referred to Heister et al. (2005), where the calculation of the coefficients is described.

All measured and calculated parameters are listed in Table 5.2.

These data clearly show that the electrical induced water flow counteracts the hydraulic water flow, if the electrical gradient is negative of sign. Applying a positive electrical potential gradient that accelerates the hydraulic water flow results in a co-acting J_e, which then has a positive sign.

To discuss the reliability of the obtained coefficients, they are compared to literature data and to a former streaming potential experiment performed in the same laboratory device with gold electrodes, where the induced streaming potential was measured on the same type of bentonite and 0.01 M NaCl solution (Heister et al., 2005). Those data are also listed in Table 5.2.

The hydraulic conductivity coefficient, k_h^*, was obtained under shorted conditions and is therefore equal in all three experiments performed in this study. The k_h^* is very close to the k_h^* determined in the former investigation. Both are in the same order of magnitude and are close to the minimum value of the hydraulic conductivity expected for highly compacted bentonites.

The electroosmotic conductivity coefficients, k_e, vary slightly in the three experiments and are in the same order of magnitude as the value obtained in the previous experiment. All calculated k_e values are close to the minimum value for saturated fine-grained soils, even a little lower. Although

Table 5.2: Comparison of the measured and calculated parameters of this study with a previous experiment and literature data.

			no extra electrical gradient	+300 mV electrical gradient	-300 mV electrical gradient	previous experiment with gold electrodes	literature data maximum	literature data minimum
			this study			(Heister et al., 2005)	(Mitchell, 1993)	
measured values								
total water flux density under non-shorted conditions	J_v	m/s	$2.81 \cdot 10^{-8}$	$6.05 \cdot 10^{-8}$	$2.76 \cdot 10^{-8}$	$2.65 \cdot 10^{-8}$		
hydraulic induced water flux density under shorted conditions	J_h	m/s	$3.21 \cdot 10^{-8}$	$3.21 \cdot 10^{-8}$	$3.21 \cdot 10^{-8}$	$3.05 \cdot 10^{-8}$		
hydraulic gradient	i_h	-	$9.84 \cdot 10^{2}$	$9.84 \cdot 10^{2}$	$9.84 \cdot 10^{2}$	$1.30 \cdot 10^{3}$		
electrical gradient measured by the Ag/AgCl gel electrodes	i_e	V/m	-6.79	88.28	-23.43	-24.00 [1]		
calculated values								
electrical induced water flux density	J_e	m/s	$-4.08 \cdot 10^{-9}$	$2.83 \cdot 10^{-8}$	$-4.59 \cdot 10^{-9}$	$-3.91 \cdot 10^{-9}$		
hydraulic conductivity coefficient	k_h^*	m/s	$5.36 \cdot 10^{-11}$	$5.36 \cdot 10^{-11}$	$5.36 \cdot 10^{-11}$	$2.34 \cdot 10^{-11}$	$1 \cdot 10^{-6}$	$1 \cdot 10^{-11}$
electroosmotic conductivity coefficient	k_e	m^2/Vs	$9.86 \cdot 10^{-10}$	$5.26 \cdot 10^{-10}$	$3.21 \cdot 10^{-10}$	$1.63 \cdot 10^{-10}$	$1 \cdot 10^{-8}$	$1 \cdot 10^{-9}$
electrical conductivity coefficient	κ	S/m	$1.40 \cdot 10^{-3}$	$5.75 \cdot 10^{-5}$	$1.32 \cdot 10^{-4}$	$8.68 \cdot 10^{-5}$	1.0	0.01

[1] measured by gold electrodes

there is some variation in this coefficient, there is no clear trend visible.

Even though these two coefficients are in good agreement with each other, the electrical conductivity coefficient, κ, however, varies stronger and not systematically (up to almost two orders of magnitude). Even more remarkable is the fact that all calculated electrical conductivity coefficients are clearly lower than even the minimum value in literature for fine-grained soils. It is assumed that this can be attributed to the compact and homogeneous clay fabric with overlapping diffuse double layers of the clay platelets within the pores of the clay. As the solid phase is only a poor conductor, electrical conduction takes place in the fluid phase. Subsequently, the transport of ions is hindered by the strong overlap of the diffuse double layers. Anyhow, electrical conduction does not only occur in the free pore fluid but also within the diffuse double layers. The so-called surface conductivity (Lyklema and Minor, 1998; Fievet et al., 2001) plays a more important role, as the electrical conductivity of the pore fluid gets lower. Although, it seems that surface conductivity is of importance in highly compacted clays, ionic conduction within the diffuse double layers is not taken into account by the classical theory of electrokinetics (Sbaï et al., 2003).

Generally speaking, comparing the experiments of this study with the former investigation, it strikes that the results are quite similar although they are obtained with different types of electrodes. This is surprising as it was afore concluded that inert gold electrodes do not produce reliable potential measurements. Therefore, the results obtained in the former study with the gold electrodes are reproducible and comparable to literature data. Moreover, in this study, it was shown that comparable results could also be obtained with the employment of Ag/AgCl gel electrodes and that polarization of the gold electrodes could be quantified. Seemingly, other effects are also playing a role in the performance of the gold electrodes. But apparently, as these effects are not known yet, it seems that if some luck in the choice of the electrode material is necessary to achieve good data.

5.7 Conclusions

In laboratory investigations regarding streaming potential and electroosmosis in earth materials like clays or soils, there are mainly two types of electrodes used. Both types – the noble metal oxidation-reduction electrode and the Ag/AgCl electrode – are reversible electrodes. Due to their modes of functioning, both types of electrodes can pose problems regarding their stability and reliability of their measurements. Whereas the Ag/AgCl electrodes often need to be stabilized by liquid junctions, inert oxidation-reduction electrodes like platinum or gold show other deviant effects, and not only polarization as stated in literature.

In a laboratory set-up consisting of a flexible-wall permeameter, equipped with gold and Ag/AgCl electrodes, streaming potential and electroosmosis experiments were conducted with commercially available bentonite and 0.01 M NaCl solution. It turned out that Ag/AgCl electrodes with thickened liquid junction electrolyte are not stable enough and are very sensitive to the development of air bubbles in the outflow reservoir. On the other hand, in an electroosmosis experiment, inert gold electrodes were influenced by polarization and additional unknown effects. Therefore, it was concluded that the Ag/AgCl gel electrodes were the better choice.

With the aid of coupled flow equations of irreversible thermodynamics, hydraulic, electroosmotic and electrical conductivity coefficients were calculated and compared with literature data and data of a previous performed study with this laboratory device. Comparing the results of the previous study

using gold electrodes, the present coefficients, which are calculated with the data obtained from the Ag/AgCl electrodes, are in quite good agreement. Compared to literature data, the hydraulic conductivity coefficients and the electroosmotic conductivity coefficients of the experiments are close to the minimum values noted for fine-grained soils; indeed, the electrical conductivity coefficients are all very much lower. This is explained by the compact and homogeneous clay fabric resulting in a strong overlap of the diffuse double layers of the clay particles, which hinders the transport of ions in the pore water of the bentonite.

In summary, it seems that reliable results had also been obtained with gold electrodes in a previous study, although it was shown that polarization and additional deviating effects occur. Comparable results were obtained with Ag/AgCl gel electrodes. But since many factors influence the performance of the electrodes, that are not all known yet, the choice of electrodes is a crucial point in designing a laboratory device to measure electrokinetic effects in clays and other earth materials. Consequently, neither of these two types of electrodes, the Ag/AgCl gel electrode and the gold electrode, can be recommended for streaming potential and electroosmosis experiments. For enhancement of the laboratory set-up, more reliable electrodes should be employed. Since the use of Ag/AgCl electrodes is established for decades in this kind of experiments, Ag/AgCl reference electrodes, stabilized with a liquid junction, are recommended, even though their use makes it almost impossible to apply hydraulic gradients due to the mode of functioning of the liquid junction.

References

Abaza, M.M.I. and Clyde, C.G., 1969. *Evaluation of the rate of flow through porous media using electrokinetic phenomena.* Water Resources Research, 5(2): 470 - 483.

Ahmad, M.U., 1964. *A laboratory study of streaming potentials.* Geophysical Prospecting, 12: 49 - 64.

Ariza, M.J., Cañas, A. and Benavente, J., 2001. *Electrokinetic and electrochemical characterization of porous membranes.* Colloids and Surfaces A: Physicochemical and Engineering Aspects, 189: 247 - 256.

Azzam, R. and Oey, W., 2001. *The utilization of electrokinetics in geotechnical and environmental engineering.* Transport in Porous Media, 42: 293 - 314.

Baraud, F., Tellier, S. and Astruc, M., 1997. *Ion velocity in soil solution during electrokinetic remediation.* Journal of Hazardous Materials, 56: 315 - 332.

Benaventea, J. and Jonsson, G., 1998. *Electrokinetic characterization of a microporous non-commercial polysulfone membrane: Phenomenological coefficients and transport parameters.* Colloids and Surfaces A: Physicochemical and Engineering Aspects, 140: 339 - 346.

Cao, Q.-Z., Wong, P.-Z. and Schwartz, L.M., 1994. *Numerical studies of the impedance of blocking electrodes with fractal surfaces.* Physical Review B, 50(8): 5571 - 5574.

Chung, H.I. and Kang, B.H., 1999. *Lead removal from contaminated marine clay by electrokinetic soil decontamination.* Engineering Geology, 53: 139 - 150.

Crow, D.R., 1994. *Principles and Applications of Electrochemistry.* Blackie Academic and Professional, London, 282 pp.

Elrick, D.E., Smiles, D.E., Baumgartner, N. and Groenevelt, P.H., 1976. *Coupling phenomena in saturated homo-ionic montmorillonite: I. Experimental.* Soil Science Society of America Journal, 40: 490 - 491.

Fievet, P., Szymczyk, A., Aoubiza, B. and Pagetti, J., 2000. *Evaluation of three methods for the*

characterisation of the membrane-solution interface: streaming potential, membrane potential and electrolyte conductivity inside pores. Journal of Membrane Science, 168: 87 - 100.

Fievet, P. et al., 2001. *Determining the zeta potential of porous membranes using electrolyte conductivity inside pores.* Journal of Colloid and Interface Science, 235: 383 - 390.

Galster, H., 1991. *pH Measurements: Fundamentals, Methods, Applications, Instrumentation.* VCH Verlagsgesellschaft mbH, Weinheim, 356 pp.

Grundl, T. and Michalski, P., 1996. *Electroosmotically driven water flow in sediments.* Water Research, 30(4): 811 - 818.

Hamed, J.T. and Bhadra, A., 1997. *Influence of current density and pH on electrokinetics.* Journal of Hazardous Materials, 55: 279 - 294.

Hicks, R.E. and Tondorf, S., 1994. *Electrorestoration of metal contaminated soils.* Environmental Science and Techology, 28(12): 2203 - 2210.

Heister, K., Kleingeld, P.J., Keijzer, T.J.S. and Loch, J.P.G., 2005. *A new laboratory set-up for measurements of electrical, hydraulic, and osmotic fluxes in clays.* Engineering Geology, 77(3-4): 295 - 303.

Jacazio, G., Probstein, R.F., Sonin, A.A. and Yung, D., 1972. *Electrokinetic salt rejection in hyperfiltration through porous materials. Theory and experiment.* Journal of Physical Chemistry, 76(26): 4015 - 4023.

Katchalsky, A. and Curran, P.F., 1967. *Non-Equilibrium Thermodynamics in Biophysics.* Harvard University Press, Cambridge, MA, USA, 248 pp.

Korpi, G.K. and de Bruyn, P.L., 1972. *Measurement of streaming potentials.* Journal of Colloid and Interface Science, 40(2): 263 - 266.

Koryta, J., Dvoràk, J. and Kavan, L., 1993. *Principles of Electrochemistry.* John Wiley & Sons, Chichester, 486 pp.

Lyklema, J. and Minor, M., 1998. *On surface conduction and its role in electrokinetics.* Colloids and Surfaces A: Physicochemical and Engineering Aspects, 140: 33 - 41.

Mitchell, J.K., 1993. *Fundamentals of Soil Behavior.* John Wiley & Sons, Inc., New York, 437 pp.

Morgan, F.D., Williams, E.R. and Madden, T.R., 1989. *Streaming potential properties of Westerly granite with applications.* Journal of Geophysical Research, 94(B9): 12449 - 12461.

Olsen, H.W., 1962. *Hydraulic flow through saturated clays.* Clays and Clay Minerals, 9: 131 - 161.

Onsager, L., 1931a. *Reciprocal relations in irreversible processes I.* Physical Review, 37: 405 - 426.

Onsager, L., 1931b. *Reciprocal relations in irreversible processes II.* Physical Review, 38: 2265 - 2279.

Raistrick, I.D., Macdonald, J.R. and Franceschetti, D.R., 1987. *Theory.* In: J.R. Macdonald (Editor), Impedance Spectroscopy: Emphasizing Solid Materials and Systems. John Wiley and Sons, New York, pp. 27 - 132.

Renaud, P.C. and Probstein, R.F., 1987. *Electroosmotic control of hazardous wastes.* Physicochemical Hydrodynamics, 9(1/ 2): 345 - 360.

Rieger, P.H., 1994. *Electrochemistry.* Chapman and Hall, New York, 483 pp.

Sbaï, M. et al., 2003. *Streaming potential, electroviscous effect, pore conductivity and membrane potential for the determination of the surface potential of a ceramic ultrafiltration membrane.* Journal of Membrane Science, 215: 1 - 9.

Sprunt, E.S., Mercer, T.B. and Djabbarah, N.F., 1994. *Streaming potential from multiphase flow.* Geophysics, 59(5): 707 - 711.

Suèr, P., Gitye, K. and Allard, B., 2003. *Speciation and transport of heavy metals and macroelements during electroremediation.* Environmental Science and Techology, 37(1): 177 - 181.

Wong, P.-Z., 1999. *Conductivity, permeability, and electrokinetics.* In: P.-Z. Wong (Editor), Methods in the Physics of Porous Media. Experimental Methods in the Physical Sciences. Academic Press, San Diego, pp. 119 - 159.

Yeung, A.T., 1990. *Coupled flow equations for water, electricity and ionic contaminants through clayey soils under hydraulic, electrical and chemical gradients.* Journal of Non-Equilibrium Thermodynamics, 15(3): 247 - 267.

Yeung, A.T. and Mitchell, J.K., 1993. *Coupled fluid, electrical and chemical flows in soil.* Geotechnique,

43(1): 121 - 134.

Yeung, A.T., 1994. *Effects of electro-kinetic coupling on the measurement of hydraulic conductivity.* In: D.E. Daniel and S.J. Trautwein (Editors), Hydraulic Conductivity and Waste Contaminant Transport in Soils. American Society for Testing and Materials, Philadelphia, pp. 569 - 585.

Yu, T.R. and Ji, G.L., 1993. *Electrochemical Methods in Soil and Water Research.* Pergamon Press, Oxford, 462 pp.

Chapter 6

Quantifying the effect of membrane potential in chemical osmosis across bentonite membranes by virtual short-circuiting*

Katja Heister, Pieter J. Kleingeld and J.P. Gustav Loch

Abstract

Clay liners are charged membranes and show semipermeable behaviour regarding the flow of fluids, electrical charge, chemicals and heat. At zero gradients of temperature and hydrostatic pressure, a salt concentration gradient across a compacted clay sample induces not only an osmotic flux of water and diffusion of salt across the membrane but also an electrical potential gradient, defined as membrane potential. Laboratory experiments were performed on commercially available bentonite samples in a rigid-wall permeameter connected to two electrically insulated fluid reservoirs filled with NaCl solutions of different concentrations and equipped with Ag/AgCl electrodes to measure the electrical potential gradient. The effect of membrane potential could be cancelled out by short-circuiting the clay with the so-called virtual shortcut. Therewith the potential gradient across the sample is brought to zero with a negative feedback circuit. It was observed that the water flux and the diffusion of Cl^- were hindered by the occurrence of a membrane potential, indicating that an electroosmotic counterflow is induced. Flow parameters were calculated with modified coupled flow equations of irreversible thermodynamics. They were in excellent agreement with values reported in literature. Comparing the method of short-circuiting with a study elsewhere, where the electrodes were physically short-circuited, it was shown that the virtual shortcut is more appropriate because physically shortening induces additional effects that attribute to the fluxes.

Keywords
bentonite, clay membrane, coupled flow equations, diffusion, irreversible thermodynamics, membrane potential, osmosis, short-circuiting

* Heister, K., Kleingeld, P.J. and Loch, J.P.G. Quantifying the effect of membrane potential in chemical osmosis across bentonite membranes by virtual short-circuiting. Journal of Colloid and Interface Science. In press.

6.1 Introduction

Electrical potentials generated by chemical concentration gradients, so-called membrane potentials, play an important role in water transport in sediments of low hydraulic conductivity (< 10^{-9} m/s) like clays and clayey soils and sediments (Mitchell, 1991). A membrane separating two phases may be semipermeable regarding the transport of fluid, electrical charge, solutes and heat. These transport phenomena can be subdivided in direct and coupled phenomena depending on driving force considered and resulting flux across the membrane. Whereas direct flows are simply induced by their conjugated driving forces (e.g., a water flow induced by a hydraulic pressure difference across the membrane), coupled flows can be induced by various non-conjugated forces (e.g., osmosis, which is water flow induced by a chemical potential gradient).

The membrane potential is defined as the electrical potential gradient induced by a concentration gradient across a semipermeable membrane under isothermal conditions and constant pressure (Kobatake et al., 1965). Clay liners are charged membranes and show semipermeable behaviour. In the absence of a membrane, the presence of a salt concentration difference induces a liquid-junction diffusion potential due to the differences between the transport numbers of the cations and anions. Inserting a membrane between the two solutions results in a larger potential difference due to increase of the differences between the cation and anion transport numbers in the membrane. The change in transport numbers can be ascribed to anion exclusion in the negatively charged clay, while cations can freely enter the membrane but may be retarded inside. Consequently, a membrane potential develops with the concentrated solution negative with respect to the dilute solution (van Olphen, 1977). This potential counteracts further separation of charge (Revil, 1999). The maximum possible potential difference occurs across a perfect membrane that blocks the passage of one kind of ions, in this case anions, completely. These are called ideal semipermeable membranes (Katchalsky and Curran, 1967). However, membranes are seldom ideal and exhibit a leakage of the blocked ions. Accordingly, the membrane is less efficient and the membrane potential decreases. In addition, the observed membrane potential also has to be corrected for the transport of water through the membrane by chemical osmosis or by electroosmosis. After all, if water flow arises, also a streaming potential will be generated (van Olphen, 1977).

The analysis of these interrelated phenomena is important for understanding the motion of salt and water in soils and sediments. Recent research on membrane potentials within the framework of irreversible thermodynamics is mainly focused on artificial membranes (Benaventea and Jonsson, 1998; Fievet et al., 2000; Chaudry, 2002; Sbaï et al., 2003). However, the results of these studies are not applicable to clays because the cross-coupling of the fluxes and driving forces is not taken into account to the extent described above. Only few references dealing with clayey membranes are known with results relevant to this study (Elrick et al., 1976; Kocherginsky and Stucki, 2001).

In this study, laboratory experiments were performed on bentonite clay. An experimental set-up was designed that enables to quantify the effect of membrane potential by eliminating it and comparing the fluxes of water and solutes across the clay membrane in presence and absence of membrane potentials. From the data obtained, transport parameters were calculated making use of modified coupled flow equations of irreversible thermodynamics. It is shown that membrane potentials clearly affect osmotic water flow and diffusion of ions.

6.2 Governing equations

Under isothermal conditions, the fluxes to be considered across a semipermeable clay membrane are the flow of water, the electrical current and the flow of solutes. Accordingly, the set of equations from irreversible thermodynamics is established as

$$\begin{aligned} J_v &= L_{11}\nabla(-P) + L_{12}\nabla(-E) + L_{13}\nabla(-\mu) \\ I &= L_{21}\nabla(-P) + L_{22}\nabla(-E) + L_{23}\nabla(-\mu) \\ J_s &= L_{31}\nabla(-P) + L_{32}\nabla(-E) + L_{33}\nabla(-\mu) \end{aligned} \tag{6.1}$$

where J_v is the water flux density in m/s, I is the electrical current density in A/m², J_s is the solute flux density in mol/m²·s, P is the hydraulic pressure in N/m², E is the electrical potential in V, μ is the chemical potential in J/mol and L_{11} to L_{33} are the phenomenological coefficients in their corresponding units (Katchalsky and Curran, 1967; Yeung and Mitchell, 1993).

At zero value of all forces, all fluxes must vanish; so all relationships will have a first range, which may be considered to be linear within a required degree of accuracy (Groenevelt and Bolt, 1969).

The on-diagonal coefficients (L_{11}, L_{22}, L_{33}) describe direct flow processes according to Darcy's law, Ohm's law and Fick's law, respectively. It is assumed that Onsager's reciprocal relations are valid (Onsager, 1931a, b). So, the off-diagonal coefficients, known as 'cross-coefficients' are related as follows

$$L_{ij} = L_{ji} \quad (i, j = 1,2,3,\ldots) \tag{6.2}$$

According to the experimental conditions, it is assumed that the pressure gradient is negligible as the development of a hydraulic head is very small compared to e.g. the head applied in common hydraulic conductivity experiments in the laboratory, which often is rather high. Consequently, the set of equations reduces to

$$\begin{aligned} J_v &= L_{12}\nabla(-E) + L_{13}\nabla(-\mu) \\ I &= L_{22}\nabla(-E) + L_{23}\nabla(-\mu) \\ J_s &= L_{32}\nabla(-E) + L_{33}\nabla(-\mu) \end{aligned} \tag{6.3}$$

However, it should be noted that the Onsager's reciprocal relations are valid, if the driving forces are expressed as hydraulic pressure, electrical potential and chemical potential, respectively. In the laboratory, it is sometimes easier to express the driving forces in different units. Therefore, the set of equations has to be modified, as the phenomenological coefficients have to be expressed with other variables. The necessary transformations, parameter units and notations used, which are according to soil science literature, cf. Mitchell (1993), are described in the appendix, and finally, the set of equations is modified to

$$\begin{aligned} J_v &= k_e \cdot i_e + \frac{\nu\sigma k_h^*}{\gamma_f} RT \cdot i_c \\ I &= \kappa \cdot i_e + D|z|F \cdot i_c \\ J_s &= \frac{cD|z|F}{RT} \cdot i_e + D \cdot i_c \end{aligned} \tag{6.4}$$

Each of these fluxes can be partitioned as:

$$J_v = J_{ve} + J_{vc} \tag{6.5}$$

and

$$I = I_e + I_c \tag{6.6}$$

and

$$J_s = J_{se} + J_{sc} \tag{6.7}$$

The subscripts e and c denote the flux induced by the electrical gradient and the chemical gradient, respectively. However, the partition of the electrical current density (Eq. 6.6) has no use because the electrical gradient occurs in an isolated system in which the electrical current is zero.

With the modified set of equations described above, it is possible to determine some characteristic flow parameters like for example the diffusion coefficient, D, which can be compared with experimental data from the literature.

6.3 Materials and methods

In this study, a commercially available Wyoming bentonite marketed under the name Portaclay A90 (Ankerpoort, Maastricht, The Netherlands) is used as sample material. It consists mainly of montmorillonite with some traces of illite and quartz. Additional sample properties are given in Table 6.1. An amount of 5 g of air-dry powder is weighed into a mould with an internal diameter of 50 mm between two 15 µm nylon filters and two porous stones (ELE Intertest, Etten-Leur, The Netherlands) as support of the clay membrane. The pedestal on which the mould is placed has several channels to allow a homogeneous water flow in the porous stone lying on top of the pedestal. The piston placed on top of the upper porous stone has two flow channels connected to the outside of the piston. All parts of the rigid-wall permeameter consist of polyoxymethylene (POM) to ensure electrical insulation of the sample.

Table 6.1: Sample properties of the bentonite clay.

cation exchange capacity		$cmol_c/kg$	75.7 ± 2.8
cation occupation by	Na^+	$cmol_c/kg$	53.0 ± 1.9
	K^+	$cmol_c/kg$	1.5 ± 0.1
	Ca^{2+}	$cmol_c/kg$	26.6 ± 0.6
	Mg^{2+}	$cmol_c/kg$	7.8 ± 0.0
C_{org}-content		wt%	0.13
carbonate content		wt%	0.63
specific surface area	EGME[1]	m^2/g	611 ± 9

[1] ethylene glycol monoethyl ether

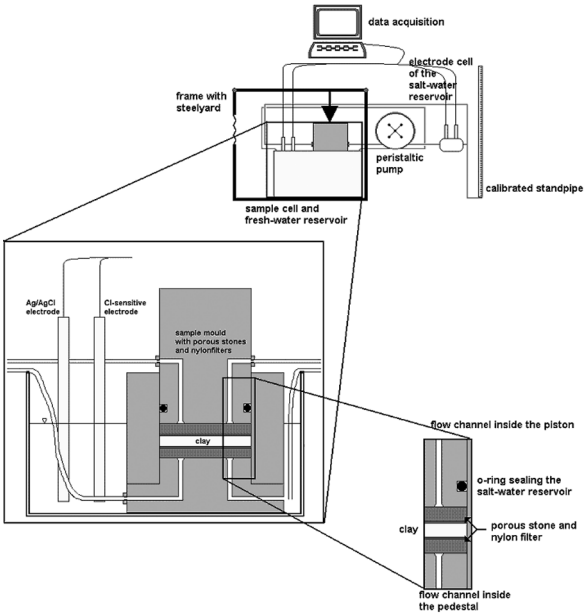

Figure 6.1: Schematic drawing of the experimental set-up. The rigid-wall permeameter with the clay sample in it and the fresh-water reservoir are shown enlarged and in transect in the bottom left corner.

Prior to the experiment, a fully saturated homogeneous clay membrane has to be obtained. Therefore, the bentonite powder inside the mould is first subjected to an overburden pressure of 20.3 MPa for approximately 30 minutes to obtain sufficient compaction. Then, the whole rigid-wall permeameter is placed in a bowl with NaCl solution of fresh-reservoir concentration (0.01 M NaCl). The clay is now able to take up the solution from below and to swell and get fully saturated. This takes two to three days and can be seen by monitoring the position of the piston relative to the mould.

After saturation, the rigid-wall permeameter is placed in a temperature-controlled chamber at 25 ± 0.4°C. By means of a frame with a steelyard, an overburden pressure can be applied through the piston on the clay membrane. It is of importance to apply a sufficient overburden load on the clay to avoid swelling of the specimen. The connectors of the permeameter are connected to the fluid reservoirs with PharMed tubings (Dépex, Houten, The Netherlands) whereby the bottom porous stone and the bowl of saturating solution act as fresh-water reservoir. The upper porous stone is connected to the salt-water reservoir that contains a calibrated standpipe to measure the induced water flow. Both reservoirs are continuously homogenized with a peristaltic pump (Ismatec Reglo-MS Analog – Dépex, Houten, The Netherlands) and are equipped with Cl^--sensitive electrodes (model 94-17B – Orion, Cambridge, MA, USA) and double-junction Ag/AgCl reference electrodes (model 90-02 – Thermo Orion, Beverly, MA, USA) to measure the salt concentration in the reservoirs and the electrical potential difference across the clay, respectively. As the salt-water reservoir is quite small compared to the fresh-water reservoir, the electrodes in the salt-water reservoir are mounted in an electrode-cell, whereas the electrodes in the fresh-water reservoir are directly placed into the bowl of solution. The potentials are monitored with an electrometer multi-channel controller (R305 – Consort, Turnhout, Belgium). A schematic overview of the set-up is given in Figure 6.1.

Before starting the experiment, both reservoirs are filled with the fresh-water solution (0.01 M NaCl). Thereby, attention has to be paid that the water level in the standpipe is equal to the water level in the fresh-water bowl to avoid an undesirable hydraulic gradient. Now, the set-up gets some

time to equilibrate. As there are no hydraulic or chemical gradients across the clay, the Ag/AgCl electrodes measure the zero potential. Then the solution in the salt reservoir is replaced by the salt-water solution; also here, care is taken that the water level in the standpipe equals the water level in the fresh-water bowl. The membrane potential induced by the salt concentration gradient can be measured directly in the reservoirs with the Ag/AgCl electrodes, since these reference electrodes have a well-defined electrical potential, which is independent to chemical and thermal difference within the accuracy of ± 1 mV of the measured membrane potentials. When the solution in the salt reservoir is completely replaced by the salt-water solution, the experiment starts. Membrane potential, salt concentrations and water flow will be monitored during the whole experiment.

To quantify the effect of membrane potential on the water flow and the diffusion of ions, a similar experiment has to be performed when the membrane potential is cancelled out by short-circuiting the Ag/AgCl electrodes. Physical shortening of electrodes based on salt bridges and AgCl solubility equilibrium is not viable because conducting electrical current through these electrodes induces unpredictable additional electrical junction-potentials. Electrodes capable of draining current, e.g. noble metal electrodes, develop high static potentials due to redox reactions in the order of hundreds of millivolts, which is an order of magnitude higher than the expected membrane potentials. Therefore, the membrane potential gradient is ruled out with a negative feedback compensation with a current that brings the potential gradient across the membrane to zero, the so-called 'virtual shortcut'. This compensation current is applied by two noble metal electrodes also inserted into the two reservoirs, respectively. Due to the fact that a current source is used to gain a zero potential across the separate Ag/AgCl electrodes, any additional junction-potential on the noble metal electrodes can be neglected.

For this 'shorted' experiment, sample preparation and launch are the same as described before. But after the salt water is pumped into the salt-water reservoir and the membrane potential is achieved, which occurs instantaneously, the noble metal electrodes are inserted into the reservoirs and connected to the current source, and by means of the negative feedback the potential difference is regulated until a zero potential gradient across the clay is obtained. During this shorted experiment, the water flow, the salt concentration in the reservoirs and the applied current are monitored.

When a set of experiments, consisting of a non-shorted and a shorted experiment, is completed, flow parameters can be calculated with the modified coupled flow equations.

Table 6.2: Test conditions of the three sets of experiments. In all experiments, the same commercially available bentonite is used as sample material.

name	overburden load	reservoir salt concentrations
experiment 1	0.18 bar	0.01 M — 0.1 M NaCl
experiment 2	1 bar	0.01 M — 0.1 M NaCl
experiment 3	1 bar	0.01 M — 0.05 M NaCl

6.4 Results

In the present study, three sets of experiments have been performed on samples of the same bentonite. The experimental conditions were chosen in that way that the effect of overburden pressure on the sample and the effect of salt concentration gradient could be studied. The specific test conditions are listed in Table 6.2.

In principle, all three sets of experiments showed the same behaviour. Applying a salt concentration gradient across the bentonite induced an electrical potential difference over the clay with the concentrated solution negative compared to the low concentrated solution. This behaviour is predicted by theory (van Olphen, 1977) and was experimentally confirmed by a comparable experiment on Fe-rich smectite by Kocherginsky and Stucki (2001). The extent of the electrical potential difference was directly proportional to the salt concentration difference; a higher salt concentration difference caused a larger electrical potential gradient. As the salt concentration difference decreases over time due to diffusion of ions from the high to the low concentration side and osmotic water flux vice versa, the electrical potential difference also vanishes (Fig. 6.2). Short-circuiting with aid of the virtual shortcut resulted in an increased osmotic water flow into the high concentration reservoir. The maximum height in the standpipe was reached sooner and was even larger than in the non-shorted experiments (Fig. 6.3). Moreover, the salt flux density increased in the shorted experiments, too, compared to the non-shorted experiments (Tab. 6.3).

By comparing the fluxes in the shorted and non-shorted experiments, the electrical induced fluxes can be calculated. As they are counteracting the total fluxes, they have a negative sign. All measured

Table 6.3: Measured and calculated fluxes and driving forces of the three experiments. The electrical water flux density and the electrical salt flux density are calculated by subtracting the osmotical flux densities from the total flux densities.

			experiment 1	experiment 2	experiment 3
total water flux density	J_v	m/s	$9.62 \cdot 10^{-10}$	$2.26 \cdot 10^{-9}$	$1.43 \cdot 10^{-9}$
osmotical water flux density	J_{vc}	m/s	$1.63 \cdot 10^{-9}$	$2.87 \cdot 10^{-9}$	$1.51 \cdot 10^{-9}$
electrical water flux density	J_{ve}	m/s	$-6.70 \cdot 10^{-10}$	$-6.09 \cdot 10^{-10}$	$-8.00 \cdot 10^{-11}$
electrical current density	I	A/m^2	$8.97 \cdot 10^{-3}$	$7.36 \cdot 10^{-5}$	$3.04 \cdot 10^{-5}$
total salt flux density	J_s	$mol/s \cdot m^2$	$6.13 \cdot 10^{-7}$	$1.99 \cdot 10^{-6}$	$1.28 \cdot 10^{-6}$
osmotical salt flux density	J_{sc}	$mol/s \cdot m^2$	$7.80 \cdot 10^{-6}$	$8.32 \cdot 10^{-6}$	$2.43 \cdot 10^{-6}$
electrical salt flux density	J_{se}	$mol/s \cdot m^2$	$-7.19 \cdot 10^{-6}$	$-6.32 \cdot 10^{-6}$	$-1.10 \cdot 10^{-6}$
chemical gradient	i_c	mol/m^4	$1.42 \cdot 10^{4}$	$3.09 \cdot 10^{4}$	$1.19 \cdot 10^{4}$
electrical gradient	i_e	V/m	-5.79	-7.67	-3.92

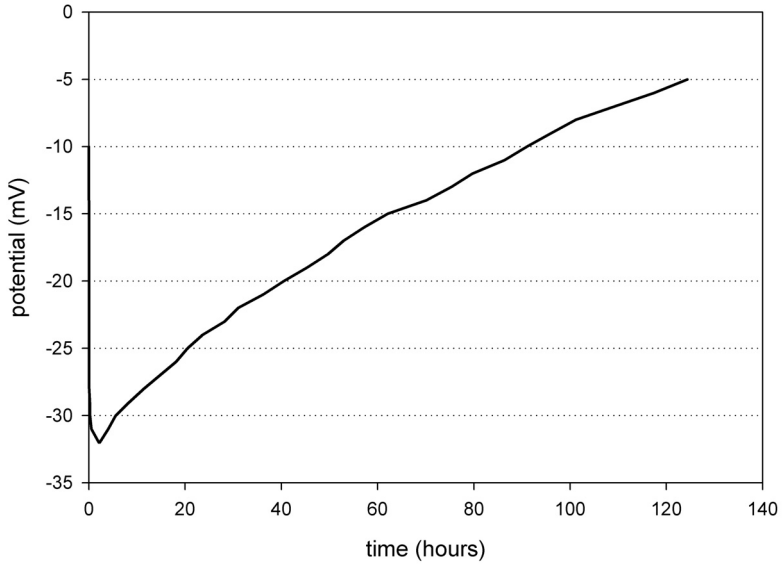

Figure 6.2: Development of the membrane potential over time in experiment 2 (0.01 M – 0.1 M NaCl, 1 bar overburden load).

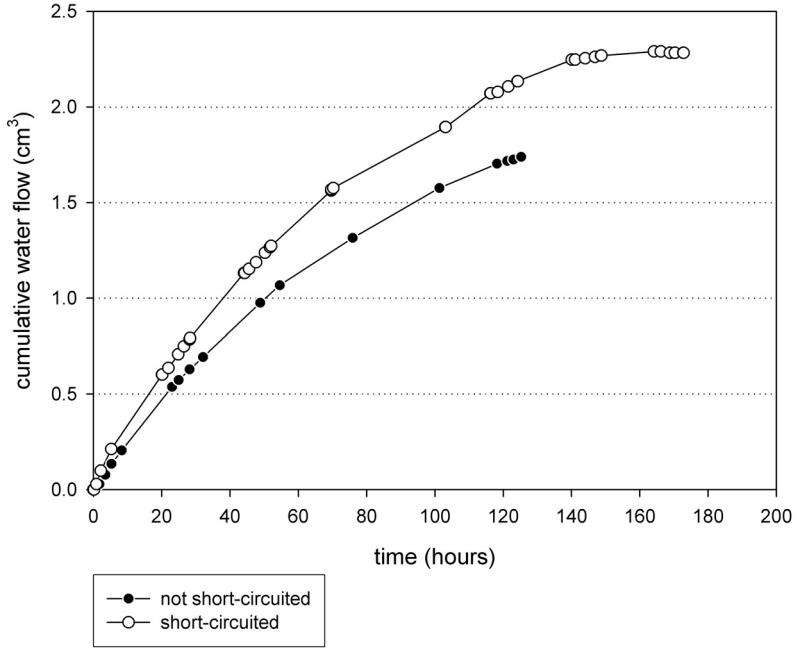

Figure 6.3: Cumulative water flow into the salt-water reservoir in experiment 2 (0.01 M – 0.1 M NaCl, 1 bar overburden load).

and calculated fluxes and driving forces are summarized in Table 6.3.

Therefore, it is concluded that the membrane potential occurring in the non-shorted experiments hinders the flow of ions and water in a way that the electrical potential gradient induces a counterflow of ions and water, respectively.

As can be seen from the values, the magnitude of electrically induced fluxes is not negligible. In experiment 2 (1 bar overburden, 0.01 M – 0.1 M NaCl), the electrical induced water flux amounts to 21% of the chemically induced water flux. At lower overburden load (experiment 1), this is higher, namely 41%; and at lower salt concentration gradient (experiment 3), 5% of the water flux is attributed to the induced electrical gradient. The same trend, but with even more noticeable values, is observed when comparing the salt flux densities in the shorted and non-shorted experiments. 76% of the salt flux is related to the electrical gradient in experiment 2. At lower salt concentration gradient (experiment 3), 45% of the salt flux is assigned to the membrane potential; and at lower overburden pressure and high salt concentration gradient (experiment 1), 92% of the salt flux is induced by the electrical gradient. This is not surprising, if we look at the electrical current density applied for virtual shorting, which was measured two orders of magnitude higher in experiment 1 than in the other two experiments.

It is assumed that the low overburden pressure in experiment 1 causes little overlap of the electrical double layers of the clay platelets. Consequently, the ions can move more freely through the pores. The differences between experiments 2 and 3 can be attributed to the halved salt concentration gradient. This results in an approximately halved membrane potential and subsequently, in smaller differences in the various fluxes. Because the membrane potential is by definition directly related to the salt concentration gradient, it is believed that the differences between the fluxes will also become smaller as the membrane potential becomes smaller due to a smaller salt concentration gradient.

6.5 Discussion

With the coupled flow equations derived in the appendix, various flow parameters were calculated. The hydraulic conductivity coefficient under shorted conditions, $k_h^\star$, necessary to calculate the reflection coefficient, σ, was adopted from an earlier experiment on streaming potentials by the authors with the same sample material at a solution concentration of 0.01 M NaCl and an overburden pressure of 1 bar (Heister et al., 2005). This parameter could not be measured within the laboratory set-up as described above due to the type of Ag/AgCl reference electrodes used. It is likely that the hydraulic conductivity coefficient will vary slightly between the three experiments; in earlier experiments, a factor of about 2 was observed. This will result in a slight variation of the reflection coefficient, σ. The flow parameters derived from all three experiments are listed in Table 6.4.

Comparing the flow parameters of the three experiments, it is noticeable that they vary only slightly which indicates that they are characteristic values of the sample material studied. The diffusion coefficient, D, is highest in experiment 1 and lowest in experiment 3. The same holds for the ionic mobility, u, that is linearly related to D. The calculated values of both parameters fall within the practical ranges of flow parameters for saturated fine-grained soils listed by Mitchell (1993): the diffusion coefficient between $2{\cdot}10^{-10}$ and $2{\cdot}10^{-9}$ m²/s, and the ionic mobility between $3{\cdot}10^{-9}$ and $1{\cdot}10^{-8}$ m²/Vs. As expected, the obtained coefficients of these experiments are very close to the minimum of these ranges because compacted bentonite is known to be very impermeable. The obtained

Table 6.4: Flow parameters of the three experiments calculated with the modified coupled flow equations of irreversible thermodynamics. The hydraulic conductivity coefficient under shorted conditions, k_h^*, is taken from a previous investigation and assumed to be constant for all experiments.

			experiment 1	experiment 2	experiment 3
diffusion coefficient	D	m^2/s	$5.49 \cdot 10^{-10}$	$2.70 \cdot 10^{-10}$	$2.04 \cdot 10^{-10}$
ionic mobility	u	m^2/Vs	$2.14 \cdot 10^{-8}$	$1.05 \cdot 10^{-8}$	$7.94 \cdot 10^{-9}$
electroosmotic conductivity coefficient	k_e	m^2/Vs	$1.16 \cdot 10^{-10}$	$7.94 \cdot 10^{-11}$	$2.05 \cdot 10^{-11}$
hydraulic conductivity coefficient	k_h^*	m/s	$2.34 \cdot 10^{-11}$	$2.34 \cdot 10^{-11}$	$2.34 \cdot 10^{-11}$
electrical conductivity coefficient	κ	S/m	0.13	0.105	0.0598
reflection coefficient	σ	-	0.0194	0.0157	0.0214

Table 6.5: Calculated flow parameters of the three experiments, if the membrane potential is not taken into account. Only those three parameters, on which this has a bearing, are listed.

			experiment 1	experiment 2	experiment 3
apparent diffusion coefficient	D'	m^2/s	$4.31 \cdot 10^{-11}$	$6.46 \cdot 10^{-11}$	$1.08 \cdot 10^{-10}$
apparent ionic mobility	u'	m^2/Vs	$1.68 \cdot 10^{-9}$	$2.52 \cdot 10^{-9}$	$7.12 \cdot 10^{-9}$
apparent electrical conductivity coefficient	κ'	S/m	0.0102	0.0251	0.0536

electroosmotic conductivity coefficients, k_e, are all somewhat lower than the minimum value mentioned by Mitchell (1993), who set the range between $1 \cdot 10^{-9}$ and $1 \cdot 10^{-8}$ m^2/Vs. The deviation is very small and also ascribed to the low permeability due to the high compaction of the sample. The hydraulic conductivity coefficient, k_h^*, obtained from an earlier experiment, is also very close to the minimum value of Mitchell (1993), which is $1 \cdot 10^{-11}$ m/s. Considering the range of electrical conductivity coefficients, κ, of 0.01 to 1.0 S/m as stated by Mitchell (1993), it is concluded that also this parameter is in perfect agreement with literature data, although the variation of this coefficient is definitely higher than of the other coefficients calculated here. The electrical conductivity coefficient decreases with decreasing salt concentration difference across the clay membrane. The decrease in electrical conductivity can be explained with electrical double-layer theory. The lower the salt concentration in the pores of the clay, the thicker the electrical double layers of the clay platelets are, subsequently, the more they overlap. Overlapping double layers hinder the transport of ions through the pores. Only surface conduction will be possible, if the overlap and the blockage of the pores are ideal (Fievet et al., 2001). Finally, the variation in the reflection coefficient, σ, which is the degree of semipermeability of the membrane, is again very small (cf. Keijzer and Loch, 2001). Ideal semipermeable membranes have a reflection coefficient of 1, whereas the reflection coefficient of membranes without semipermeability equals zero (Katchalsky and Curran, 1967). All calculated values of the reflection coefficient are close to zero, indicating that the semipermeable property of the bentonite is not very high. However, to calculate the reflection coefficient, the hydraulic conductivity coefficient has to be known. As this value is taken from another experiment and set equal for all three experiments, the actual reflection coefficients could vary somewhat more.

The effect of membrane potential on the flow parameters is illustrated by calculating the coefficients again while neglecting the membrane potential, e.g. by calculating the diffusion coefficient from the salt flux density in the non-shorted experiment. From the coupled flow equations, it can be seen, that the membrane potential affects not only the diffusion coefficient but also subsequently the ionic mobility and the electrical conductivity coefficient. The values, which would be obtained if the membrane potential was not taken into account, are listed in Table 6.5. It can be seen that, if membrane potential is not taken into account, diffusion coefficient, ionic mobility and electrical conductivity coefficient are clearly lower. The deviation is largest in experiment 1, which was shown to have the largest difference in salt flux and water flux density between non-shorted and shorted conditions due to the low compaction of the sample. The smallest deviation is observed in experiment 3. It is concluded that the deviation becomes smaller as the gradients are smaller. The virtual shortcut is expected to have the largest effect in experiments with high chemical and subsequently electrical gradients.

Fievet et al. (1999) presented a theoretical study of diffusion-driven transport phenomena by means of the space-charge model. Thereby, the assumption was made that the hydraulic pressure gradient is taken equal to zero, which is also assumed in the present investigation. But contrary to this study, Fievet et al. subsequently omitted the equation describing the water flux density, thus neglecting osmotically driven water flow, which is of great importance in clayey materials. Consequently, this study and also other studies already mentioned dealing with artificial membranes cannot be used for comparison.

More recently, coupled flow equations for a bentonite plug were reported by Chatterji (2004), whose equations are not complete as he neglected the hydraulic pressure gradient. This is justified by the fact that the hydraulic pressure evolving is very small. The same assumption was made in the

present study to derive the modified coupled flow equations. However, Chatterji (2004) also neglected the equation describing the water flux, which is only considered appropriate in the case of diffusion experiments, if no water flow occurs. But this is not negligible in the system described here, where a definite osmotic water flow is measured. Consequently, this set of equations is also not viable to compare the results with the ones of the present study. But apart from the formulation of the coupled flow equations, he drew some other interesting conclusions.

While looking at the diffusion experiment from Dutt and Low (1962), Chatterji (2004) explained their results regarding the transport of ions through bentonite pastes by the presence of an electrical induced flux simultaneous with the chemical induced flux. The sum of these two components form the phenomenological ion flux observed in the experiment. Although, Chatterji did not employ the term membrane potential, his explanation agrees very well with the results obtained in this study. As in the present paper, Chatterji observed that the diffusivity of Cl^- ions due to the chemical gradient is higher than the observed phenomenological diffusivity, and that consequently, an electrically induced component counteracts the chemical diffusivity. This is in perfect agreement with the results of this study, where short-circuiting the clay plug results in an increased salt flux, which was determined with Cl^--sensitive electrodes. On the other hand, Chatterji stated that the chemical diffusivity of Na^+ions is lower than the measured phenomenological diffusivity, and that the electrical potential gradient that decreases the diffusivity of Cl^- simultaneously increases that of Na^+. So, the developed electrical potential gradient unifies the diffusivities of the two species by counteracting the charge separation (Revil, 1999). Unfortunately, Chatterji's findings regarding the behaviour of sodium cannot be confirmed from our experiments, as sodium concentrations have not been measured.

The only investigation with a comparable experimental approach was reported by Elrick et al. (1976). A saturated montmorillonite sample was clamped between two solution reservoirs filled with NaCl solutions of different concentrations. The salt concentrations in their reservoirs were determined by intermittent conductivity measurements. The hydraulic pressure and the electrical potential, the latter by means of Ag/AgCl electrodes, were continuously recorded. To investigate the effect of the induced electrical potential gradient, the Ag/AgCl electrodes were periodically physically shorted. The results obtained in the non-shorted part are very similar to the results of this paper. First, a hydraulic pressure gradient evolved due to osmosis, which subsequently decreased slightly over time, ascribed to the deficiency of the semipermeability of the clay membrane. The concentration difference decreased slightly due to diffusion and was directly related to the small decrease in electrical potential gradient measured. Although these results are in excellent agreement with the findings of this study, the observed behaviour in the shorted part of the experiment and the explanations are very different. As the electrical potential gradient vanished, Elrick et al. (1976) observed an evident decrease in the concentration difference and a reversal of the hydraulic pressure across the clay, subsequently returning to zero.

Although the acceleration of the diffusion of Cl^- ions by short-circuiting the clay membrane was also found in our study, their effect on the hydraulic pressure was not reproduced in the behaviour of the water flow by virtual short-circuiting. The water flow was accelerated by short-circuiting, which we explain by the abolition of the electrically induced counterflow, but this cannot explain the observations by Elrick et al. (1976). We concluded that the behaviour of the hydraulic pressure is produced by the physical short-circuiting of the Ag/AgCl electrodes. Shorting the electrodes means that an electrical current is conducted through the electrodes. In our case, shorting salt-bridge

electrodes means adding an unpredicted voltage due to serial resistance of the electrodes and an additional voltage due to enhanced different mobilities of the potassium and chloride ions in the liquid junction. Moreover, also an unknown part of the AgCl will be mobilized. In fact, in the experiment of Elrick et al., a water flow is induced by the enhanced different mobilities of the ions in solution. These effects are minimized by a four-electrode system like the virtual shortcut, where the actual potential measurement is performed by non-(ion-)current conducting electrodes. Groenevelt et al. (1978) calculated an even greater change in the hydraulic pressure difference and attributed this and its subsequent decrease to the 'shorting efficiency' of the electrodes. Of course, conducting electrical current through the Ag/AgCl electrodes causes dissolution of AgCl at one electrode. Consequently, the shorting efficiency finally drops to zero when this electrode has lost all its AgCl. Then the system would behave as in a non-shorted situation again. The maximum shorting efficiency was found to be only 18% (Groenevelt et al., 1978). In contrast, the virtual shortcut takes the continuous change in the electrical potential gradient into account and therefore leads to a shorting efficiency of 100% throughout the whole shorting period. Thus, it is concluded that short-circuiting a clay membrane in this kind of experimental set-up is more appropriate by the virtual shortcut. As a consequence, the results obtained in this study better reflect the effect of membrane potential on the induced water flow and diffusion of ions across the membrane.

6.6 Conclusions

In the laboratory, membrane potentials – electrical gradients across a semipermeable membrane induced by a salt concentration gradient – on compacted bentonite samples were measured in a rigid-wall permeameter with Ag/AgCl reference electrodes. To quantify the effect of membrane potential on osmotic water flow and diffusion of ions, the membrane potential was cancelled out with a negative feedback current applied by means of two noble metal electrodes inserted in the solution reservoirs on both sides of the clay, the so-called virtual shortcut.

It was observed that membrane potentials are directly related to the salt concentration difference, and that short-circuiting the clay with the virtual shortcut resulted in an increased osmotic water flow and accelerated diffusion of Cl^- ions. Obviously, the membrane potential induces an electroosmotic counterflow. This effect is larger as the salt concentration difference increases. Within the range of overburden loads studied, it was observed that the higher the compaction, the smaller the effect of shorting.

Using the coupled flow equations and Onsager's reciprocal relations of irreversible thermodynamics, various transport parameters were calculated. As not much research is done on the effect of membrane potentials in clays, it is difficult to compare the obtained results with literature data. However, the calculated flow parameters are all in the range expected from literature.

Comparing the results with a similar experiment reported in literature, where the Ag/AgCl reference electrodes have been physically shorted, it was concluded that the virtual shortcut is a more appropriate way to quantify the effect of membrane potential.

6.7 Appendix: Modification of the coupled flow equations

To calculate characteristic flow parameters, like for example the diffusion coefficient, the valid coupled flow equations of irreversible thermodynamics (Eq. 6.3) need to be modified. This section deals with the derivation of the six phenomenological coefficients, so that an utilizable set of equations will emerge (Eq. 6.4).

Because the units of the water flux density and the electrical gradient remain unchanged, the L_{12}-coefficient is identical to the electroosmotic conductivity coefficient, k_e (m^2/Vs). So, the term relating the water flux density and the electrical gradient can be expressed as

$$J_{ve} = k_e \cdot i_e \tag{6.A.1}$$

in which J_{ve} is the water flux density due to the electrical gradient in m/s, and i_e is the electrical gradient in V/m.

According to Ohm's law, the L_{22}-term can be rephrased as

$$I_e = \kappa \cdot i_e \tag{6.A.2}$$

where I_e is the electrical current density due to the electrical gradient in A/m^2 and κ is the electrical conductivity coefficient in S/m.

According to Mitchell (1993), L_{32} can be rewritten as the product of the concentration c and the ionic mobility u. Subsequently, the ionic mobility can also be rewritten according to the Nernst-Einstein equation. So, it follows that

$$J_{se} = c\frac{D|z|F}{RT} \cdot i_e \tag{6.A.3}$$

where J_{se} is the solute flux density due to the electrical gradient in $mol/m^2 \cdot s$, D is the diffusion coefficient according to Fick's law in m^2/s, z is the valence of the ion, F is the Faraday constant in C/mol, and R and T are the gas constant in J/K·mol and the temperature in K, respectively.

According to Fick's law, the L_{33}-coefficient can be replaced by the diffusion coefficient D as follows:

$$J_{sc} = D \cdot i_c \tag{6.A.4}$$

where J_{sc} is the solute flux density due to the chemical gradient in $mol/m^2 \cdot s$, and i_c is the chemical gradient in mol/m^4.

The second term in the expression for J_v will be expressed as

$$J_{vc} = \frac{\nu\sigma k_h^*}{\gamma_f} RT \cdot i_c \tag{6.A.5}$$

where J_{vc} is the water flux density due to chemical osmosis in m/s, ν is the dissociation factor coming from the van't Hoff equation, σ is the dimensionless reflection coefficient, k_h^* is the hydraulic conductivity coefficient under short-circuited conditions in m/s, and γ_f is the unit weight of the fluid in N/m^3.

Finally, the second term in the expression for I will be rephrased as

$$I_c = D|z|F \cdot i_c \tag{6.A.6}$$

where I_c is the electrical current density due to the chemical gradient in A/m^2.

Combining all this, the complete set of equations is as follows:

$$\begin{aligned} J_v &= k_e \cdot i_e + \frac{\nu\sigma k_h^*}{\gamma_f} RT \cdot i_c \\ I &= \kappa \cdot i_e + D|z|F \cdot i_c \\ J_s &= \frac{cD|z|F}{RT} \cdot i_e + D \cdot i_c \end{aligned} \tag{6.A.7}$$

References

Benaventea, J. and Jonsson, G., 1998. *Electrokinetic characterization of a microporous non-commercial polysulfone membrane: Phenomenological coefficients and transport parameters.* Colloids and Surfaces A: Physicochemical and Engineering Aspects, 140: 339 - 346.

Chatterji, S., 2004. *Ionic diffusion through thick matrices of charged particles.* Journal of Colloid and Interface Science, 269: 186 - 191.

Chaudry, M.A., 2002. *Water and ions transport mechanism in hyperfiltration with symmetric cellulose acetate membranes.* Journal of Membrane Science, 206: 319 - 332.

Dutt, G.R. and Low, P.F., 1962. *Diffusion of alkali chlorides in clay-water systems.* Soil Science, 93: 233 - 240.

Elrick, D.E., Smiles, D.E., Baumgartner, N. and Groenevelt, P.H., 1976. *Coupling phenomena in saturated homo-ionic montmorillonite: I. Experimental.* Soil Science Society of America Journal, 40: 490 - 491.

Fievet, P., Aoubiza, B., Szymczyk, A. and Pagetti, J., 1999. *Membrane potential in charged porous membranes.* Journal of Membrane Science, 160: 267 - 275.

Fievet, P., Szymczyk, A., Aoubiza, B. and Pagetti, J., 2000. *Evaluation of three methods for the characterisation of the membrane-solution interface: streaming potential, membrane potential and electrolyte conductivity inside pores.* Journal of Membrane Science, 168: 87 - 100.

Fievet, P. et al., 2001. *Determining the zeta potential of porous membranes using electrolyte conductivity inside pores.* Journal of Colloid and Interface Science, 235: 383 - 390.

Groenevelt, P.H. and Bolt, G.H., 1969. *Non-equilibrium thermodynamics of the soil-water system.* Journal of Hydrology, 7: 358 - 388.

Groenevelt, P.H., Elrick, D.E. and Blom, T.J.M., 1978. *Coupling phenomena in saturated homo-ionic montmorillonite: III. Analysis.* Soil Science Society of America Journal, 42(5): 671 - 674.

Heister, K., Kleingeld, P.J., Keijzer, T.J.S. and Loch, J.P.G., 2005. *A new laboratory set-up for measurements of electrical, hydraulic, and osmotic fluxes in clays.* Engineering Geology, 77(3-4): 295 - 303.

Katchalsky, A. and Curran, P.F., 1967. *Non-Equilibrium Thermodynamics in Biophysics.* Harvard University Press, Cambridge, MA, USA, 248 pp.

Keijzer, T.J.S. and Loch, J.P.G., 2001. *Chemical osmosis in compacted dredging sludge.* Soil Science Society of America Journal, 65: 1045 - 1055.

Kobatake, Y., Takeguchi, N., Toyoshima, Y. and Fujita, H., 1965. *Studies of membrane phenomena. I. Membrane potential.* Journal of Physical Chemistry, 69(11): 3981 - 3988.

Kocherginsky, N.M. and Stucki, J. W., 2001. *Supported clay membrane: A new way to characterize water and ion transport in clays.* Advances in Environmental Research, 5: 197 - 201.

Mitchell, J.K., 1991. *Conduction phenomena: From theory to geotechnical practice.* Geotechnique, 41(3): 229 - 340.

Mitchell, J.K., 1993. *Fundamentals of Soil Behavior.* John Wiley & Sons, Inc., New York, 437 pp.

Onsager, L., 1931a. *Reciprocal relations in irreversible processes I.* Physical Review, 37: 405 - 426.

Onsager, L., 1931b. *Reciprocal relations in irreversible processes II.* Physical Review, 38: 2265 - 2279.

Revil, A., 1999. *Ionic diffusivity, electrical conductivity, membrane and thermoelectric potentials in colloids and granular porous media: A unified model.* Journal of Colloid and Interface Science, 212: 503 - 522.

Sbaï, M. et al., 2003. *Streaming potential, electroviscous effect, pore conductivity and membrane potential for the determination of the surface potential of a ceramic ultrafiltration membrane.* Journal of Membrane Science, 215: 1 - 9.

van Olphen, H., 1977. *An Introduction to Clay Colloid Chemistry.* John Wiley, New York, 318 pp.

Yeung, A.T. and Mitchell, J.K., 1993. *Coupled fluid, electrical and chemical flows in soil.* Geotechnique, 43(1): 121 - 134.

Chapter 7

Induced membrane potentials in chemical osmosis across clay membranes*

Katja Heister, Pieter J. Kleingeld and J.P. Gustav Loch

Abstract

Clay layers act as semipermeable membranes in the flow of fluids, electrical charge, chemicals and heat. At zero gradients of temperature and hydrostatic pressure, a salt concentration gradient across compacted clay induces osmotic flow of water, diffusion of salt and an electrical potential gradient, the so-called membrane potential. Laboratory experiments were performed on samples of Boom Clay (Mol, Belgium) and Calais Clay (polder Groot Mijdrecht, The Netherlands) in a rigid-wall permeameter set-up. With this set-up, the induced osmotic flow of water, the diffusion of Cl^- ions and the membrane potential were measured. To quantify the effect of membrane potential, the electrical potential gradient was cancelled out by virtual short-circuiting the clay membrane. In the experiments with Boom Clay, it was shown that the occurrence of a membrane potential hindered the water flux and the diffusion of Cl^- by inducing an electroosmotic counterflow. Flow parameters calculated with coupled flow equations of irreversible thermodynamics were in excellent agreement with values reported in literature. In the experiments with oxidized Calais Clay, no osmotic water flow and membrane potential were observed. Calculated diffusion coefficients suggest that the clay membranes are intact. In a control experiment with kaolinite, believed to be a less efficient semipermeable membrane, apart from diffusion very small osmotic water flow and membrane potential were observed, indicating that the semipermeable behaviour of the Calais Clay is less than that of kaolinite or even nonexistent.

Keywords
clay membrane, coupled flow equations, diffusion, irreversible thermodynamics, membrane potential, osmosis, semipermeability

* Heister, K., Kleingeld, P.J. and Loch, J.P.G. Induced membrane potentials in chemical osmosis across clay membranes. Submitted.

7.1 Introduction

Experimental and modelling investigations have shown that clay liners exhibit semipermeable properties (Fritz, 1986). These semipermeable properties are caused by the negative charge of the clay platelets and the compaction of the clay causing diffuse double layers to overlap in the pore space of the clay liners. Due to overlapping double layers, the passage of ions through the clay is hindered, whereas water and non-charged molecules can pass (Mitchell, 1993). So, if a clay layer separates two solutions of different ionic strength, osmotic water flow occurs, i.e. water will flow through the clay from the low-concentration side to the high-concentration side.

Osmosis belongs to the coupled flow phenomena and can be described within the framework of irreversible thermodynamics. In this context, a distinction is made between direct and coupled flows. Direct flows are flows induced by their conjugated driving force, like e.g. water flow induced by a hydraulic gradient. Coupled flows are flows induced by non-conjugated driving forces, like e.g. osmotic water flow, a water flow induced by a chemical potential gradient (Yeung and Mitchell, 1993). Across a semipermeable membrane, flows of water, chemicals, electrical charge and heat can occur directly by hydraulic, chemical, electrical and temperature gradients, respectively. Table 7.1 gives an overview of all possible phenomena that can occur. The direct flows are on-diagonal, whereas the coupled flows are off-diagonal (Mitchell, 1993; Yeung, 1994; Horseman et al., 1996).

Under isothermal conditions, the set of equations from irreversible thermodynamics is established as:

$$\begin{aligned} J_v &= L_{11}\nabla(-P) + L_{12}\nabla(-E) + L_{13}\nabla(-\mu) \\ I &= L_{21}\nabla(-P) + L_{22}\nabla(-E) + L_{23}\nabla(-\mu) \\ J_s &= L_{31}\nabla(-P) + L_{32}\nabla(-E) + L_{33}\nabla(-\mu) \end{aligned} \tag{7.1}$$

Table 7.1: Direct and coupled flow phenomena (Mitchell, 1993; Yeung, 1994; Horseman et al., 1996).

Flow J	Gradient X			
	Hydraulic	Electrical	Chemical	Thermal
Fluid	Hydraulic conduction *Darcy s law*	Electroosmosis	Chemical osmosis	Thermoosmosis
Current	Streaming potential	Electrical conduction *Ohm s law*	Diffusion and membrane potentials	Thermoelectricity Seebeck effect
Ion	Streaming current	Electrophoresis	Diffusion *Fick s law*	Thermal diffusion of electrolyte Soret effect
Heat	Isothermal heat transfer	Peltier effect	Dufour effect	Thermal conduction *Fourier s law*

where J_v is the water flux density in m/s, I is the electrical current density in A/m² and J_s is the salt flux density in mol/m²·s; P is the hydraulic pressure in N/m², E is the electrical potential in V, μ is the chemical potential in J/mol and finally, L_{11} to L_{33} are the phenomenological coefficients in their corresponding units (Katchalsky and Curran, 1967; Yeung and Mitchell, 1993).

The direct flow processes according to Darcy's law, Ohm's law and Fick's law are described by the on-diagonal coefficients L_{11}, L_{22} and L_{33}, respectively. As it is assumed that Onsager's reciprocal relations are valid, the off-diagonal coefficients, also called cross-coefficients, describing the coupled flow processes are related as follows (Onsager 1931a, b):

$$L_{ij} = L_{ji} \quad (i, j = 1,2,3,...) \tag{7.2}$$

Osmosis in clays is of importance in various environments, e.g. in salt-water intrusion in near coastal areas or in sealing applications of waste deposits. Especially, where clays are employed due to their low hydraulic permeability, osmotic induced water flow can be of significance.

However, the ability of a clay layer to act as a semipermeable membrane is influenced by several factors, e.g. type of clay and porosity (Marine and Fritz, 1981; Fritz, 1986). The efficiency of the membrane is expressed in the reflection coefficient, σ (Katchalsky and Curran, 1967). The reflection coefficient varies between zero and one. If the membrane is ideal, the reflection coefficient is one; if a membrane does not have semipermeable properties at all, the reflection coefficient equals zero. However, clay membranes are seldom ideal. Salt ions leak through the membrane due to diffusion lowering the osmotic efficiency (Katchalsky and Curran, 1967).

Until today, many bench-scale experiments were performed in the laboratory to study osmotic behaviour of clays and clayey materials (Elrick et al., 1976; Cey et al., 2001; Keijzer and Loch, 2001; Malusis et al., 2001). Moreover, osmosis was investigated by modelling field situations (Marine and Fritz, 1981; Soler, 2001; Noy et al., 2004) and laboratory experiments with pure homoionic clays and single salt solutions (Groenevelt and Elrick, 1976). In the latter case, cation exchange is absent. Irreversible thermodynamics is often used for modelling (Yeung, 1990; Yeung and Mitchell, 1993), by which also other coupled flow phenomena can be quantified.

If a saturated clay membrane is subjected to a salt concentration gradient under isothermal conditions without hydrostatic pressure differences, not only osmotic water flow and diffusion of ions will be induced, but also an electrical potential gradient across the clay membrane, called the membrane potential (Kobatake et al., 1965). It has been shown that the membrane potential in turn influences the fluxes of water and ions (Elrick et al., 1976; Groenevelt et al., 1978; Heister et al., in press). However, the effect of membrane potential is not taken into account in laboratory studies on natural clays and clayey sediments (e.g. Cey et al., 2001).

In the present study, laboratory experiments were performed on several natural clayey materials. To quantify the effect of membrane potential, it was cancelled out by virtual short-circuiting the clay membrane. With modified coupled flow equations of irreversible thermodynamics, flow parameters were calculated and the effect of membrane potential was demonstrated.

7.2 Materials and methods

7.2.1 Materials

Two different natural clay deposits were investigated in the present study. The first is the Boom Clay coming from northern Belgium, the second is a Calais Clay sampled in the polder Groot Mijdrecht southeast of Amsterdam, The Netherlands.

The Boom Clay Formation is an Oligocene formation extending in northeastern Belgium (Aertsens et al., 2004). The clay sample was kindly provided by SCK·CEN, located in Mol, where the Boom Clay is found at 170 – 270 m depth (Bernier et al., 1997) and extensively studied in an underground research laboratory to investigate its feasibility to serve as a candidate host rock for geological disposal of high-level and long-lived radioactive waste. Boom Clay is supposed to be the main barrier for the isolation of the radionuclides whose migration through the clay is mainly by diffusion (Maes et al., 1998).

The Boom Clay sample investigated in this study originates from excavation works of a connexion gallery in February 2002 between the second shaft and the Test drift of the Hades Underground Research Laboratory of SCK·CEN. The depth of the connexion gallery is 223 m below the ground level at Mol. The clay sample is from the Rupelian Putte Member of the Boom Formation, which is characterized by dark clay and a relatively high organic matter content (cf. Tab. 7.2). After excavation, the clay was immediately packed in an aluminium-coated polyethylene foil under vacuum to avoid pyrite oxidation and desiccation. The clay was kept at 4°C to minimize microbial growth before it was transported to our laboratory.

The Boom Clay consists of about 60% of clay minerals (illite, smectite and kaolinite) and about 20% of quartz. It may also contain feldspars, pyrite, siderite and organic matter (Bernier et al., 1997; Aertsens et al., 2004). The existence of pyrite indicates that anaerobic conditions are prevailing in-

Table 7.2: Sample properties of the two investigated field clays. The cation exchange capacity of the Calais Clay is expected to be higher due to cation occupation of Al^{3+} on the exchange sites. Al^{3+} originates from degeneration of the clay particles by acidification indicated by the low pH. However, Al^{3+} could not be measured with the method used.

			Boom Clay	Calais Clay
cation exchange capacity		$cmol_c/kg$	22.9 ± 3.0	14.0 ± 0.4
cation occupation by	Na^+	$cmol_c/kg$	11.2 ± 0.2	3.5 ± 0.2
	K^+	$cmol_c/kg$	3.6 ± 0.1	1.0 ± 0.0
	Ca^{2+}	$cmol_c/kg$	10.7 ± 0.2	11.6 ± 0.4
	Mg^{2+}	$cmol_c/kg$	7.2 ± 0.2	9.0 ± 0.2
C_{org}-content		wt%	1.26	3.69
carbonate content		wt%	2.76	0.29
specific surface area	with EGME*	m^2/g	129 ± 9	88 ± 8
pH			9	3

* ethylene glycol monoethyl ether

situ (Beaucaire et al., 2000). Consequently, the Boom Clay is a moderately swelling clay that shows self-healing capacity. Additional sample properties for characterization of the clay are given in Table 7.2.

The Calais Clay is sampled in the polder Groot Mijdrecht near Nessersluis at a depth of 1.6 – 1.8 m. It is a brackish tidal sediment deposited in the Atlanticum and early Subboreal during marine transgressions. During the regressions, peat layers were formed, which are intercalated in the clay (Stichting voor Bodemkartering, 1970). Under anaerobic conditions, pyrite is accumulated in the organic matter, since soil bacteria reduce the marine sulphate in the sediments. But if the soil is drained, oxidation will occur. Depending on the amount of lime and alkaline cations, the soil will become acidic. Finally, the clay will exhibit characteristic yellow spots of acid reacting sulphate precipitates like e.g. jarosite and is termed 'acid sulphate soil' (Poelman, 1966). In the grassland, where the clay is sampled, the groundwater table is so high that the samples taken are under anaerobic conditions in the field. However, because the clay has a low carbonate content, it is expected that acid sulphate soil will be formed by oxidation in the laboratory. Such a clay is also named 'potential acid sulphate soil' (in Dutch: katteklei).

The Calais Clay consists of a mixture of illite, smectite and kaolinite. The main non-clay mineral is quartz. Swelling of the clay during saturation is expected to be negligible. Moreover, the clay contains a high amount of organic matter. Additional sample properties for characterization are also given in Table 7.2. These data were determined on the clays after a storage period of 17 months.

To facilitate comparison, both sample materials were primarily air-dried and ground in an agate mortar. As both initial sedimentary conditions were anaerobic, oxidation of the clay is expected during drying. However, oxidation reactions were not observed by visual inspection in the Boom Clay, whereas oxidation of the Calais Clay into an acid sulphate soil was evident. The degree of oxidation is noticeable in the pH of the clay. The Boom Clay was measured to have pH 9 and did not differ significantly from anaerobic Boom Clay samples, which have a pH of about 8.5 (Maes et al., 1998, 1999). The pH of the Calais Clay dropped to pH 3 after oxidation during storage.

The clay membranes were prepared by weighing the dry clay powder into the sample mould for compaction and subsequent saturation as described below. Accordingly, the porosities obtained by this method are not comparable to the corresponding field situations. For the Boom Clay at 223 m depth, a porosity of 36 – 40% is reported (Bernier et al., 1997), whereas for the shallow Calais Clay, a much higher porosity can be expected.

It should be emphasized that the objective was to compare directly the different materials as present in the laboratory and not to quantify the processes in the field situation.

7.2.2 Method

The dry clay powder is weighed into a mould with an internal diameter of 50 mm between two 15 μm nylon filters and two porous stones (ELE Intertest, Etten-Leur, The Netherlands) that act as support of the clay membrane. The pedestal in the base of the mould has several channels to allow a homogeneous water flow in the porous stone. The piston on top of the upper porous stone has two flow channels leading to the outside of the piston. Those three parts, which consist all of polyoxymethylene (POM) to ensure electrical insulation of the sample, form a rigid-wall permeameter. Inside this permeameter, the clay powder is first subjected to an overburden pressure of 20.3 MPa for approximately 30 minutes to obtain sufficient compaction. Then, the whole

permeameter is placed into a bowl of 0.01 M NaCl solution ('fresh-water' concentration). The dry clay powder takes up this solution to get fully saturated and possibly swell. Depending on the amount and type of clay, this takes one to three days.

After saturation, the rigid-wall permeameter is placed in a temperature-controlled chamber at 25 ± 0.4°C. An overburden pressure of 1 bar is applied through the piston on the clay membrane by means of a frame with a steelyard. The bowl, in which the rigid-wall permeameter is immersed, acts as the fresh-water reservoir. The upper porous stone is connected to a salt-water reservoir via the flow channels of the piston. Both reservoirs are equipped with Cl^--sensitive electrodes (model 94-17B – Orion, Cambridge, MA, USA) and double-junction Ag/AgCl reference electrodes (model 90-02 – Thermo Orion, Beverly, MA, USA) to measure the salt concentration in the reservoirs and the electrical potential difference across the clay, respectively. The potentials are monitored with a multi-channel controller (R305 – Consort, Turnhout, Belgium) acting as electrometer data logging system. The salt-water reservoir is additionally equipped with a calibrated standpipe to measure the osmotic water flow into the salt-water reservoir. To avoid an undesirable hydraulic gradient at the beginning of each experiment, the water level in the standpipe equals the water level in the fresh-water bowl. During the whole experiment, both reservoirs are continuously homogenized with a peristaltic pump (Ismatec Reglo-MS Analog – Dépex, Houten, The Netherlands). A more detailed description of the set-up and the experimental procedure is given by Heister et al. (in press).

To quantify the effect of membrane potential on water flow and diffusion of ions, two similar experiments have to be performed, one with induced membrane potential, and one, in which the membrane potential is cancelled out. This is done by 'virtual short-circuiting' the clay membrane with the so-called 'virtual shortcut'. Hereby, the electrical potential gradient across the sample is ruled out with a negative feedback compensation current that brings the potential gradient to zero. The compensation current is applied through two noble metal electrodes also inserted in the two reservoirs. The electrical current is controlled with a negative feedback circuit comparable with a four-electrode bipotentiostat. The advantage of this method is that unpredictable additional electrical potentials that will be induced by conducting current through the reference electrodes will be avoided. It was shown that the method of virtual short-circuiting is a more appropriate way to quantify the effect of membrane potential than physical shortening of the electrodes (Heister et al., in press).

With a full set of experiments, consisting of a non-shorted and a shorted experiment, flow parameters can be calculated with modified coupled flow equations of irreversible thermodynamics.

Table 7.3: Test conditions of the two sets of experiments with Boom Clay.

name	overburden load	reservoir salt concentrations
experiment 1	1 bar	0.01 M — 0.1 M NaCl
experiment 2	1 bar	0.01 M — 0.05 M NaCl

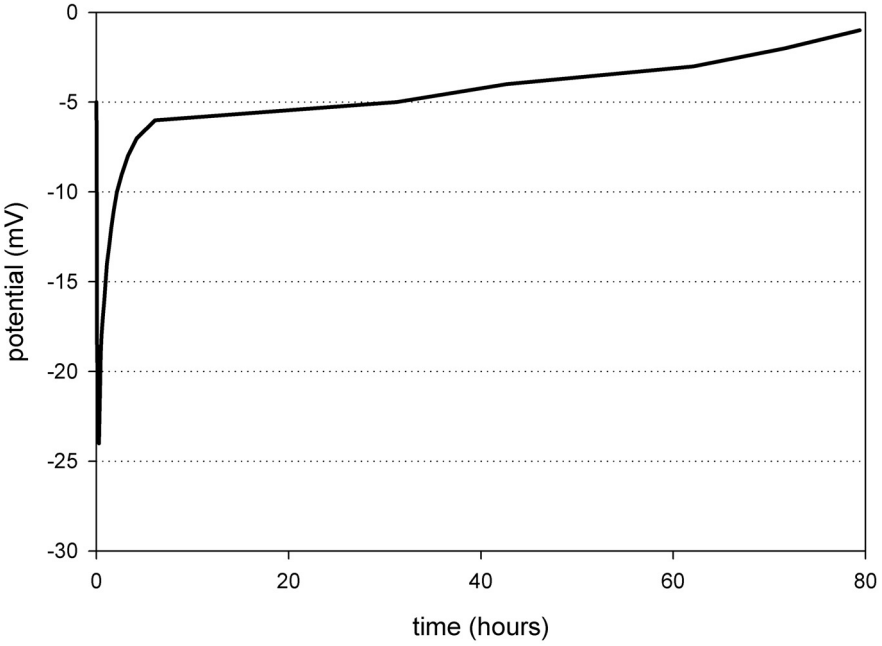

Figure 7.1: Development of the membrane potential over time in experiment 1 with Boom Clay (0.01 M – 0.1 M NaCl). When the salt-water concentration in the salt-water reservoir is increased up to the desired ionic strength, the electrical potential gradient immediately develops. Thereafter, the potential gradient gradually vanishes due to the decrease in salt concentration difference and the build-up of an electrical potential due to water flow.

7.3 Results and discussion

7.3.1 Boom Clay

With Boom Clay, two sets of experiments, each consisting of a non-shorted and a shorted experiment, were performed. Therefore, for each experiment, 5 g of air-dry clay powder was used to produce a clay membrane. The porosity of these samples ranged from 47% to 59% and their thickness varied between 1.1 mm and 1.6 mm. The specific experimental conditions are listed in Table 7.3.

Both sets of experiments showed the same behaviour, which is comparable to a previous investigation with bentonite samples in the same laboratory set-up (Heister et al., in press). The applied salt concentration gradient induced an electrical potential difference across the clay. As predicted by theory (van Olphen, 1977) and confirmed also by another experimental study (Kocherginski and Stucki, 2001), the solution of high concentration was negative compared to that of low concentration. The higher salt concentration difference caused a larger electrical potential gradient. The electrical potential gradient vanished over time as the salt concentration difference decreased by osmotic water flow and diffusion of ions (Fig. 7.1).

Comparing the non-shorted experiments with the respective shorted experiments, it was seen that short-circuiting with the virtual shortcut resulted in an increased osmotic water flow into the high-concentration reservoir. The maximum rise in the standpipe was larger and sooner reached than in the non-shorted experiments (Fig. 7.2). Additionally, also the salt flux density increased by short-

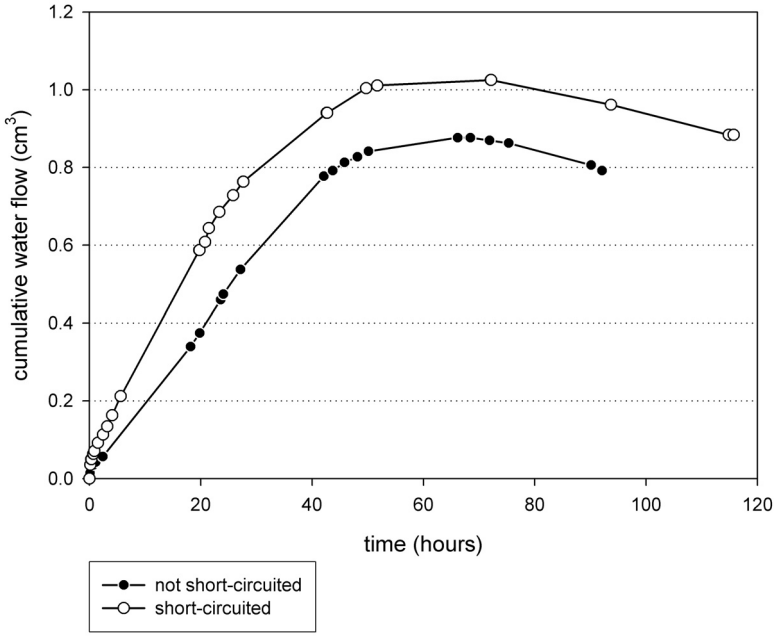

Figure 7.2: Cumulative water flow into the salt-water reservoir in experiment 1 with Boom Clay (0.01 M – 0.1 M NaCl). The rate of osmotic rise and the maximum height were larger in the short-circuited experiment, which indicates that in the presence of an electrical gradient across the sample (non-short-circuited), a counterflow of water is present.

circuiting the clay membrane.

The fluxes can be divided into an electrical and a chemical induced part:

$$\begin{aligned} J_v &= J_{ve} + J_{vc} \\ I &= I_e + I_c \\ J_s &= J_{se} + J_{sc} \end{aligned} \qquad (7.3)$$

with the subscripts e and c denoting the electrical and chemical induced part, respectively.

In the short-circuited experiments, the chemical induced fluxes are measured, whereas in the non-shorted experiments, the combined fluxes are quantified. However, the partition of the electrical current density has no use because the electrical potential gradient occurs in an isolated system in which the electrical current is zero, i.e. $I_e = 0$.

It is concluded that the induced membrane potential hinders the flow of water and ions by inducing a counterflow of water and ions, respectively. The electrical induced fluxes can be calculated according to Eq. 7.3. Because they are counteracting the others, they have a negative sign. All measured and calculated fluxes and driving forces are given in Table 7.4.

These values show that electrical induced fluxes are not negligible. In experiment 1 (0.01 M – 0.1 M NaCl), the electrical induced salt flux amounts to 73% of the chemical induced salt flux, and the electrical induced water flux amounts to even 98% of the chemical induced water flux. In experiment 2 (0.01 M – 0.05 M NaCl), the salt concentration gradient is smaller and therefore, also the

differences between the fluxes are smaller. This is caused by the smaller electrical potential gradient. The electrical induced salt flux amounts to 21% of the chemical induced flux, but the electrical induced water flux still amounts to 92% of the chemical induced water flux. These results are in excellent agreement with previous performed experiments on bentonite (Heister et al., in press).

Various flow parameters were derived with the coupled flow equations of irreversible thermodynamics. Therefore, the set of equations (Eq. 7.1) had to be modified. In the experiments, the build-up of hydraulic pressure is small compared to common hydraulic conductivity experiments. Consequently, the pressure-induced terms are neglected. Moreover, the phenomenological coefficients had to be reformulated. After modification, the set of equation is rewritten as follows:

$$\begin{aligned} J_v &= k_e \cdot i_e + \frac{\nu\sigma k_h^*}{\gamma_f} RT \cdot i_c \\ I &= \kappa \cdot i_e + D|z|F \cdot i_c \\ J_s &= \frac{cD|z|F}{RT} \cdot i_e + D \cdot i_c \end{aligned} \qquad (7.4)$$

where k_e is the electroosmotic conductivity coefficient in m^2/Vs, i_e is the electrical potential gradient in V/m, ν is the dissociation factor from the van't Hoff equation, σ is the reflection coefficient, k_h^* is the hydraulic conductivity coefficient under short-circuited conditions in m/s, γ_f is the unit weight of the fluid in N/m^3, R is the gas constant in J/K·mol, T is the temperature in K, i_c is the chemical concentration gradient in mol/m^4, κ is the electrical conductivity coefficient in S/m, D is the diffusion coefficient in m^2/s, z is the valence of the ion and F is the Faraday constant in C/mol.

One disadvantage of the laboratory set-up used is that the hydraulic conductivity coefficient cannot de determined because no hydraulic pressure gradients can be applied. Subsequently, neither the reflection coefficient can be calculated because both parameters are clustered in one phenomenological coefficient. It would be possible to employ a hydraulic conductivity coefficient obtained from another type of experiment, but as the samples are never perfectly identical, small

Table 7.4: Measured and calculated fluxes and driving forces of the two experiments with Boom Clay. The electrical water flux density and the electrical salt flux density are calculated by subtracting the osmotic flux densities at shorted condition from the total flux densities at non-shorted condition.

			experiment 1	experiment 2
total water flux density	J_v	m/s	$3.43 \cdot 10^{-8}$	$1.79 \cdot 10^{-8}$
osmotic water flux density	J_{vc}	m/s	$1.60 \cdot 10^{-6}$	$2.20 \cdot 10^{-7}$
electrical water flux density	J_{ve}	m/s	$-1.57 \cdot 10^{-6}$	$-2.03 \cdot 10^{-7}$
electrical current density	I	A/m^2	$1.36 \cdot 10^{-4}$	$2.56 \cdot 10^{-5}$
total salt flux density	J_s	$mol/s \cdot m^2$	$3.18 \cdot 10^{-6}$	$2.28 \cdot 10^{-6}$
osmotic salt flux density	J_{sc}	$mol/s \cdot m^2$	$1.20 \cdot 10^{-5}$	$2.88 \cdot 10^{-6}$
electrical salt flux density	J_{se}	$mol/s \cdot m^2$	$-8.82 \cdot 10^{-6}$	$-5.94 \cdot 10^{-7}$
concentration gradient	i_c	mol/m^4	$6.43 \cdot 10^{4}$	$9.59 \cdot 10^{3}$
electrical potential gradient	i_e	V/m	-8.97	-6.37

Table 7.5: Flow parameters of the two experiments with Boom Clay calculated with the modified coupled flow equations of irreversible thermodynamics and literature data for fine-grained soils.

			experiment 1	experiment 2	literature data maximum	literature data minimum
					(Mitchell, 1993)	
diffusion coefficient	D	m^2/s	$1.87 \cdot 10^{-10}$	$3.00 \cdot 10^{-10}$	$2 \cdot 10^{-9}$	$2 \cdot 10^{-10}$
ionic mobility	u	m^2/Vs	$7.26 \cdot 10^{-9}$	$1.17 \cdot 10^{-8}$	$1 \cdot 10^{-8}$	$3 \cdot 10^{-9}$
electroosmotic conductivity coefficient	k_e	m^2/Vs	$1.74 \cdot 10^{-7}$	$3.18 \cdot 10^{-8}$	$1 \cdot 10^{-8}$	$1 \cdot 10^{-9}$
electrical conductivity coefficient	κ	S/m	0.129	0.043	1.0	0.01

differences would lead to incorrect values if they are directly adopted into the equation. Under the experimental conditions, it is estimated from the data obtained that the reflection coefficient of the Boom Clay samples is lower than for bentonite. For comparison, reflection coefficients for bentonite are reported around 0.02 (Heister et al., in press).

All flow parameters derived from the two sets of experiments are summarized in Table 7.5, where they are compared to a range of literature values for saturated fine-grained soils listed by Mitchell (1993). It can be seen from Table 7.5 that all calculated flow parameters fit well within the literature range. There is, however, one exception: the k_e value of experiment 1 exceeds the maximum value found in literature. There is no explanation for this except the possible concurrence of several inaccuracies in the measurements of one of the particular samples, which causes this deviation.

In general, the diffusion coefficients and ionic mobilities are close to the minimum literature value, which is expected because the Boom Clay is quite an impermeable medium. The deviation between the parameters from the two experiments is small indicating that they are specific for the clay. The variation between the two experiments in the electrical conductivity coefficient, κ, is about a factor two suggesting that this parameter is influenced by the salt concentration gradient, which is halved in experiment 2.

If the effect of membrane potential on the flow parameters would not be taken into account, i.e. when the diffusion coefficient is calculated from the salt flux density in the non-shorted experiment, different values for the diffusion coefficient, the ionic mobility and the electrical conductivity coefficient are obtained. These calculations, however, do not have any influence on the

Table 7.6: Calculated flow parameters of the two experiments with Boom Clay, if the membrane potential is not taken into account. The electroosmotic conductivity coefficient, k_e, is not listed, as this has no effect on this parameter.

			experiment 1	experiment 2
apparent diffusion coefficient	D'	m^2/s	$4.94 \cdot 10^{-11}$	$2.38 \cdot 10^{-10}$
apparent ionic mobility	u'	m^2/Vs	$1.92 \cdot 10^{-9}$	$9.28 \cdot 10^{-9}$
apparent electrical conductivity coefficient	κ'	S/m	0.0342	0.0346

electroosmotic conductivity coefficient, k_e, which remains the same. The apparent parameters, when neglecting the membrane potential, are listed in Table 7.6. In this case, all flow parameters are clearly lower. The deviation is largest in experiment 1 with the largest salt concentration gradient. Therefore, it is concluded that the deviation becomes smaller as the gradients are smaller. The virtual shortcut is expected to have the largest effect in experiments with large salt concentration gradients and subsequently large electrical potential gradients.

Unfortunately, there are only a few studies known which attempt to quantify the effects of membrane potentials on diffusion and water flux, although the build-up of an electrical potential gradient and its subsequent decrease were observed in laboratory experiments (Kocherginski and Stucki, 2001). Besides Heister et al. (in press), only one study is found in literature that attempts to quantify the effects of membrane potential. Elrick et al. (1976) performed laboratory experiments on homoionic bentonite where a salt concentration difference was applied and the gradients of hydraulic pressure and electrical potential were monitored. However, to quantify the effects of membrane potential, the electrodes were physically shortened which was shown to be less appropriate than virtual short-circuiting (Heister et al., in press).

For a continuing discussion of research elsewhere on the effect of induced membrane potential gradients in clays, the reader is referred to Heister et al. (in press). The achieved conclusions there comply very well with the present results. Comparing the results obtained from Boom Clay with those from bentonite samples, it is concluded that under the defined conditions in the laboratory experiments, the bentonite is more semipermeable than the Boom Clay. However, this does not hold for samples of Boom Clay under field conditions, e.g. in the underground research laboratory at Mol, where different conditions, e.g. of the overburden load, are prevailing.

7.3.2 Calais Clay

Different samples of oxidized Calais Clay were prepared ranging from 1.87 mm to 3.64 mm thickness corresponding to 5 g and 10 g of air-dry clay, respectively. However, in none of the experiments, which were all non-short-circuited, neither an electrical potential gradient, which is evoked by the membrane and its interfaces and not by the different salt concentrations in the reservoirs, nor an osmotic water flux was observed. Nevertheless, diffusion of ions from the salt-

reservoir through the clay into the fresh-reservoir was measured in the experiments with thin (5 g) clay samples. It was expected that thicker clay membranes would exhibit the desired semipermeable properties since an increase in membrane thickness would result in an increase in electrical potential. However, no electrical potential gradient or osmotic water flux arose even across the thick (10 g) sample. Moreover, diffusion of Cl^- ions could not be measured continuously in the experiment with the thick membrane due to repeated malfunctioning of the Cl^--sensitive electrodes.

The malfunctioning of the Cl^--sensitive electrodes can be ascribed to interfering ions at the electrode membrane causing a fast potential drift to corresponding unreal chloride concentrations. A possible source for these interfering ions is pyrite oxidation in the clay.

It is concluded that the oxidized Calais Clay does not show semipermeable behaviour, or at least no sufficient semipermeable behaviour to be detected in this kind of experiments.

To check how sensitive the laboratory set-up is, experiments were performed with kaolinite. Kaolinite is thought to be a less efficient membrane due to its low cation exchange capacity (Fritz, 1986). For these experiments, a commercially available kaolinite marketed for moulding purposes under the name Kaolin (Artie, Oss, The Netherlands) was used.

Unfortunately, no semipermeable behaviour was observed in experiments with thin kaolinite membranes. However, diffusion of chloride was measured in all experiments. The weighed 5 g clay yielded a membrane with a thickness of about 1.7 mm, as kaolinite is a non-swelling clay. Accordingly, a thicker membrane (3.65 mm corresponding to 10 g kaolinite) was prepared. In this experiment, additional to salt diffusion, a small membrane potential was measured and very little osmotic water flow was observed.

One may expect that thin membranes are quite susceptible to damage and that possible leakage through the membrane precludes osmotic water flow and build-up of an electrical potential gradient as both reservoirs will be short-circuited. Calculation of the diffusion coefficients can prove that the membranes were not damaged. For this purpose, the salt flux equation is used and the membrane potential term is neglected because no electrical potential gradient was measured. The calculated diffusion coefficients lie between $7.51 \cdot 10^{-10}$ and $9.16 \cdot 10^{-10}$ m^2/s for the Calais Clay samples. The diffusion coefficients for the kaolinite range between $1.3 \cdot 10^{-9}$ and $3.5 \cdot 10^{-9}$ m^2/s. Compared to the Boom Clay samples, diffusion here is quite a fast process. This can be explained by the higher moisture content and less overlapping double layers in the pores, which hinder the flux of ions. However, the values are too low for membrane damage to be probable.

Therefore, it is concluded that the laboratory set-up is sensitive enough to detect semipermeable properties of kaolinite clay. Consequently, the semipermeable properties of the oxidized Calais Clay are less than those of kaolinite or even nonexistent because the diffuse double layers do not sufficiently overlap. This can be confirmed with the measured cation occupation of the exchange complex, where sodium is nearly negligible. Accordingly, the presence of sodium is advantageously for a clay to exhibit semipermeable properties (Malusis et al., 2003).

Another explanation for the lack of semipermeability is the very low pH of the oxidized Calais Clay. At pH 3, the clay is below the point of zero charge (PZC) of most of its constituent clay minerals. The PZCs of illite and kaolinite are 3.2 and 4.3, respectively (Chantawong et al., 2003); only smectites have a PZC lower than 3, e.g. montmorillonite has a PZC of 2.5 (Sparks, 1995). At pH lower than the PZC, the clay particles will exhibit a positive charge. Consequently, the oxidation of the clay modified the surface of the minerals and thus the semipermeable properties of the clay.

Obviously, the oxidation of pyrite seems to play an important role. As the Boom Clay contains

pyrite, too, it is expected that the Boom Clay will also loose its semipermeability when it becomes fully oxidized. To verify this, a comparable experiment with a fully oxidized Boom Clay sample should be performed. However, oxidation of the Boom Clay under laboratory conditions is a very time-consuming process. Therefore, an enhanced oxidation process should be established, e.g. heating in an oxygen-rich atmosphere. But the effects of enhanced oxidation are not sufficiently investigated yet.

7.4 Conclusions

In a rigid-wall permeameter, osmotic water flow, diffusion and induced membrane potentials were measured in different clays in chemical osmosis experiments. To quantify the effect of membrane potential on water flux and diffusion, the electrical potential gradient was cancelled out by virtual short-circuiting the clay membrane.

Semipermeable behaviour was clearly observed in samples of Boom Clay (Mol, Belgium). The induced membrane potential was directly related to the salt concentration gradient applied and decreased over time due to osmotic water flow and diffusion of ions. Short-circuiting the clay resulted in an increased osmotic water flow and accelerated diffusion of Cl^- ions. It is concluded that the membrane potential induces an electroosmotic counterflow. This effect is larger as the salt concentration gradient increases.

Flow parameters were calculated with coupled flow equations of irreversible thermodynamics, assuming that Onsager's reciprocal relations are valid. The flow parameters were in good agreement with literature data. Furthermore, it is concluded that, under the same experimental conditions, Boom Clay is less efficient than bentonite.

No osmotic water flow or membrane potentials were observed in samples of oxidized Calais Clay from polder Groot Mijdrecht, The Netherlands. The possibility of leakage through the clay membrane was excluded by calculating the diffusion coefficient that is in good agreement with data expected from literature values.

The sensibility of the experimental set-up was tested with experiments on kaolinite samples because kaolinite is thought to be a less efficient semipermeable membrane due to its low cation exchange capacity. With experiments on relatively thick kaolinite membranes, additional to diffusion, a small membrane potential and very little osmotic water flux was observed. Accordingly, the set-up is sensitive enough to detect semipermeable properties of kaolinite. So, the semipermeable properties of the oxidized Calais Clay are less than those of kaolinite or even nonexistent.

The lack of semipermeability of the Calais Clay can be explained by the low pH, which is lower than the point of zero charge of most of its constituent clay minerals, which indicates that the clay surfaces are modified and thus also the semipermeable properties of the clay, and by the very low quantity of sodium ions on the exchange complex. Subsequently, a significant amount of Al^{3+} is expected on the exchange complex decreasing the diffuse double-layer thickness, which cannot sufficiently overlap to exhibit semipermeable properties.

In general, the laboratory set-up has sensitivity to detect even slight semipermeable behaviour of clay samples. The method of virtual short-circuiting is appropriate to quantify the effects of membrane potential on osmotic water flow and diffusion. The different clays investigated show different degrees of semipermeable behaviour.

Acknowledgements

We thank Dr. Pierre De Cannière and his colleagues from SCK·CEN in Mol, Belgium for collaboration and providing us with Boom Clay material.

We also like to thank Ana Maria Garavito and her colleagues at the Vrije Universiteit of Amsterdam, The Netherlands, who provided us with Calais Clay material.

References

Aertsens, M., Wemaere, I. and Wouters, L., 2004. *Spatial variability of transport parameters in the Boom Clay.* Applied Clay Science, 26: 37 - 45.

Beaucaire, C., Pitsch, H., Toulhoat, P., Motellier, S. and Louvat, D., 2000. *Regional fluid characterisation and modelling of water-rock equilibria in the Boom Clay Formation and in the Rupelian aquifer at Mol, Belgium.* Applied Geochemistry, 15: 667 - 686.

Bernier, F., Volckaert, G., Alonso, E. and Villar, M., 1997. *Suction-controlled experiments on Boom clay.* Engineering Geology, 47: 325 - 338.

Cey, B.D., Barbour, S.L. and Hendry, M.J., 2001. *Osmotic flow through a Cretaceous clay in southern Saskatchewan, Canada.* Canadian Geotechnical Journal, 38: 1025 - 1033.

Chantawong, V., Harvey, N.W. and Bashkin, V.N., 2003. *Comparison of heavy metal adsorption by Thai kaolin and ballclay.* Water, Air and Soil Pollution, 148: 111 - 125.

Elrick, D.E., Smiles, D.E., Baumgartner, N. and Groenevelt, P.H., 1976. *Coupling phenomena in saturated homo-ionic montmorillonite: I. Experimental.* Soil Science Society of America Journal, 40: 490 - 491.

Fritz, S.J., 1986. *Ideality of clay membranes in osmotic processes: A review.* Clays and Clay Minerals, 34(2): 214 - 223.

Groenevelt, P.H. and Elrick, D.E., 1976. *Coupling phenomena in saturated homo-ionic montmorillonite: II. Theoretical.* Soil Science Society of America Journal, 40: 820 - 823.

Groenevelt, P.H., Elrick, D.E. and Blom, T.J.M., 1978. *Coupling phenomena in saturated homo-ionic montmorillonite: III. Analysis.* Soil Science Society of America Journal, 42(5): 671 - 674.

Heister, K., Kleingeld, P.J. and Loch, J.P.G., in press. *Quantifying the effect of membrane potential in chemical osmosis across bentonite membranes by virtual short-circuiting.* Journal of Colloid and Interface Science.

Horseman, S.T., Higgo, J.J.W., Alexander, J. and Harrington, F.J., 1996. *Water, Gas and Solute Movement Through Argillaceous Media.* CC-96/1, Nuclear Energy Agency, Organisation for Economic Co-Operation and Development, Paris, France.

Katchalsky, A. and Curran, P.F., 1967. *Non-Equilibrium Thermodynamics in Biophysics.* Harvard University Press, Cambridge, MA, USA, 248 pp.

Keijzer, T.J.S. and Loch, J.P.G., 2001. *Chemical osmosis in compacted dredging sludge.* Soil Science Society of America Journal, 65: 1045 - 1055.

Kobatake, Y., Takeguchi, N., Toyoshima, Y. and Fujita, H., 1965. *Studies of membrane phenomena. I. Membrane potential.* Journal of Physical Chemistry, 69(11): 3981 - 3988.

Kocherginsky, N.M. and Stucki, J. W., 2001. *Supported clay membrane: A new way to characterize water and ion transport in clays.* Advances in Environmental Research, 5: 197 - 201.

Maes, N., Moors, H., De Cannière, P., Aertsens, M. and Put, M., 1998. *Determination of the diffusion coefficient of ionic species in Boom Clay by electromigration: Feasibility study.* Radiochimica Acta, 82: 183 - 189.

Maes, N., Moors, H., Dierckx, A., De Cannière, P. and Put, M., 1999. *The assessment of electromigration as a new technique to study diffusion of radionuclides in clayey soils.* Journal of Contaminant Hydrology, 36: 231 - 247.

Malusis, M.A., Shackelford, C.D. and Olsen, H.W.,

2001. *A laboratory apparatus to measure chemico-osmotic efficiency coefficients for clay soils.* Geotechnical Testing Journal, 24(3): 229 - 242.

Malusis, M.A., Shackelford, C.D. and Olsen, H.W., 2003. *Flow and transport through clay membrane barriers.* Engineering Geology, 70: 235 - 248.

Marine, I.W. and Fritz, S.J., 1981. *Osmotic model to explain anomalous hydraulic heads.* Water Resources Research, 17(1): 73 - 82.

Mitchell, J.K., 1993. *Fundamentals of Soil Behavior.* John Wiley & Sons, New York, 437 pp.

Noy, D.J., Horseman, S.T., Harrington, J.F., Bossart, P. and Fisch, H.R., 2004. *An experimental and modelling study of chemico-osmotic effects in the Opalinus Clay of Switzerland.* In: P. Heitzmann (Editor), Mont Terri Project - Hydrogeological Synthesis, Osmotic Flow. Geology Series. Federal Office for Water and Geology, Bern, Switzerland, pp. 95 - 126.

Onsager, L., 1931a. *Reciprocal relations in irreversible processes I.* Physical Review, 37: 405 - 426.

Onsager, L., 1931b. *Reciprocal relations in irreversible processes II.* Physical Review, 38: 2265 - 2279.

Poelman, J.N.B., 1966. *De Bodem van Utrecht, Toelichting bij Blad 6 van de Bodemkaart van Nederland, Schaal 1:200.000.* Stichting voor Bodemkartering, Wageningen, The Netherlands, 107 pp.

Soler, J.M., 2001. *The effect of coupled transport phenomena in the Opalinus Clay and implications for radionuclide transport.* Journal of Contaminant Hydrology, 53: 63 - 84.

Sparks, D.L., 1995. *Environmental Soil Chemistry.* Academic Press, San Diego, 267 pp.

Stichting voor Bodemkartering, 1970. *Toelichting bij Kaartblad 31 Oost Utrecht.* Bodemkaart van Nederland, Schaal 1:50.000, Wageningen, The Netherlands, 153 pp.

van Olphen, H., 1977. *An Introduction to Clay Colloid Chemistry.* John Wiley, New York, 318 pp.

Yeung, A.T., 1990. *Coupled flow equations for water, electricity and ionic contaminants through clayey soils under hydraulic, electrical and chemical gradients.* Journal of Non-Equilibrium Thermodynamics, 15(3): 247 - 267.

Yeung, A.T. and Mitchell, J.K., 1993. *Coupled fluid, electrical and chemical flows in soil.* Geotechnique, 43(1): 121 - 134.

Yeung, A.T., 1994. *Effects of electro-kinetic coupling on the measurement of hydraulic conductivity.* In: D.E. Daniel and S.J. Trautwein (Editors), Hydraulic Conductivity and Waste Contaminant Transport in Soils. American Society for Testing and Materials, Philadelphia, pp. 569 - 585.

Chapter 8

Synthesis

A critical review on the modifications of the experimental set-up

As this thesis is a compilation of several research articles, a clear chronological development is visible. At the beginning, our idea was to realize a laboratory set-up that is able to measure hydraulic, electrical and chemical induced fluxes simultaneously. Therefore, we adapted the design of an existing flexible-wall permeameter developed in our laboratory by which chemical osmosis across clay membranes had been successfully measured (Keijzer, 2000).

Because many clays can swell in contact with water, an overburden load has to be applied on the clay sample in order to maintain a constant shape of the specimen. In contact with concentrated salt solutions, the clay sample can shrink. According to diffuse double-layer theory, the thickness of the diffuse double layers of clay particles decreases at increasing salt concentration so that the clay particles can approach each other more closely (Bolt, 1976; Bolt, 1979). Shrinkage can cause side-wall leakage in the permeameter. Side-wall leakage, however, will be avoided by using a flexible-wall permeameter (Daniel et al., 1984), and its suitability was proven in experiments by Keijzer (2000).

Since we are interested in electrical potential gradients, the complete flexible-wall permeameter had to be built with electrically insulating materials like plastics, and also the cell filling surrounding the clay, used to apply the overburden pressure on the sample, had to be electrically insulating; in our case, we used silicone oil because aqueous solutions would partially electrically short-circuit the sample and various membranes were shown to be permeable for gaseous cell filling.

Peristaltic pumps were employed to fill and to homogenize the solution reservoirs on both sides of the clay membrane. Consequently, due to the use of tubings in the pumps, the solution reservoirs were not rigid, and instead of osmotic and hydraulic pressure, only flows could be measured. This will possibly restrict the accuracy of the measurements, since it takes some time to obtain a measurable amount of flow across a low-permeable clay sample.

During the experiments, we realized that the electrode material is a crucial parameter. First, to attain our goal to design a set-up useable for all our purposes, we chose electrodes that were able to both measure and apply electrical potentials and that were chemically inert. As noble-metal electrodes are widely applied and described (e.g. Renaud and Probstein, 1987; Baraud et al., 1997), we used gold electrodes as first choice and employed them in the electrically insulating flexible-wall permeameter (cf. Chapter 4).

Additional to the measurements of electrical potential gradients, our intention was to monitor the development of pH at the clay – solution interface during experiments in which electrical potential gradients occur, because it was expected that electroosmosis evokes extreme pH conditions, below 2 at the anode side and above 12 at the cathode side, depending on the electrical current applied (Acar et al., 1990; Acar and Alshawabkeh, 1993). Therefore, we installed a solid state pH ISFET electrode (Sentron, Roden, The Netherlands) to measure the pH at the clay sample surface. However, this attempt was not successful because measuring the pH with the ISFET electrode induced heavy interferences with the potential measurements in such a way that even periodical measurements were

not possible. Consequently, we had to abandon this effort, although we are aware that pH is an important parameter in experiments on electroosmosis.

Flows that may occur across clay membranes are flows of fluid, electrical charge and solutes. In all of our experiments, the temperature is kept constant, so heat flow is absent. Consequently, a set of transport equations is established according to the theory of irreversible thermodynamics:

$$\begin{aligned} J_v &= L_{11}\nabla(-P) + L_{12}\nabla(-E) + L_{13}\nabla(-\mu) \\ I &= L_{21}\nabla(-P) + L_{22}\nabla(-E) + L_{23}\nabla(-\mu) \\ J_s &= L_{31}\nabla(-P) + L_{32}\nabla(-E) + L_{33}\nabla(-\mu) \end{aligned} \qquad (8.1)$$

where J_v is the water flux density in m/s, I is the electrical current density in A/m², J_s is the solute flux density in mol/m²·s, P is the hydraulic pressure in N/m², E is the electrical potential in V, μ is the chemical potential in J/mol and L_{11} to L_{33} are the phenomenological coefficients in their corresponding units (Katchalsky and Curran, 1967; Yeung, 1990; Yeung and Mitchell, 1993).

In the beginning, we limited our experiments to the coupling of hydraulic and electrical fluxes, i.e. without any imposed chemical concentration gradients. Accordingly, the set of equations is reduced to

$$\begin{aligned} J_v &= L_{11}\nabla(-P) + L_{12}\nabla(-E) \\ I &= L_{21}\nabla(-P) + L_{22}\nabla(-E) \end{aligned} \qquad (8.2)$$

We first investigated streaming potentials (electrical potential gradients induced by hydraulic water flow). The flexible-wall permeameter was found suitable, as experimental results matched our expectations, namely that streaming potentials induced an electroosmotic counterflow. Moreover, the calculated flow parameters were in good agreement with literature data (cf. Mitchell, 1993), except for the very low electrical conductivity coefficients. It was assumed that these low values were due to the compact homogeneous fabric of the clay samples, causing the mobility of the ions to be hindered by the strong overlap of the diffuse double layers of the clay particles.

These results were presented at an international conference (Loch et al., in press), where it was suggested to use reversible Ag/AgCl electrodes instead of the inert gold electrodes because inert electrodes are susceptible to polarization. Therefore, we drew the conclusion to investigate this further.

From a literature review on various types of electrodes, it was concluded that also inert electrodes belong to the group of reversible electrodes (Chapter 5). We agree that Ag/AgCl electrodes are a

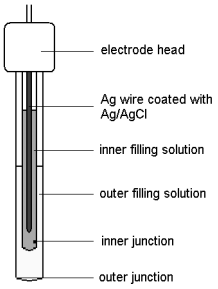

Figure 8.1: Schematic drawing of a double-junction Ag/AgCl reference electrode. The drawing is not to scale. The inner junction consists of a ceramic plug, whereas the outer junction is simply a very small slit at the bottom of the electrode. For proper functioning, the inner filling solution has to discharge into the outer filling solution and the outer filling solution in turn into the measuring solution. This is achieved by differences in filling level.

better choice since they do not show polarization, like gold electrodes do, and other – for us – unpredictable effects. But the most suitable type, the double-junction Ag/AgCl reference electrode, could not be employed in the existing permeameter set-up because of the liquid junction of the electrodes (Fig. 8.1). For successful operation of the electrode, the filling solution of the salt bridge has always to flow from the inside to the outside. So, if the solution reservoir is pressurized because a hydraulic gradient is applied, the reservoir solution will flow into the electrode liquid junction; however, for good performance of the electrode, the opposite should hold. Consequently, by employing double junction Ag/AgCl electrodes, no hydraulic gradients can be applied. Overpressurizing the electrodes to prevent inflow of reservoir solution is too complicated. Moreover, Ag/AgCl gel electrodes with a thickened liquid junction appeared to be too unstable. Thus, only electrical and chemical concentration gradients could be applied in a laboratory set-up with Ag/AgCl reference electrodes.

During modification of the set-up, it was decided to simplify it further. As no hydraulic pressure can be exerted on the clay membrane, the flexible-wall permeameter can be reduced to a rigid-wall permeameter. One major advantage of a rigid-wall permeameter is that it is much easier to handle than a flexible-wall permeameter because the permeameter cell itself is simplified. In this permeameter, an axial overburden load is applied on top of the sample. Side-wall leakage is avoided because the clay is palmed off laterally.

With this new design it is possible to measure membrane potentials, i.e. electrical potential gradients induced by a chemical concentration gradient, in clayey materials (Chapters 6 and 7). Flow parameters derived from the measurements using the coupled flow equations were in good agreement with literature (cf. Mitchell, 1993). Moreover, electrical conductivity coefficients, which were very low in streaming potential experiments, now agreed better with literature values. However, calculated reflection coefficients, σ, indicating the ideality of semipermeability of the membrane, were significantly lower than expected ($\sigma = 0$ implies the absence of semipermeability, $\sigma = 1$ implies ideal semipermeability), but are in agreement with results obtained by Keijzer et al. (1999) who studied chemical osmosis in electrically shorted, comparable bentonite.

It can be concluded that our first objective to realize a universal laboratory set-up, in which hydraulic, electrical and chemical concentration gradients can be varied simultaneously, was not reached. Modification of the set-up appeared to be too time-consuming, in part due to the mentioned problem of electrodes. In the author's opinion, amendments of the set-up are still feasible, although it is possible to determine most of the parameters of interest with the existing versions.

Retrospect on the data and comparison with the primary expectations

The experimental results obtained are in good agreement with our expectations. Both in the presence of streaming potential and membrane potential, the induced electrical potential gradient evoked an electroosmotic counterflow of water. The membrane potential also caused a counterflow of ions. Moreover, the flow parameters calculated with the coupled flow equations are in good agreement with literature values for saturated fine-grained soils (Mitchell, 1993). However, there are two exceptions that attract our attention, as already mentioned in the previous section.

Firstly, the electrical conductivity coefficients are quite different in the streaming potential and the membrane potential experiments, although the same bentonite and salt solutions were used. Whereas the values from the membrane potential experiments are in good agreement with literature data, the

values from the streaming potential experiments are up to two orders of magnitude lower. Furthermore, the high overburden load on the clay causing strong overlap of the diffuse double layers of the clay particles and subsequent hindrance of transport of ions through the pores cannot be (solely) responsible for this phenomenon because the overburden load is identical in both types of experiments.

Secondly, reflection coefficients were calculated from the membrane experiments with bentonite that are lower than expected from literature. Compacted bentonite is believed to be very capable to act as a semipermeable membrane. Thus, high reflection coefficients are expected, but the values obtained from the experiments indicate very low semipermeability. Although our results are in good agreement with a previous study on osmosis on bentonite (Keijzer et al., 1999), these values are remarkable.

The expectation of high reflection coefficients is based on model calculations. The models regarded to be appropriate include the Groenevelt-Bolt model, the Kemper-Bresler model and the Fritz-Marine membrane model. The Groenevelt-Bolt model is based on the Gouy-Chapman theory of diffuse double layers and irreversible thermodynamics (Bolt, 1955; Groenevelt and Bolt, 1969, 1972; Bolt, 1982); the Kemper-Bresler model is based on the same theory (Kemper and Rollins, 1966; Bresler, 1973); the Fritz-Marine membrane model is a refinement of the Teorell-Meyer-Siever model and supports laboratory scale hyperfiltration experiments and field scale data of anomalous hydraulic heads in the Dunbarton Triassic Basin, USA (Marine and Fritz, 1981; Fritz and Marine, 1983; Fritz, 1986).

All models overestimate the reflection coefficient. For the Fritz-Marine membrane model, Keijzer (2000) suggested that the difference in contact time between the salt solution and the clay membrane is a cause for deviating values. Contrary to osmosis experiments, hyperfiltration experiments have a relatively short contact time of sample and salt solution, which minimizes salt diffusion into the clay. The longer contact time in an osmosis experiment would therefore lead to flocculation of the clay, increasing the permeability, which in turn reduces the reflection coefficient. However, compared to the experiments of Keijzer, the membrane potential experiments performed in this study are significantly shorter, consequently minimizing salt diffusion. Furthermore, the effect of flocculation can be disregarded since it was shown that, under sufficient overburden load, clay particles are not able to flocculate (Heister et al., 2004).

In the author's opinion, the main cause for overestimated reflection coefficients are some additional model assumptions. In all three models, it is assumed that the clay is monomineral, completely dispersed and that the exchange complex is completely occupied by one monovalent cation (Na^+ in the Fritz-Marine membrane model). These assumptions do not hold for the bentonite used in the experiments because the cation exchange complex is significantly occupied by Ca^{2+}, a divalent cation that is known to form tactoids of clay particles resulting in an incompletely dispersed structure of the clay. For natural clays, the situation is even more deviating from the model assumptions due to inhomogeneities in the mineralogical composition. Consequently, these models are not appropriate to describe complex natural clays. Therefore, ion exchange should be included into the models.

The problem of ion exchange may be enforced by an experimental problem brought up by Keijzer (2000): the incomplete mixing of the solution reservoirs. To obtain homogenized solutions, both reservoirs are continuously pumped around. Nevertheless, the possibility remains that a small water film within the porous stones that act as membrane support, adjacent to the clay membrane, is not

mixed with the bulk reservoir solution. As osmosis proceeds, a fresh-water film will develop in the salt-water reservoir due to osmotic water flow, and a salt-water film will develop in the fresh-water reservoir due to salt sieving by the membrane. Unfortunately, these water films cannot be avoided by increasing the pump speed because at high pumping rates, the so-called 'stirring effect' is induced at the electrodes. Stirring affects the distribution of ions within the interface layer between the liquid junction and the reservoir solution. Consequently, disturbance of this interface layer results in unstable electrical potential readings. So, if ion exchange occurs, this will in first instance take place in the unmixed water films close to the clay membrane and thus probably be not measurable before a large amount of cations is exchanged.

According to Keijzer (2000), the Kemper-Bresler model is the best choice when estimating the semipermeability of natural clayey sediments, since it offers a simple but straightforward approach based on the Gouy-Chapman theory, that probably is the most suitable for incorporation of the effect of divalent cations on the exchange complex. With the Kemper-Bresler model, good results were obtained for various clayey materials like shales and harbour sludge (Keijzer et al., 1999; Keijzer and Loch, 2001; Neuzil, 2000).

In this thesis, it is shown that in general the theory of homoionic, completely dispersed clays is also applicable to clays with the exchange complex partly occupied by divalent cations and to natural clayey sediments. We assume that the occurrence of tactoids is the reason for the lowered semipermeability. Moreover, we think that the very small electrical conductivity coefficients in the streaming potential experiments are also due to divalent cations on the exchange complex. In these experiments, fresh water is forced by a hydraulic pressure gradient through the clay membrane which can result in the build-up of a water layer with increased ion concentration at the inflow site of the clay membrane as described above. This water layer will participate in ion exchange with the adjacent clay, probably inducing a membrane potential that enforces the actual measured streaming potential. However, the contribution of the membrane potential in the measured electrical potential gradient could not be quantified. Accordingly, this was not taken into account in the calculations of the flow parameters, so that deviating values were generated.

Comparison of natural and homoionic clays

To confirm that our results obtained with natural clays are comparable to the almost ideal homoionic situation, a homoionic bentonite with sodium on the exchange complex was prepared by repeated washing of the bentonite with 1 M NaCl solutions followed by repeated washing with demineralized water to remove the excess of salt. With this homoionic sodium bentonite, membrane potential experiments were performed as described in Chapter 6. The particular experimental conditions were 1 bar overburden load and salt concentrations in the respective reservoirs of 0.01 M and 0.1 M NaCl.

At present, however, only preliminary results are obtained. Therefore, it is not possible to compare directly the results of a 'mixed-ionic' bentonite with a homoionic Na-bentonite. Moreover, not all flow parameters can be calculated since no additional experiments to determine the hydraulic conductivity coefficient were performed until now. Besides, other sample properties like the actual cation occupation of the exchange complex, necessary for model calculations, are not measured yet. Thus, only some general trends can de discussed here.

First of all, it can be concluded that the trends observed in the homoionic bentonite are

comparable to those observed in the previously described experiments on natural clays. As in all membrane potential experiments, also in the Na-bentonite experiment the induced electrical potential gradient induced an electroosmotic counterflow of water and Cl^- ions across the clay membrane. The membrane potential vanished over time due to osmotic water flow and diffusion of ions. All these observations are in agreement with the results from the experiments described in Chapter 6 and 7. Preliminary results indicate that the osmotic and electrically induced fluxes are much larger in the homoionic than in the mixed-ionic experiments; but, because they counteract each other, the total fluxes are almost equal in both experiments. Consequently, coupled transport phenomena probably are of more importance in homoionic systems. Additionally, first model calculations yielded an increase of the reflection coefficient, i.e. in the ideality of the semipermeable membrane. This is expected because the presence of more sodium on the exchange complex enhances the semipermeable properties of the clay (Malusis et al., 2003).

In general, it can be concluded that our findings on natural clays also hold for homoionic systems.

Concluding remarks and outlook

In this thesis, induced electrical potential gradients in clay layers are demonstrated in laboratory experiments and their effect on the flow of water and ions is quantified by means of coupled flow equations. All sample materials studied are mixed-ionic clays and act as non-ideal semipermeable membranes.

First results of homoionic Na-bentonite show that the cation occupation of the exchange complex influences the semipermeability of the clay. If a mixed-ionic clay is in contact with a single-salt solution, ion exchange will take place, which, apparently, affects the hydraulic and/ or osmotic induced electrical potential gradient. A mixed-ionic clay deviates from the ideal situation that is assumed in models or aspired in laboratory studies elsewhere (e.g. Kemper and Rollins, 1966; Elrick et al., 1976; Groenevelt and Elrick, 1976). Due to tactoid formation, the clay is not fully dispersed resulting in an inhomogeneous pore size distribution. Accordingly, diffuse double layers do not sufficiently overlap in larger pores. Besides, the exchange of cations influences the diffusivity of the salt anion because the mobility of the cation will affect the mobility of the anion.

It is conceivable that in a mixed-ionic clay, the ideality of semipermeability is lower due to less overlap of diffuse double layers and enhanced diffusion of salt ions due to exchange of cations with a higher mobility (e.g. the release of Ca^{2+} from the exchange complex by exchange with Na^+, which has a lower ionic mobility, will increase the diffusivity of Cl^- in solution). This can explain the low reflection coefficients obtained by Keijzer et al. (1999) and in the present study. Nevertheless, no clear explanation could be found yet to explain the differences in the electroosmotic conductivity coefficients between the streaming potential and the membrane potential experiments. But also here, an impact of cation exchange is imaginable.

Consequently, a direction for further research is obvious. Firstly, the author recommends improving the 'virtual shortcut' in such a way that also online measurements of cation concentrations in the solution reservoirs and pH measurements are possible without interferences. Subsequently, the effect of ion exchange should be investigated in more detail. These results can be helpful to extend existing transport models.

To gain more insight in processes occurring at the interfaces of the system, measurements of complex impedances with impedance spectroscopy are recommended. In addition, the employment

of micro Luggin capillaries appears to be useful to obtain electrical potential gradient profiles through clay membranes. These results can also improve transport models.

Another direction for further research is electroosmosis. Up to now, the suitability of clays for electroosmosis was indicated by electroosmotic conductivity coefficients derived from streaming potential experiments. Results from experiments on actively applied electroosmosis can extend existing transport models further. In practice, it can be desirable to obtain such data because application of an appropriately dosed electrical potential gradient for e.g. soil consolidation or soil remediation can save expenses and avoid disadvantageous additional effects in the soil or sediment like extreme pH values.

References

Acar, Y.B., Gale, R.J., Putnam, G.A., Hamed, J. and Wong, R.L., 1990. *Electrochemical processing of soils: Theory of pH gradient development by diffusion, migration, and linear convection.* Journal of Environmental Science and Health, A25(6): 687 - 714.

Acar, Y.B. and Alshawabkeh, A.N., 1993. *Principles of electrokinetic remediation.* Environmental Science and Techology, 27(13): 2638 - 2647.

Baraud, F., Tellier, S. and Astruc, M., 1997. *Ion velocity in soil solution during electrokinetic remediation.* Journal of Hazardous Materials, 56: 315 - 332.

Bolt, G.H., 1955. *Analysis of the validity of the Gouy-Chapman theory of the electric double layer.* Journal of Colloid Science, 10(2): 206 - 218.

Bolt, G.H., 1976. *Surface interaction between the soil solid phase and the soil solution.* In: G.H. Bolt and M.G.M. Bruggenwert (Editors), Soil Chemistry. A. Basic Elements. Developments in Soil Science. Elsevier, Amsterdam, pp. 43 - 53.

Bolt, G.H., 1979. *The ionic distribution in the diffuse double layer.* In: G.H. Bolt (Editor), Soil Chemistry. B. Physico-Chemical Models. Developments in Soil Science. Elsevier, Amsterdam, pp. 1 - 25.

Bolt, G.H., 1982. *Electrochemical phenomena in soil and clay systems.* In: G.H. Bolt (Editor), Soil Chemistry. B. Physico-Chemical Models. Developments in Soil Science. Elsevier, Amsterdam, pp. 387 - 423.

Bresler, E., 1973. *Anion exclusion and coupling effects in nonsteady transport through unsaturated soils: I. Theory.* Proceedings of the Soil Science Society of America, 37(5): 663 - 669.

Daniel, D.E., Trautwein, S.J., Boynton, S.S. and Foreman, D.E., 1984. *Permeability testing with flexible-wall permeameters.* Geotechnical Journal, 7(3): 113 - 122.

Elrick, D.E., Smiles, D.E., Baumgartner, N. and Groenevelt, P.H., 1976. *Coupling phenomena in saturated homo-ionic montmorillonite: I. Experimental.* Soil Science Society of America Journal, 40: 490 - 491.

Fritz, S.J. and Marine, I.W., 1983. *Experimental support for a predictive osmotic model of clay membranes.* Geochimica et Cosmochimica Acta, 47: 1515 - 1522.

Fritz, S.J., 1986. *Ideality of clay membranes in osmotic processes: A review.* Clays and Clay Minerals, 34(2): 214 - 223.

Groenevelt, P.H. and Bolt, G.H., 1969. *Non-equilibrium thermodynamics of the soil-water system.* Journal of Hydrology, 7: 358 - 388.

Groenevelt, P.H. and Bolt, G.H., 1972. *Permiselective properties of porous materials as calculated from diffuse double layer theory.* In: International Association for Hydraulic Research (Editor), Fundamentals of Transport Phenomena in Porous Media. Developments in Soil Science. Elsevier, Amsterdam, pp. 241 - 255.

Groenevelt, P.H. and Elrick, D.E., 1976. *Coupling phenomena in saturated homo-ionic montmorillonite: II. Theoretical.* Soil Science Society

of America Journal, 40: 820 - 823.

Heister, K., Keijzer, T.J.S. and Loch, J.P.G., 2004. *Stability of clay membranes in chemical osmosis.* Soil Science, 169(9): 632 - 639.

Katchalsky, A. and Curran, P.F., 1967. *Non-Equilibrium Thermodynamics in Biophysics.* Harvard University Press, Cambridge, MA, USA, 248 pp.

Keijzer, T.J.S., Kleingeld, P.J. and Loch, J.P.G., 1999. *Chemical osmosis in compacted clayey material and the prediction of water transport.* Engineering Geology, 53: 151 - 159.

Keijzer, T.J.S., 2000. *Chemical Osmosis in Natural Clayey Materials.* Ph.D. Thesis, Universiteit Utrecht, Utrecht, The Netherlands, 166 pp.

Keijzer, T.J.S. and Loch, J.P.G., 2001. *Chemical osmosis in compacted dredging sludge.* Soil Science Society of America Journal, 65: 1045 - 1055.

Kemper, W.D. and Rollins, J.B., 1966. *Osmotic efficiency coefficients across compacted clays.* Proceedings of the Soil Science Society of America, 30(5): 529 - 534.

Loch, J.P.G., Richter, K. and Keijzer, T.J.S., in press. *Coupling between chemical and electrical osmosis in clays.* Proceedings of the IUTAM-symposium on The Mechanics of Physicochemical and Electromechanical Interactions in Porous Media. May 2003, Kerkrade, The Netherlands. Kluwer Academic Publishers.

Malusis, M.A., Shackelford, C.D. and Olsen, H.W., 2003. *Flow and transport through clay membrane barriers.* Engineering Geology, 70: 235 - 248.

Marine, I.W. and Fritz, S.J., 1981. *Osmotic model to explain anomalous hydraulic heads.* Water Resources Research, 17(1): 73 - 82.

Mitchell, J.K., 1993. *Fundamentals of Soil Behavior.* John Wiley & Sons, Inc., New York, 437 pp.

Neuzil, C.E., 2000. *Osmotic generation of 'anomalous' fluid pressures in geological environments.* Nature, 403: 182 - 184.

Renaud, P.C. and Probstein, R.F., 1987. *Electroosmotic control of hazardous wastes.* Physicochemical Hydrodynamics, 9(1/ 2): 345 - 360.

Yeung, A.T., 1990. *Coupled flow equations for water, electricity and ionic contaminants through clayey soils under hydraulic, electrical and chemical gradients.* Journal of Non-Equilibrium Thermodynamics, 15(3): 247 - 267.

Yeung, A.T. and Mitchell, J.K., 1993. *Coupled fluid, electrical and chemical flows in soil.* Geotechnique, 43(1): 121 - 134.

Samenvatting

Transport van water en opgeloste stoffen in bodems en sedimenten met een hoog kleigehalte speelt een belangrijke rol in het beheer van grondwater en afvalstoffen. Het transport van water in kleilagen wordt niet alleen veroorzaakt door gradiënten in hydraulische potentiaal en dichtheid van de oplossing maar ook door gradiënten in zoutconcentratie en elektrische potentiaal. Chemisch en elektrisch gedreven watertransport, chemische osmose en elektro-osmose genoemd, zijn van belang in poreuze materialen met een hydraulische doorlatendheid van minder dan $1 \cdot 10^{-9}$ m/s, zoals bijvoorbeeld kleien.

Hoewel het belang van deze processen in kleiige bodems en sedimenten al sinds het midden van de 20e eeuw bekend is, worden chemische osmose en elektro-osmose niet toegepast in grondwater modellering. Binnen de bodemkunde is in de laatste decennia veel fundamenteel onderzoek verricht naar hydraulisch, chemisch en thermisch gedreven transport. Ook is hier en daar elektro-osmose toegepast voor het ontwateren van bodems en voor stabilisatie van hellingen en elektromigratie als in-situ remediatie techniek voor verontreinigde grond en slib. Het verwaarlozen van elektrisch en chemisch geïnduceerde processen is niet gerechtvaardigd bij bijvoorbeeld zoutwater-intrusie in laaggelegen kustgebieden, opslagplaatsen van verontreinigde baggerspecie en langdurige opslag van radioaktief of toxisch afval in kleiformaties. In deze gevallen wordt vertrouwd op de lage waterdoorlatendheid en het hoge adsorptievermogen van de klei. In kustgebieden wordt verondersteld dat zoutwater-intrusie in grondwatervoerende pakketten door holocene kleilagen ingeperkt wordt belemmerd. Verontreinigde klei, kleiige bagger of kleiig sediment zijn onderhevig aan emissie-eisen voor verspreiding van verontreinigingen naar de omgeving. Hierbij dient rekening gehouden te worden met alle drijvende krachten voor stoftransport. Bij langdurige opslag van radioaktief afval in kleiformaties kunnen kleine stromingen van belang zijn omdat het transport gedurende een lange tijd kan plaatsvinden tegelijkertijd het gevaar voor mens en milieu groot is.

Chemische osmose en elektro-osmose zijn gekoppelde transportprocessen die kunnen worden beschreven met de irreversibele thermodynamica. In het algemeen zijn kleilagen onderworpen aan stroming van vloeistof, elektrische lading, opgeloste stoffen en warmte. Deze vormen van transport kunnen geïnduceerd worden door de bijhorende drijvende kracht, zoals bijvoorbeeld vloeistofstroming door een hydraulische potentiaalgradiënt. Dit wordt 'direct transport' genoemd. Daarnaast kan transport ook door niet-bijbehorende drijvende krachten geïnduceerd worden, zoals bijvoorbeeld vloeistofstroming door een gradient in zoutconcentratie, wat chemische osmose wordt genoemd. Dit is gekoppeld transport.

Kleilagen gedragen zich als semipermeabele membranen. Ze zijn dus in staat transport van bepaalde komponenten van een oplossing toe te staan terwijl andere geblokkeerd worden. Zo kan een semipermeabel membraan de doorgang van opgeloste stoffen verhinderen zonder de doorstroom van het oplosmiddel te beïnvloeden. De oorzaak hiervan in klei is het overlappen van diffuse dubbellagen van de kleideeltjes in de poriën. Anionen, die zich door de poriën willen verplaatsen, worden afgestoten door de negatieve lading van de kleiplaatjes. Vervolgens wordt ook de beweging van de kationen door de klei beperkt, doordat elektrische neutraliteit in de evenwichtsoplossing gehandhaafd moet blijven. Als een klei in staat is het transport van een opgeloste stof helemaal te voorkomen is het membraan ideaal. In de natuur is een membraan zelden ideaal en passeert een deel van de zout-ionen het membraan door diffusie. Dus niet-ideale membranen beperken het transport van opgeloste stoffen niet volledig. De mate van idealiteit wordt uitgedrukt in de reflektiecoëfficiënt, die – samen met een aantal andere parameters voor het transport van ionen en water door een

semipermeabel membraan – met de vergelijkingen voor gekoppeld transport berekend kan worden.

Het doel van dit proefschrift is het effekt van geïnduceerde elektrische potentiaalgradiënten op het transport van water en ionen in klei met behulp van laboratorium experimenten te kwantificeren. In experimenten worden elektrische potentiaalgradiënten geïnduceerd door hydraulische drukgradiënten (stromingspotentialen) en door gradiënten in zoutconcentratie (membraanpotentialen). Voor dit doel zijn opstellingen gemaakt om experimenten op laboratorium schaal met verschillende kleiige materialen uit te voeren. In de literatuur worden deze opstellingen permeameters genoemd. De bestudeerde materialen zijn een Wyoming bentoniet en twee veldkleien. Met de vegelijkingen voor gekoppeld transport zijn transportparameters berekend en is het effekt van geïnduceerde elektrische potentiaalgradiënten op de stroming van water en ionen gedemonstreerd. De geïnduceerde elektrische potentiaalgradiënten belemmeren het transport van water en opgeloste stoffen door de klei. Als hiermee geen rekening wordt gehouden heeft dit een signifikante invloed op de berekende transportparameters. De resultaten van deze laboratoriumstudie worden gebruikt door de groep Environmental Hydrogeology van het Departement Aardwetenschappen, Universiteit Utrecht, om een transportmodel te valideren dat chemische osmose en elektro-osmose in grondwater omvat.

Opbouw van het proefschrift

Hoofdstuk 1 geeft een algemene inleiding en benadrukt de relevantie van dit onderwerp voor de praktijk. Na een beschrijving van de in de experimenten gebruikte kleimaterialen (**Hoofdstuk 2**), wordt de stabiliteit van kleimembranen in **Hoofdstuk 3** onderzocht. Dit is belangrijk voor alle volgende experimenten waar klei in kontakt komt met oplossingen met een ionsterkte boven de flocculatiewaarde. Wanneer veranderingen in de micro-structuur van de klei ontstaan door een herschikking van de kleideeltjes door flocculatie, dan hebben deze veranderingen naar verwachting een signifikante invloed op de semipermeabiliteit van het membraan. Hierna zijn stromingspotentialen (elektrische potentiaalgradiënten) in bentoniet membranen, geïnduceerd door hydraulische stroming, onderzocht in een permeameter met flexibele wand, en hun effekt op watertransport is gekwantificeerd (**Hoofdstuk 4**). In deze opstelling zijn goud elektroden gebruikt om de elektrische potentiaalgradiënt te meten. De prestatie van goud elektroden kan in twijfel getrokken worden vanwege de mogelijke polarisatie van de elektroden. Daarom zijn de verschillende soorten reversibele elektroden besproken en de toepasbaarheid van goud elektroden is vergeleken met die van Ag/AgCl gel-elektroden voor meting van stromingspotentialen en voor elektro-osmose experimenten in bentoniet (**Hoofdstuk 5**). Op grond van de conclusie dat beide soorten elektroden niet geschikt zijn voor het meten van membraanpotentialen, is een permeameter met vaste wand en 'double junction' Ag/AgCl referentie elektroden gemaakt (**Hoofdstuk 6**). Met deze opstelling zijn membraanpotentialen (elektrische potentiaalgradiënten geïnduceerd door een gradient in zoutconcentratie) in bentoniet membranen gemeten, en hun effekt op transport van water en opgeloste stoffen is kwantificeerd. Dezelfde experimenten aan monsters van twee veldkleien zijn gerapporteerd in **Hoofdstuk 7**, die, vergeleken met bentoniet, een ander semipermeabel gedrag vertonen. Tenslotte worden in **Hoofdstuk 8** de bereikte resultaten kritisch samengevat, de conclusies van deze studie gegeven en een perspektief geboden op mogelijk toekomstig onderzoek aan dit complexe onderwerp.

Zusammenfassung

Der Transport von Wasser und gelösten Stoffen in tonigen Böden und Sedimenten spielt eine wichtige Rolle im Grundwasser- und Abfallmanagement. Neben dem Transport entlang hydraulischer und Dichte-Gradienten spielt in Tonschichten auch der Transport entlang von Gradienten in der Salzkonzentration und dem elektrischen Potential eine Rolle. Chemisch und elektrisch induzierter Wassertransport, sogenannte chemische Osmose und Elektroosmose, sind wichtig in porösen Materialien mit einer hydraulischen Durchlässigkeit von weniger als $1 \cdot 10^{-9}$ m/s, wie z.B. Tone.

Obwohl die Bedeutung dieser Prozesse in tonigen Böden und Sedimenten bereits in der Mitte des 20. Jahrhunderts erkannt wurde, werden chemische Osmose und Elektroosmose bis heute nicht in Grundwassermodellen berücksichtigt. In der Bodenkunde wurde in den vergangenen Jahrzehnten viel fundamentelle Forschung nach hydraulisch, chemisch und thermisch angetriebenen Strömen betrieben. So wurde auch die Nutzung von Elektroosmose für das Entwässern von Böden und zur Stabilisierung von Hängen sowie Elektromigration als in-situ Sanierungstechnik für verunreinigte Böden untersucht. Bei z.B. Salzwasserintrusionen in tiefgelegene Küstengebiete, in Deponien von verschmutztem Baggerschlamm und bei der Langzeitlagerung von radioaktiven oder toxischen Abfällen in Tonformationen, ist es nicht gerechtfertigt, elektrisch und chemisch induzierte Prozesse zu vernachlässigen. In diesen Fällen verläßt man sich auf die geringe Permeabilität und das hohe Adsorptionsvermögen des Tons, um die Verlagerung von gelösten Verunreinigungen zu begrenzen. Man geht davon aus, daß Seewasserintrusionen in grundwasserführende Schichten in Küstengebieten durch holozäne Tonschichten eingeschränkt werden. Verunreinigter Ton, toniger Schlamm oder toniges Sediment sind Emissionsrichtlinien unterworfen, die das Austreten von Schadstoffen in die Umwelt regeln. Im Falle der Langzeitlagerung von radioaktiven Abfällen in Tonformationen können sogar sehr kleine Ströme bedeutsam sein, da diese Prozesse über einen langen Zeitraum andauern, und die Gefährdung für Mensch und Umwelt groß ist.

Chemische Osmose und Elektroosmose sind gekoppelte Transportphänomene, die im Rahmen der irreversibelen Thermodynamik beschrieben werden können. Im allgemeinen kann Transport von Flüssigkeiten, elektrischer Ladung, gelösten Stoffen und Wärme durch Tonschichten auftreten. Diese Ströme können von ihren dazugehörigen Antriebskräften induziert werden, wie z.B. ein Wasserstrom durch einen hydraulischen Potentialgradienten; sie werden direkte Ströme genannt. Darüberhinaus können Ströme auch von nicht-dazugehörigen Antriebskräften induziert werden, wie z.B. ein Wasserstrom durch einen Salzkonzentrationsgradienten, was chemische Osmose genannt wird. Dies ist gekoppelter Transport.

Tonschichten können sich als semipermeabele Membranen verhalten. Sie sind imstande, den Transport von bestimmten Komponenten einer Lösung zuzulassen, während sie gleichzeitig den von anderen verhindern. Dementsprechend unterbindet eine semipermeabele Membran die Passage von gelösten Stoffen, ohne den Durchfluß des Lösungsmittels zu beeinflussen. Dies wird durch die sich innerhalb der Poren der Tonmembran überschneidenden diffusen Doppelschichten der Tonteilchen verursacht. Anionen, die versuchen durch die Poren zu wandern, werden von der negativen Ladung der Tonteilchen abgestoßen, wodurch auch die Bewegung der Kationen durch den Ton eingeschränkt wird, da nur so elektrische Neutralität in der Lösung aufrecht erhalten werden kann. Wenn ein Ton in der Lage ist, den Transport eines gelösten Stoffes komplett zu unterbinden, ist die Membran ideal. In der Natur jedoch sind Membranen selten ideal, und ein Teil der Salzionen passiert die Membran durch Diffusion. Folglich verhindern derartige nicht-ideale Membranen die Passage

von gelösten Stoffen nicht vollständig. Der Grad der Idealität wird mit dem Reflektionskoeffizienten ausgedrückt, der – zusammen mit einer Anzahl anderer Transportparameter für den Transport von Ionen und Wasser durch semipermeabele Membranen – mit Hilfe der gekoppelten Transportgleichungen berechnet werden kann.

Das Ziel dieser Dissertation ist die Quantifizierung des Effekts von induzierten elektrischen Potentialgradienten auf den Transport von Wasser und Ionen in Tonschichten mit Hilfe von Laborexperimenten. In Experimenten werden elektrische Potentialgradienten durch hydraulische Druckgradienten (Strömungspotentiale) oder durch Salzkonzentrationsgradienten (Membranpotentiale) induziert. Für diesen Zweck wurden Versuchsanordnungen realisiert, um Experimente im Labormaßstab mit verschiedenen Tonen durchzuführen. In der Literatur werden diese Versuchsanordnungen Permeameter genannt. Die untersuchten Materialien waren ein handelsüblicher Wyoming Bentonit und zwei unterschiedliche Geländeproben. Mit gekoppelten Transportgleichungen wurden Transportparameter berechnet, und der Effekt der induzierten elektrischen Potentialgradienten auf die Ströme von Wasser und Ionen wurde demonstriert. Es wurde festgestellt, daß induzierte elektrische Potentialgradienten den Transport van Wasser und Ionen durch den Ton behindern. Werden diese Effekte nicht berücksichtigt, so hat dies einen signifikanten Einfluß auf die berechneten Transportparameter. Die Ergebnisse dieser Laborstudie werden genutzt, um ein von der Environmental Hydrogeology Gruppe des Department of Earth Sciences, Universität Utrecht entwickeltes Modell zu validieren, welches chemische Osmose und Elektroosmose in Grundwassertransport einbezieht.

Gliederung der Arbeit

Kapitel 1 gibt eine allgemeine Einleitung und hebt die praktische Relevanz dieses Themas hervor. Nach einer Beschreibung der tonigen Materialien, die in den Versuchen verwendet werden (**Kapitel 2**), ist die Stabilität der Tonmembranen in **Kapitel 3** untersucht. Dies ist wichtig für alle nachfolgenden Experimente mit Tonmembranen, die in Kontakt mit Lösungen kommen, deren Ionenstärke über dem Flockulationswert des Tons liegt. Wenn durch Flockulation strukturelle Veränderungen durch eine Neuanordnung der Tonpartikel auftreten, hat dies einen maßgeblichen Einfluß auf die Semipermeabilität der Membran. Anschließend werden Strömungspotentiale (elektrische Potentialgradienten hervorgerufen durch hydraulische Strömung) in Bentonitmembranen in einem Permeameter mit flexibler Wand untersucht, und der Effekt von Strömungspotentialen auf den Wassertransport wird quantifiziert (**Kapitel 4**). In dieser Versuchsanordnung werden Goldelektroden verwendet, um die elektrischen Potentialgradienten zu messen. Die Anwendbarkeit der Goldelektroden kann wegen ihrer möglichen Polarisierbarkeit in Frage gestellt werden. Deshalb werden die verschiedenen Arten von reversibelen Elektroden diskutiert, und die Eignung von Goldelektroden wird in Strömungspotential- und Elektroosmose-Experimenten in Bentonitmembranen mit der von Ag/AgCl-Gel-Elektroden verglichen (**Kapitel 5**). Da hierbei festgestellt wurde, daß beide Elektrodenarten für das Messen von Membranpotentialen ungeeignet sind, wurde ein Permeameter mit fester Wand und ‘double junction’ Ag/AgCl Referenzelektroden realisiert (**Kapitel 6**). Mit dieser Versuchsanordnung werden Membranpotentiale, d.h. elektrische Potentialgradienten hervorgerufen durch einen Salzkonzentrationsgradienten, in Bentonitmembranen gemessen, und ihr Einfluß auf den Transport von Wasser und den darin gelösten Stoffen wird quantifiziert. In **Kapitel 7** sind ähnliche

Experimente mit zwei unterschiedlichen Geländeproben beschrieben. Diese zeigen im Vergleich zum Bentonit eine andere Semipermeabilität. Schließlich werden in **Kapitel 8** die erzielten Ergebnisse kritisch zusammengefaßt, die Schlußfolgerungen dieser Studie hervorgehoben und ein Ausblick auf mögliche zukünftige Studien innerhalb dieses komplexen Themengebietes gegeben.

Dankwoord/ Acknowledgements

First of all, I like to thank my promotor Philippe Van Capellen for giving me the chance and the freedom to delve into this interesting topic resulting in this thesis.

Mijn dank geldt ook mijn begeleider Guus Loch. Zonder hem had ik zeker niet de kans gekregen om op dit gebied te promoveren. – Guus, bedankt voor je vertrouwen en je interesse. Je hebt me in deze jaren altijd gesteund, ook al was dit zeker niet altijd een even gemakkelijke taak.

Dit proefschrift zou nooit tot stand zijn gekomen zonder labwerk. Voor de hulp, die ik hier heb ervaren, dank ik Pieter Kleingeld. – Pieter, jij was onmisbaar in het lab. Zonder jou zou ik nog steeds met problemen als lekkages enzovoorts worstelen. Ik moet ook mijn dank uitspreken dat jij samen met mij 3 ½ uur in de rij bleef staan om je voor een electrochemie-congress in te schrijven. Maar ik heb meer hoogachting voor het feit, dat je na een hele dag met mij op een vliegveld rondhangend, wachtend op de reparatie van het vliegtuig, me nog steeds kan verdragen.

Voor de finaciele ondersteuning geldt mijn dank TRIAS. Dit proefschrift kwam tot stand in het project 835.80.003 'Chemically and Electrically Coupled Transport in Clayey Soils and Sediments'. Dank ook aan de leden van de TRIAS begeleidingscommissie voor hun interesse.

This thesis is only one part of the TRIAS project. I like to thank the other Ph.D. students involved, Ana Maria Garavito and Sam Bader, and their supervisors, Henk Kooi and Ruud Schotting, for the good collaboration.

I thank Pierre De Cannière and his colleagues from SCK·CEN, Mol, Belgium, for providing us with Boom Clay sample material, for their hospitality and for their collaboration in the Underground Research Laboratory in Mol.

Dank aan dhr. B. Verburg van Sentron voor het beschikbaar stellen van een aantal ISFET pH elektroden. Helaas konden wij tot nu toe hiermee geen bruikbare resultaten boeken, maar we hebben de hoop dat in een mogelijk vervolgonderzoek interessante dingen aan het daglicht komen.

Dank ook aan Ineke Joosten van ICN en Rob Fase van JEOL voor het proberen ESEM foto's van flocculerende klei te maken.

For the good time I had in Utrecht, I like to thank all members of the Geochemistry group and the Geochemistry students, especially my roommates and Thomas Keijzer. – Thomas, ook al werk je niet meer in Utrecht, je hebt me in het begin heel goed op weg geholpen. Hartelijk dank hiervoor.

Nicht zuletzt gilt mein Dank meiner Familie für die Unterstützung und das Verständnis, das ich in dieser Zeit erfahren habe. Ganz besonders möchte ich Johannes danken. – Johannes, ohne Dich hätte ich dies alles nicht geschafft. Danke, daß Du für mich da bist.

Curriculum vitae

Katja Heister, geb. Richter, geboren op 21 maart 1973 in Koblenz, Duitsland.

1983 – 1992:	Staatliches Görres-Gymnasium in Koblenz, Duitsland.
1992 – 2000:	Studie geologie aan de Rheinische Friedrich-Wilhelms-Universität in Bonn, Duitsland. M.Sc. in geologie.
2000 – 2001:	Werkervaring buiten de geologie in een hulporganisatie.
2001 – 2005:	Universiteit Utrecht, Departement Aardwetenschappen – Geochemie. Ph.D. in geochemie.